ROLE OF EXTRACELLULAR POLYMERS IN STREPTOMYCES GROWTH

THE ROLE OF EXTRACELLULAR POLYMERS IN *STREPTOMYCES* GROWTH AND DEVELOPMENT

By DANIELLE L. SEXTON, B. Sc.

A Thesis Submitted to the School of Graduate Studies in Partial Fulfilment of the Requirements for the Degree Doctor of Philosophy

McMaster University
Hamilton, Ontario

DOCTOR OF PHILOSOPHY (2018)
(Biology)

TITLE: The role of extracellular polymers in *Streptomyces* growth and development

AUTHOR: Danielle L. Sexton, B. Sc (University of Toronto)

SUPERVISOR: Dr. Marie A. Elliot

Number of pages: xiv, 131

Lay Abstract
Bacteria are all around us. In these different environments, whether in the soil, or inside our guts, or in a body of water, they will encounter stress. This can take the shape of nutrient stress, or the presence of growth inhibiting compounds. In response, bacteria can evade these poor conditions by entering into dormancy, analogous to hibernation, by building a biofilm, analogous to building a bunker, or by moving away. The surface of bacterial cells becomes decorated with different polymers as it transitions into one of these three modes of stress evasion. The cell wall holds the cell together and supports its shape, making it the most important surface polymer. I examined how rapid remodeling of the cell wall provides a competitive advantage to cells waking up from dormancy. I also examined the importance of additional polymers to the formation of biofilms that slide across surfaces, away from stressors. These works establish how important the surface of the bacterium is for surviving stressful conditions.

Abstract
Bacteria in the environment face constant stress, due to lack of nutrients or presence of growth inhibiting compounds. As a result, they have developed several strategies to evade unfavourable growth conditions. These range from entering into dormant or quiescent states, through to motility, and biofilm formation. Using the model organism *Streptomyces*, we investigated how the bacterial cell surface regulates dormancy, biofilm formation, and motility.

Dormancy via spore formation allows cells to shut down metabolism in response to poor nutrient conditions. Spores can then be dispersed throughout the environment to encounter favourable conditions. This is an incredibly resilient survival strategy, so long as the spores resuscitate from dormancy and resume growth once favourable conditions are sensed. We established that peptidoglycan remodeling by resuscitation promoting factors is critical for rapid germination of dormant *Streptomyces* spores, which likely provides a competitive advantage over slower growing microbes in the same environment. Previously it was thought that these proteins produce a signal to stimulate germination in neighbouring cells. We determined that the resuscitation promoting factors are lytic transglycosylases, and were not capable of producing a germination signal on their own. Instead, they function by cleaving the peptidoglycan to make room for new cell growth. This work highlights the importance of peptidoglycan remodeling to the germination process. Biofilms are multicellular communities of microorganisms which are adhered to each other using a protective matrix. Formation of biofilms is thought to be inversely correlated with motility. We established that *Streptomyces* forms biofilms during the exploratory growth identifying potential extracellular matrix components. These biofilms use sliding motility to expand rapidly across their environment. Components of the biofilm matrix effect colony expansion, suggesting that biofilm formation and motility are intricately linked in *Streptomyces.* These works demonstrate the importance of surface polymers to the growth and development of *Streptomyces*.

Acknowledgements

I would first like to thank Dr. Marie Elliot. I do not have words to express the depth of my gratitude for your mentorship. Thank you as well to my supervisory committee members, Dr. Lori Burrows and Dr. Turlough Finan for their guidance and feedback on my work. I would also like to say thanks to all of the post doctoral fellows, grad students and undergrads I have had the honour of working with over the last six years. I learned something from each of you. I don't think I could have ended up working with a better group of people if I tried.

I would like to thank my parents, Dan and Karen, for giving me the freedom to set my own path in life, and for never clipping my wings. Thanks to my whole family and all of my non-lab friends for keeping me humble, and for all your love and emotional support over the years. Finally, I would like to thank Harrison Lee. I could have done this without you, but it would not have been anywhere near as much fun.

Table of Contents

LIST OF TABLES

LIST OF FIGURES

LIST OF ABBREVIATIONS

A

AMP	Adenosine monophosphate
ATP	Adenosine triphosphate

B

bp	Base pair

C

C	Carbon atom or cysteine
c-di-GMP	Cyclic di guanosine monophosphate
cfu	Colony forming unit
cm	Centimeter
cDNA	Complementary DNA
ConA	Concanavalin A

D

DBA	*Dolichos biflorus* agglutinin
DNA	Difco nutrient agar or deoxyribonucleic acid
DNase	Deoxyribonuclease
DUF	Domain of unknown function

E

eDNA	Extracellular DNA
EDTA	Ethylenediaminetetraacetic acid

G

g	Gram or gravity
GlcNAc	*N*-acetylglucosamine

H

h or hr	Hours

I

IPTG	Isopropyl-β-D-thiogalactopyranoside

K

kDa	Kilodalton
kW	Kilowatt

L

LB	Lysogeny Broth
LC	Liquid chromatography
LL-DAP	Diaminopimelic acid

M

m/z	Mass to charge ratio
min	Minute
mL	Milliliter
mm	Millimeter
mg	Milligram
MS	Mannitol soya flour agar or mass spectrometry
MurNAc	*N*-acetylmuramic acid
MYM	Malt extract-yeast extract-maltose medium

N

NA	Nutrient agar medium
Ni-NTA	Nickel nitriloacetic acid
nm	Nanometer
nM	Nanomolar
NMMP	New minimal medium with phosphate
nmol	Nanomole

P

PBS	Phosphate buffered saline
PCR	Polymerase chain reaction
PNA	Peanut agglutinin

Q

Q-TOF MS	Quadrupole time of flight mass spectrometry

R

RCA120	*Ricinus communis* agglutinin
RNA	Ribonucleic acid
RNase	Ribonuclease
RNA-seq	RNA sequencing
RPKM	Reads per kilobase per million mapped reads
RT	Reverse transcriptase

S

SALP	SsgA like protein
SBA	Soybean agglutinin
SCO	*Streptomyces coelicolor*
SD	Synthetic defined medium
SDS	Sodium dodecyl sulphate
SEM	Scanning electron microscopy
SOB	Super optimal broth
SVEN	*Streptomyces venezuelae*

T

TCA	Trichloroacetic acid
TEM	Transmission electron microscopy
TSB	Tryptone soy broth

U

U	Unit
μL	Microliter
μm	Micrometer
μM	Micromolar
μmol	Micromole

W

WGA	Wheat germ agglutinin
WT	Wild type

Y

YEME	Yeast extract-malt extract medium
YP	Yeast extract peptone medium
YPDA	Yeast extract dextrose adenine medium

Symbols

˚C	degrees Celsius
Δ	mutant

Chapter 1

General Introduction

1.1 The bacterial cell envelope

The cell envelope is arguably the most important structure produced by the bacterial cell. It senses and responds to the environment, controls cell shape and prevents lysis due to the turgor pressure within the cytoplasm. Indeed, bacteria are separated into their two main classifications, Gram- positive and Gram- negative, based on cell wall structure.

Gram- negative bacteria feature a double membrane with a periplasmic space and a thin layer of peptidoglycan. The Gram- positive cell wall is composed of a single membrane surrounded by a thick layer of peptidoglycan and teichoic acids. Both cell walls also contain proteins that perform functions relating to modulating surface properties, transport of proteins and other molecules in and out of the cell, and maintaining the cell wall.

1.1.1 Teichoic acids in the Gram- positive cell wall

Teichoic acids are glycopolymers composed of phosphodiester-linked polyol repeats. These can be anchored to the cell membrane via a glycolipid (lipoteichoic acids) or covalently attached to the peptidoglycan (wall teichoic acids). Lipoteichoic acids are composed of a polyglycerolphosphate chain that is anchored to a glycolipid and embedded in the membrane (Reichmann and Gründling, 2011). In *Bacillus subtilis* and *Staphylococcus aureus*, it is estimated that roughly 10% of *N*-acetylmuramic acid residues have a covalently attached wall teichoic acid (Bera et al., 2007). Wall teichoic acid composition varies greatly between bacteria, but they all share a common structure: they are all attached to the peptidoglycan through a defined 'linkage group', from which variable repeat units extend. The linkage group is composed of *N*-acetylmannosamine ($\beta 1 \rightarrow 4$) *N*-acetylglucosamine 1-phosphate with one to two glycerol 3-phosphate moieties (Brown et al., 2013). This is attached to the peptidoglycan via a phosphodiester bond to the *N*-acetylmuramic acid in peptidoglycan (discussed below) (Brown et al., 2013). The polymer of repeat units extend from the glycerol 3-phosphate units on the other end of the linker (Brown et al., 2013). The repeat unit can be ribitol 5-phosphate, glycerol 3-phosphate, or glycosylpolyol phosphate/glycosyl phosphate-polyphosphate-based (Brown et al., 2013). Despite a considerable variation in the sugar subunits, all teichoic acids feature a negatively charged backbone.

The repeat units can also be modified in both lipoteichoic acids and wall teichoic acids. For example, D-alanylation of teichoic acids alters the surface charge by decreasing the

net negative charge of the teichoic acid polymer (Brown et al., 2013; Reichmann and Gründling, 2011). The amount of D-alanine added to ribitol 5-phosphate polymers can vary in response to changing environmental conditions, including pH, temperature, and salt concentrations (Brown et al., 2013; Jenni and Berger-Bächi, 1998; Neuhaus and Baddiley, 2003). Mono- or oligosaccharides, often glucose and *N*-acetylglucosamine, can also be added to the repeat unit, although the extent to which these sugar modification are employed does not seem to change with environmental conditions (Collins et al., 2002). These sugars can ultimately coat the entire teichoic acid polymer and can be added using an α or β glycosidic linkage. It is likely that the addition of sugars, and the type of linkage, affects interactions with cell surface protein or other components of the cell wall, or may impact interactions with the environment (Brown et al., 2013). In the case of *S. aureus,* removal of the sugar residues led to enhanced susceptibility to antibiotic treatment and reduced virulence (Brown et al., 2012; Xia et al., 2010).

1.1.2 Peptidoglycan structure

Peptidoglycan represents another major component of the bacterial cell wall, where it serves both as the attachment point for wall teichoic acids, and as a major structural entity in and of itself. It is a polymer of alternating sugar residues cross linked together by a combination of peptide stems and crossbridges (Fig. 1.1). This crosslinked polymeric mesh surrounds the cell, providing support for the membrane, while still being porous enough to allow diffusion through it.

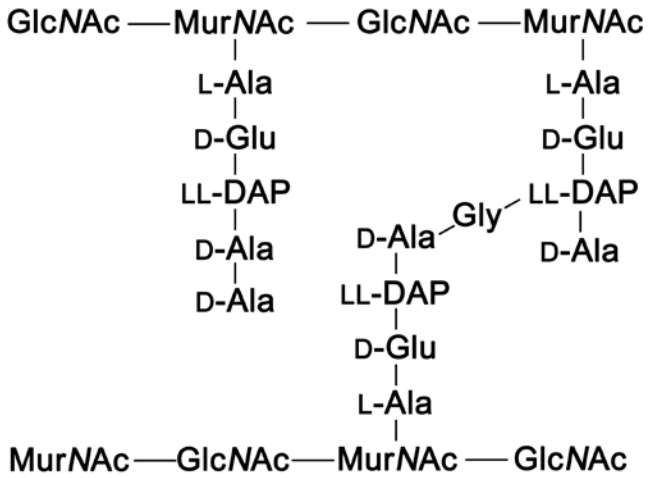

Figure 1.1: The structure of *Streptomyces* peptidoglycan. The backbone of peptidoglycan comprises alternating units of *N*-acetylglucosamine (Glc*N*Ac) and *N*-acetylmuramic acid (Mur*N*Ac). Strands of peptidoglycan are crosslinked using peptide stems composed of L-alanine (L-Ala), D-glutamine (D-Glu), diaminopimelic acid (LL-DAP), and D-alanine (D-Ala) which are bridged with single glycine (Gly) residues.

1.1.2.1 The glycan strand

The composition and organization of the glycan strand, the peptidoglycan backbone, is uniform across all bacteria. It is composed of alternating *N*-acetylglucosamine and *N*-acetylmuramic acid residues linked by β 1-4 glycosidic bonds (Fig. 1.1). Peptidoglycan polymers range from 3 to 250 repeats of these two sugar residues, depending on the strain and the growth conditions (Vollmer et al., 2008a). In rod shaped bacteria, the strands of peptidoglycan run parallel to the cell surface, and perpendicular to the long axis of the cell (Beeby et al., 2013; Gumbart et al., 2014; Turner et al., 2018). In spherical bacteria, peptidoglycan strands are highly organized into concentric rings on the division plane, but this organization is lost in the mature cell wall (Turner et al., 2014).

1.1.2.2 The peptide stem

Peptidoglycan strands are crosslinked together through peptide bonds, to provide additional strength to the cell wall. Penta-peptide stems are attached to muramic acid residues, and crosslinks/bridges between these different stems effectively serve to crosslink distinct glycan strands together (Fig. 1.1). The composition of the peptide stem varies between bacteria but it is generally composed of alternating L- and D- amino acids, with the greatest degree of variability at the third position of the peptide stem. The amino acid in the third position is typically a diamino acid and it participates in crosslinking with the fourth amino acid of a second peptide stem, either directly, or through an additional peptide crossbridge. The fifth amino acid is removed during the crosslinking process. In *Streptomyces coelicolor*, the peptide stem is composed of L-Ala – D-Glu – LL-diaminopimelic acid (DAP) – D-Ala – D-Ala, with a single glycine crossbridge linking the LL-DAP of one peptide stem, with the LL-DAP (3^{rd} position) or D-Ala (4^{th} position) of the second peptide stem (Hugonnet et al., 2014; Schleifer and Kandler, 1972) (Fig. 1.2). These two crosslinking variants (LL-DAP-LL-DAP or LL-DAP-D-Ala) occur in almost equal proportions under standard laboratory conditions (Hugonnet et al., 2014). The biological function of these two crosslinking types is unknown. The degree of crosslinking depends both on the strain and the growth conditions. Approximately 50% of stem peptides are crosslinked in *Streptomyces* growing under standard laboratory conditions (Paget et al., 1999). Sortase enzymes may also covalently anchor proteins to the peptide stem of nascent peptidoglycan; their activity therefore has the potential to spatially exclude peptide stem crosslinking.

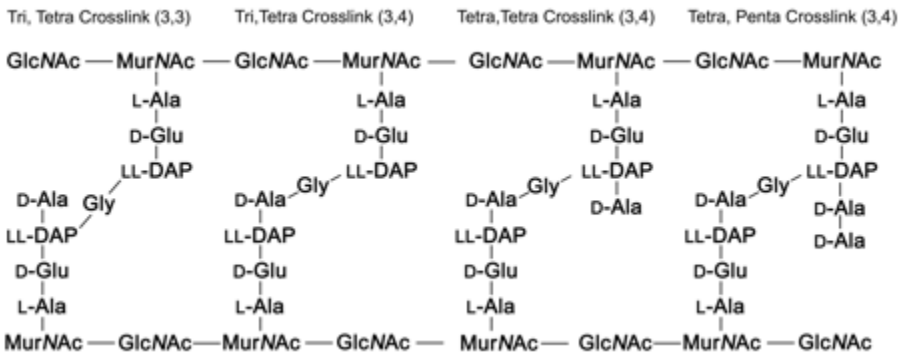

Figure 1.2: Peptidoglycan crosslinking structures in *Streptomyces*. Throughout its growth, *Streptomyces* peptidoglycan crosslinks will change in structure. Common peptidoglycan crosslinks are shown here.

1.1.3 Cell wall hydrolases – modifying peptidoglycan structure

Despite its seemingly rigid structure, peptidoglycan is necessarily a highly dynamic entity: if the cell wall was entirely inflexible, it would completely prevent growth. In order for cell growth to occur, peptidoglycan must be very carefully altered and adjusted by a suite of cell wall lytic enzymes. These cell wall lytic enzymes cleave different portions of the glycan strand or the peptide side chains to make space for new growth. In addition, a subset of cell wall lytic enzymes have specialized functions, where they are responsible for making room for the insertion of large cross-wall protein complexes, like flagella, secretion systems, and pili production complexes.

1.1.3.1 Classification of cell wall lytic enzymes

For every type of bond in the peptidoglycan, there is an enzyme that can digest it (Fig. 1.3**)**. In the backbone, *N*-acetylglucosaminidases hydrolyse the bond between Glc*N*Ac and Mur*N*Ac residues, while lysozymes hydrolyse the bonds between Mur*N*Ac and Glc*N*Ac residues. Lytic transglycosylases also cleave the glycosidic linkage between Mur*N*Ac and Glc*N*Ac residues (Fig. 1.3); however, they break the bond without using a water molecule, resulting in the formation of a 1,6 anhydro ring on the muramic acid residue (Fig. 1.4).

Like the backbone, the peptide stem is also subject to cleavage at every position. Amidases, or *N*-acetylmuramyl-L-alanine amidases, cleave the amide bond between the L-alanine in the first position of the peptide stem and Mur*N*Ac, completely removing the peptide stem. Endopeptidases cleave different amide bonds within the peptide stem. These can be further subdivided into different families, such as DD-peptidases, which cleave between two D amino acids, DL-peptidases, which cleave between L- and D-amino acids, and LL-peptidases, which cleave between two L-amino acids. Carboxypeptidases remove the C terminal amino acid from the peptide stem.

In addition to their enzymatic domains, cell wall lytic enzymes often have additional domains. These domains, including the SH3b, SPOR, LysM and G5 domains, function to enhance substrate binding and in turn are thought to increase enzyme activity. The SH3b domain is often associated with endopeptidases (Lu et al., 2006). Substitutions within the SH3b domain can modify substrate specificity to direct proteins to specific sites within the cell wall (Xu et al., 2015). The sporulation-related repeat (SPOR) domain also guides protein localization. The SPOR domain has increased affinity for peptidoglycan lacking side chains, which is often found at the septum. Proteins containing SPOR domains often have diverse functions, however they are frequently targeted to the septum (Yahashiri et al., 2015). Like the SPOR-containing proteins, LysM domain-containing proteins also have diverse functions, and again, its binding substrate is well-established: it recognizes *N*-acetylglucosamine in the backbone of peptidoglycan and other polysaccharides like chitin. LysM domain binding can be influenced by peptide stem length on neighbouring *N*-acetylmuramic acid residues, with longer stem peptides inhibiting binding more than shorter peptide stems (Mesnage et al., 2014). Similar to the LysM domain, the G5 domain is also predicted to bind to *N*-acetylglucosamine residues, however this has not been demonstrated experimentally (Bateman et al., 2005). Whether substrate binding by G5 domain-containing proteins is affected by peptide stem length on adjacent *N*-acetylmuramic acid residues remains to be seen.

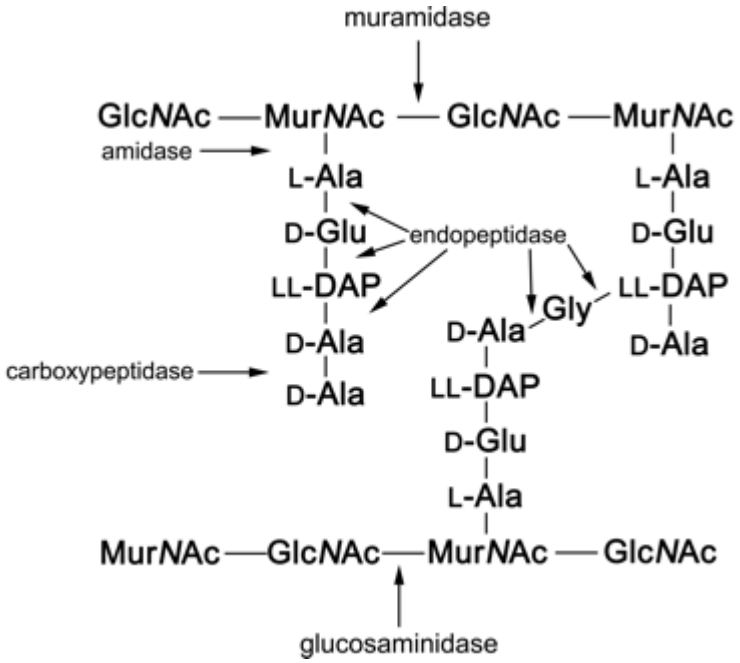

Figure 1.3: Peptidoglycan cleavage by cell wall lytic enzymes. Cleavage positions for the various classes of cell wall lytic enzymes are indicated on the structure of *Streptomyces* peptidoglycan with arrows.

1.1.4 Modifications to the glycan strand

The peptidoglycan backbone can be modified in a number of different ways, often to regulate the activity of cell wall lytic enzymes (Fig 1.4). Lysozymes are produced by a broad range of organisms ranging from phage to mammals, potentially as a mechanism to disrupt the growth of bacteria, and as a result bacteria have developed strategies to protect their cell walls from digestion. Many human pathogenic bacteria use peptidoglycan deacetylases which act on either the muramic acid or glucosamine residues to resist the activity of lysozymes produced by the host (Vollmer, 2008). Deacetylated peptidoglycan is a poor substrate for cell wall hydrolases, as lysozymes use the acetyl group for substrate binding (Vocadlo et al., 2001). These enzymes, such as in the human pathogen *Helicobacter pylori,* are controlled through the transcriptional response to reactive oxygen species produced during the host response to infection (Wang et al., 2009). Within the actinobacteria (excluding the streptomycetes), *N*-glycolation of muramic acid has been observed (Azuma et al., 1970; Uchida and Aida, 1979). While the exact function of the glycolyl group is not known, *Mycobacterium smegmatis* mutants lacking this modification are hyper-sensitive to lysozyme, suggesting a role in protecting the peptidoglycan from lysozymes (Raymond et al., 2005).

O-acetylated peptidoglycan is also resistant to digestion by muramidases. *O*-acetylation and de-*O*-acetylation are thought to represent parallel strategies for spatially and temporally regulating lytic transglycosylase activity (Weadge et al., 2005). *O*-acetylation has also been associated with *N*-acetylglucosamine residues in *Lactobacillus plantarum*, where it inhibits peptidoglycan degradation by *N*-acetylglucosaminidases (Bernard et al., 2011).

Finally, polysaccharide polymers like wall teichoic acids, can be added to the peptidoglycan. Wall-anchored teichoic acids, capsular polysaccharides, or arabinogalactans can all be attached to the peptidoglycan, and function to prevent cleavage of the peptidoglycan by cell wall lytic enzymes (Vollmer, 2008). Wall teichoic acids may function by excluding access of cell wall lytic enzymes to their substrates, and have been shown to reduce peptidoglycan degradation by lysozyme in *S. aureus* (Bera et al., 2007; Frankel and Schneewind, 2012; Schlag et al., 2010). Little is known about how the addition of other polysaccharides to the peptidoglycan impacts cell wall lytic enzymes.

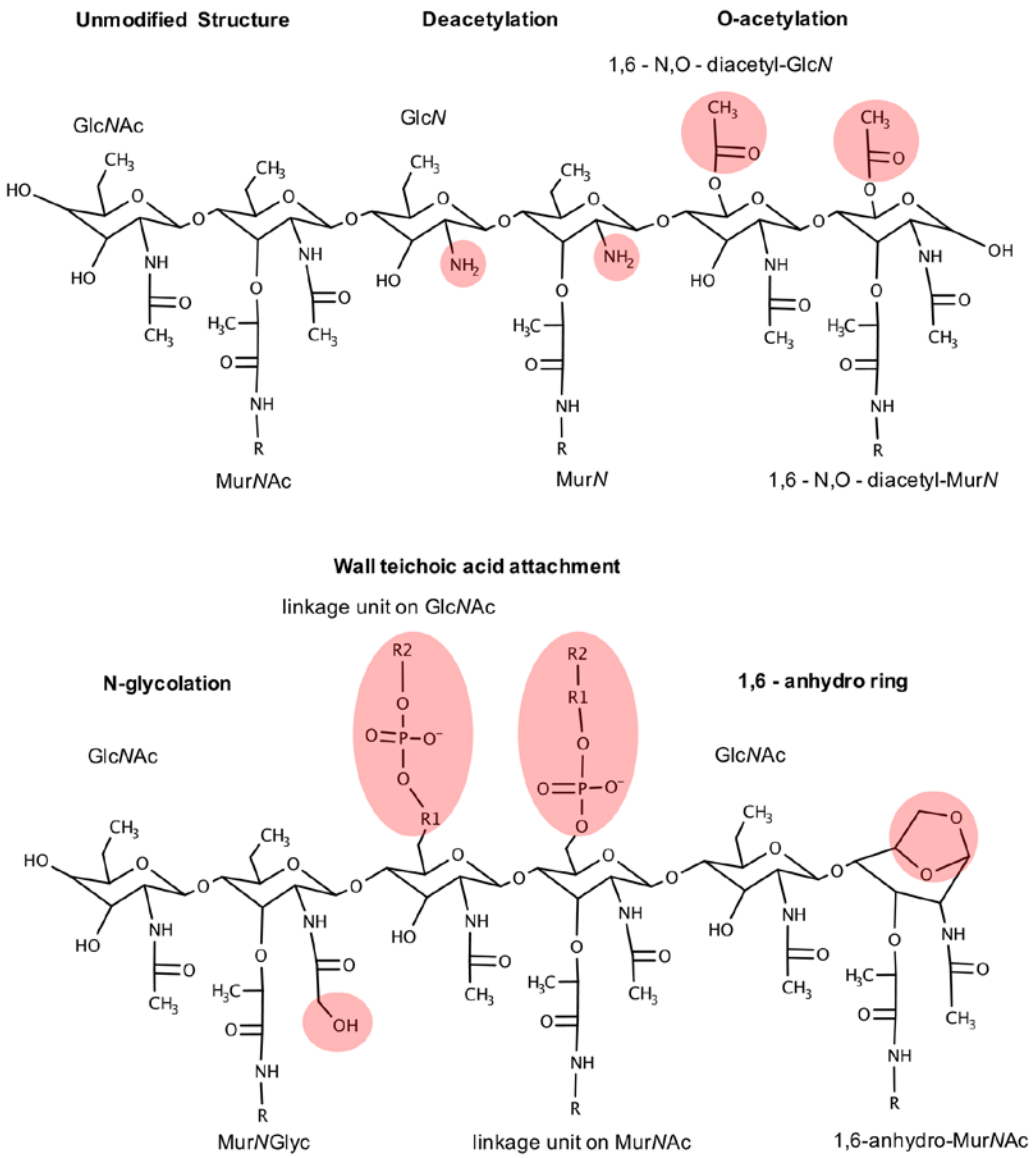

Figure 1.4: Modifications to the backbone of peptidoglycan. The peptidoglycan backbone can be modified in several ways. Acetyl groups can be added or removed (top middle and right). Glycolation can also occur. Teichoic acids can also be linked to the peptidoglycan through linkage groups (R1). The repeating units of the polymer (R2) will extent away from the linkage unit. Finally, digestion by lytic transglycosylases will leave a 1,6-anhydro ring on the *N*-acetylmuramic acid residues. Glc*N*Ac, *N*-acetylglucosamine. Mur*N*Ac, *N*-acetylmuramic acid. Modifications to the structure are highlighted in red.

1.2 *Streptomyces* growth and development

Streptomyces is a genus of Gram- positive bacteria that belong to the actinobacterial phylum. This genus has classically been studied for its ability to produce numerous medically relevant compounds, such as antibacterial, antifungal, and anti-cancer drugs. In addition to their reputation as "nature's chemists", the streptomycetes have a complex developmental cycle, more similar to that of filamentous fungi than unicellular bacteria.

1.2.1 Classical development

Life for *Streptomyces* begins as a dormant spore (Fig. 1.5). When the spore encounters favourable growth conditions, it resumes metabolic activity and initiates growth through a process known as germination. During germination, a spore will produce one or two germ tube(s) that grow via tip extension. As these germ tubes extend, they begin branching and ultimately form what is known as a vegetative mycelium. Vegetative growth continues until a signal, possibly nutrient limitation, triggers the onset of the reproductive phase of their life cycle. This phase is marked by the raising of unbranched hyphae up into the air. These aerial hyphae undergo a synchronous round of cell division to produce ~100 immature spores per hyphal filament. These pre-spore compartments are subject to a maturation process that yields mature, dormant spores that can then be released into the environment. The transitions between vegetative growth, aerial hyphae formation and sporulation are complex and highly regulated and are discussed in greater detail below.

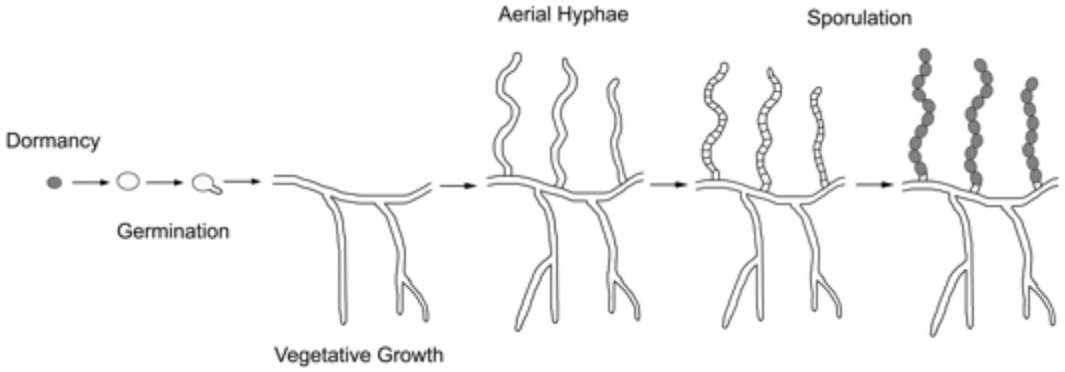

Figure 1.5: Lifecycle stages of *Streptomyces*. *Streptomyces* begins its growth cycle as a dormant spore (Dormancy). Once a germination signal is sensed, the spore swells and produce a germ tube (Germination). The germ tube grows via hyphal tip extension and branching (Vegetative Growth). Unbranched aerial hyphae are produced and extend up from the surface of the substratum (Aerial Hyphae). These aerial cells undergo a synchronous round of cell division to produce immature spores, which undergo a maturation process to become fully dormant spores (Sporulation). Once dormant, the spores are released and can begin the cycle again.

1.2.1.1 Resuscitation from dormancy

Many bacteria use some form of quiescence as a strategy to evade a range of poor environmental conditions. Once a dormant cell encounters favourable growth conditions, however, it will often resume active growth and colonize the environment. On paper this sounds quite straightforward; however, it requires the cell to sense an external signal, restart its metabolism, and modify its cell wall such that physical growth of the cell can resume.

1.2.1.2 *Bacillus* model for spore germination

Triggers of spore germination are best characterized in *Bacillus*. Endospores produced by *Bacillus* and other members of the firmicutes are metabolically inactive and are exceptionally resistant to environmental stressors. This resistance is due in large part to the unique spore structure, which will be the focus here. The spore cell wall is composed of two distinct layers of peptidoglycan, the inner germ cell peptidoglycan and the outer cortex. The cortex is surrounded by an outer membrane, (Gerhardt and Black, 1961; Henriques and Moran, Jr., 2007; Rode et al., 1962), outside of which is a layer of coat proteins, which protect against chemicals (Henriques and Moran, Jr., 2007; Mckenney et al., 2013). The cell wall and cytoplasm are also dehydrated during dormancy. The dehydration of the spore core is critical for the highly resilient nature of bacterial spores (Beaman and Gerhardt, 1986; Nakashio and Gerhardt, 1985; Setlow, 2006).

Spore germination is a multistep process. Initially, a germination signal is sensed. In its natural environment, it is thought that nutrients, including specific L-amino acids, salts, and glucose, trigger *Bacillus* spore germination (Gupta et al., 2013; Paidhungat and Setlow, 2000). There are dedicated germination receptors in the outer membrane that specifically sense and respond to these different nutrients. Spores lacking the germinant receptors are essentially not viable, with fewer than 0.001% of spores able to germinate (Gupta et al., 2013; Paidhungat and Setlow, 2000). Independent of the germinant receptors, $Ca^{2+}$and dipicolinic acid, high pressure and cationic surfactants can also promote germination (Reineke et al., 2013; Setlow, 2013; Shah et al., 2008).

There is a lag between recognizing a germination cue and the commitment to proceed with germination, lasting anywhere from a few minutes to over 24 hours. Very little is known about what occurs during this lag phase; however, commitment to germination is associated with a change in inner membrane permeability, leading to the release of monovalent cations, $Ca^{2+}$and dipicolinic acid (Setlow, 2013; Swerdlow et al., 1981; Yi and Setlow, 2010). CwlJ, a putative lytic transglycosylase and SleB, a known lytic transglycosylase, then degrade the cortex peptidoglycan (Heffron et al., 2009; Setlow, 2013). Following cortex digestion, the germ cell hydrates and swells. Increased hydration of the cell allows metabolism to resume and the spore begins outgrowth.

1.2.1.3 *Streptomyces* spore germination

Compared with *Bacillus* spore germination, we know very little about how germination is triggered in *Streptomyces*. A minimal germination medium, composed of a mixture of L-amino acids, salts, para-aminobenzoic acid, adenosine, Ca^{2+}, and Mg^{2+} ions, was found to effectively stimulate germination (Hirsch and Ensign, 1976). It has been proposed that Ca^{2+} may stimulate the function of Ca^{2+} dependent ATPases, leading to increased ATP production and germination (Grund and Ensign, 1985); however, the function of the other germination-promoting compounds remains unclear even 40+ years on. Germination can be stimulated by plating spores in close proximity to each other (Xu and Vetsigian, 2017), and depends on a heat sensitive compound(s) (Xu and Vetsigian, 2017). *S. coelicolor* can also produces germicidins, which inhibit the germination of neighbouring cells. Germicidins function by inhibiting Ca^{2+}-activated ATPases through an unknown mechanism, thereby decreasing ATP levels during germination (Grund and Ensign, 1985). This presumably confers a competitive advantage to spores that germinate early. Adding surplus Ca^{2+} can reduce the effect of germicidins on germination (Petersen et al., 1993), as can the addition of detergents or heat shock treatment (Grund and Ensign, 1982, 1985; Hirsch and Ensign, 1976b).

Once germination has initiated, the spore proceeds through three distinct phases: darkening, swelling, and germ tube emergence, as defined by Hardisson *et al* (1978). Darkening is associated with water entering into the spore cell wall, leading to the loss of divalent cations and a change in the refractive index (Eaton and Ensign, 1980; Hardisson et al., 1978). Increased spore hydration leads to an increase in spore size and marks the entry into the 'swelling' phase. This increase in cytoplasmic hydration is thought to allow for enzyme reactivation (Crowe et al., 1984). This in turn enables translation to resume, employing ribosomes and mRNAs synthesized prior to onset of dormancy (Crowe et al., 1984).

During these early stages of cellular resuscitation, saccharides like trehalose stored in the spore, serve as an integral energy source (Crowe et al., 1984). Resumption of DNA synthesis coincides with germ tube emergence (Wolanski et al., 2011), and the extension of one or two germ tubes marks the entry into vegetative growth. The positioning of the germ tubes is thought to be set by SsgA, which is deposited at the septa during sporulation (Noens et al., 2007).

To date, several cell wall lytic enzymes have been implicated in the germination process. SwlA, an NlpC/P60 endopeptidase, promotes rapid germination through an unknown mechanism (Haiser et al., 2009). SwlA shares regulatory elements with some of the resuscitation promoting factors, or Rpfs, which are also important for resuscitation from dormancy (Sexton et al., 2015). The Rpfs are family of lytic transglycosylases found largely within the actinobacteria, with anywhere from one to five Rpf proteins being encoded by any given actinobacterial species. Beyond the Swl and Rpf proteins, which are important for promoting spore germination, a newly characterized D-alanyl-D-

alanine carboxypeptidase, SCO4439, is also thought to modulate crosslinking as new peptidoglycan is being synthesized during germination (Rioseras et al., 2016).

1.2.2 Vegetative growth

Growth of the nascent germ tubes occurs via tip extension, where new growth is coordinated by a tip organizing complex. The location of this complex is dictated by extreme negative curvature, and is governed by DivIVA, which preferentially localizes to sites of negative membrane curvature, such as hyphal tips (Lenarcic et al., 2009; Ramamurthi and Losick, 2009). DivIVA foci form prior to new cell wall synthesis, suggesting that DivIVA functions to recruit and organize the cell wall biosynthetic machinery. Branching occurs when a portion of the DivIVA complex disassociates from the main tip focus and localizes to a secondary site, driving branch formation.

1.2.3 The initiation of sporulation

The growth of aerial hyphae is also driven by DivIVA, although without any associated branching. The onset of aerial hyphae formation represents the start of their dormant growth phase. As has been seen for many other bacteria (Higgins and Dworkin, 2012) nutrient limitation is likely the cue for *Streptomyces* to enter into dormancy. A wide variety of signals, including starvation, reduced oxygen, suboptimal temperature, osmotic stress, exposure to heavy metals, and white light, are used by a variety of bacteria to enter into dormancy or analogous metabolically quiescent states (Oliver, 2005, 2010). The production of exo-spores (as for *Streptomyces*) or endo-spores (as for *Bacillus*) is the culmination of specialized developmental programs, yielding metabolically inactive cells with heavily modified cell morphology and an accompanying increase in resistance to a wide variety of environmental stresses. Other forms of bacterial dormancy rely solely on metabolic quiescence or metabolic inactivity for increased survival.

In the case of spores, once dormant, these cells can remain viable but not growing for many years. For *Streptomyces,* spores have been shown to remain viable for 80 years (Renberg and Nilsson, 1992), while endospores produced by *Bacillus* have been found viable after an incredible 25 to 40 million years inside of a bee in a piece of amber (Cano and Borucki, 1995).

1.2.4 Aerial hyphae formation – the first stage of sporulation

Streptomyces sporulation is a complex process, and is highly regulated. Several classical developmental regulators control the transition from vegetative to aerial hyphae. These regulators are encoded by the so-called '*bld*' genes, and are so named due to the lack of fuzzy aerial hyphae coating mutant colonies. These Bld regulators control the transcription of many genes involved in aerial hyphae formation, including those encoding two types of surfactants, SapB and the chaplins. The chaplins are a family of functional amyloid proteins that coat the surface of the aerial hyphae in a beautiful paired rodlet ultrastructure, in association with a second family of proteins termed the

rodlins (Capstick et al., 2011; Claessen et al., 2003, 2004; Elliot et al., 2003). The chaplin/rodlin ultrastructure functions to alter the surface properties of the aerial hyphae, conferring both a hydrophobic coating and serving to reduce the surface tension at the air-medium interface under all growth conditions. In contrast, SapB is a lantibiotic-like peptide derived from the *ramCSAB* gene cluster (Willey et al., 1991) . SapB is thought to accumulate at the air-medium interface, reducing the surface tension specifically during growth on nutrient rich conditions (Capstick et al., 2007).

1.2.5 Sporulation and entrance into dormancy

Sporulation can be subdivided two distinct stages: cell division to form spores, and spore maturation, when the spores become dormant. A second set of developmental genes is required for effective sporulation: the *whi* (white) genes. These are named for the white appearance of colonies bearing mutations in these genes, indicating a failure of these strains to reach the final stage of spore maturation, where a pigment is deposited into the mature spore coat. Like the *bld* genes, many *whi* genes encode transcription factors, with a notable exception being the *whiE* gene cluster that directs the production of the pigmented polyketide that gives the spores their distinctive colour. The Whi transcription factors control the expression (both directly and indirectly) of genes with roles in chromosome compaction, cell division and spore wall thickening and maturation (discussed below). Once fully mature, spores have increased heat stress tolerance compared to vegetatively growing cells, in addition to being desiccation resistant, and more resistant to other abiotic stresses.

SsgA and SsgB are thought to be responsible for demarcating sites of future cell division within the aerial hyphae, and recruit FtsZ to these sites (Willemse et al., 2011). The resulting Z-rings are stabilized by the dynamin-like proteins DynAB, in association with SepF family proteins (Schlimpert et al., 2017). Z-ring formation is critical for recruiting the other divisome-associated proteins needed for peptidoglycan synthesis to complete cell division. Throughout the septation process, SsgA remains associated with the septa, and this has led to the proposal that SsgA also functions to mark future sites of spore germination (Traag and Wezel, 2008). Additional SALPs (SsgA-like proteins) function in later stages of spore maturation and cell separation (Noens et al., 2005).

Peptidoglycan synthesis during spore maturation is directed by MreB (Mazza et al., 2006). Deleting *mreB* results in misshapen spores with abnormally thin walls (Mazza et al., 2006). As expected, these spores are heat sensitive, suggesting a reduced capacity for survival during exposure to environmental stress (Mazza et al., 2006). Mutations in other genes in the *mre* operon also result in less robust spores that are more sensitive to both heat and osmotic stress (Kleinschnitz *et al.*, 2011). These proteins likely function in association with MreB, as has been shown in other systems (Kruse *et al.*, 2005; Soufo and Graumann, 2006)

Spore maturation requires not only new peptidoglycan synthesis, but also requires the action of several cell wall lytic enzymes. Mutations in the Swl family of enzymes result in general defects in spore maturation, with those spores that do form having thin cell walls and reduced tolerance to heat stress (Haiser et al., 2009). Interestingly, the Rpfs also appear to contribute to cell wall remodeling during entry into dormancy (Haiser et al., 2009; Sexton et al., 2015). Beyond the peptidoglycan, teichoic acid synthesis is also critical for spore formation. Deleting a *tagF* homologue involved in teichoic acid synthesis leads to the production of spores with reduced tolerance to heat and cell wall stress (Kleinschnitz *et al.*, 2011).

1.2.6 Modifications to peptidoglycan structure during dormancy

While many proteins involved in bacterial spore maturation have roles in directing peptidoglycan synthesis or altering peptidoglycan structure, little is known about how this activity relates to spore maturation and dormancy establishment in *Streptomyces*. The pre-spore compartments that are formed following septation end up being substantially modified. The cell wall itself doubles in thickness (Bradley and Ritzi, 1968; Glauert and Hopwood, 1961), and become more resistant to lysozyme treatment, suggesting changes in structure (Grund and Ensign, 1985). As mentioned above, a D,D-carboxypeptidase (SCO4439), is required for spore maturation (Rioseras et al., 2016); however, it is unclear how its activity promotes spore maturation.

The structure of *S. coelicolor* spore peptidoglycan was recently solved (van der Aart et al., 2018), and dramatic changes in the degree of crosslinking are not observed relative to that of vegetative cells. What is different, however, are the types of crosslinks. Compared to actively growing vegetative mycelia, there is an increase in 3-4 tetra,tetrapeptide crosslinks and a decrease in 3-4 tetra, pentapeptide crosslinks (Fig. 1.2). There is also an increase in the relative abundance of peptidoglycan monomers with tetrapeptide stems, which could result from D,D-carboxypeptidase activity. A small proportion of spore muramic acid is deacetylated (van der Aart et al., 2018), suggesting that spores cell walls are primed for rapid modification by cell wall lytic enzymes following resuscitation.

1.2.7 Role of glycopolymers in *Streptomyces* development

Streptomyces produce several types of teichoic acids, including a glycerol 1,3 phosphate and glycerol 2,3 phosphate based lipoteichoic acid (Cot et al., 2011; Rahman et al., 2009), teichulosonic acid (Ostash et al., 2014; Shashkov et al., 2012), and polydiglycosylphosphate polymers (Shashkov et al., 2012). The roles of these glycopolymers in *Streptomyces* growth and development are still poorly defined. Teichulosonic acid is, however, the major glycopolymer in *Streptomyces* (Ostash et al., 2014). As described above, deleting *tagF,* whose product functions to ligate the repeating units of wall teichulosonic acids together, yields poorly dormant spores that are prone to germinate prematurely (Kleinschnitz *et al.*, 2011). Unexpectedly, deleting

ptdA, whose product acts after TagF in transferring teichulosonic acid to *N*-acetylmuramic acid*,* results in severe defects in all stages of *Streptomyces* growth, including hyperbranching during vegetative growth, increased sensitivity to chemical and physical stresses during germination, and heterogeneously sized spores (Sigle et al., 2016). These results collectively demonstrate the importance of glycopolymers to *Streptomyces* growth and development, and suggest they need to be considered as important developmental determinants.

1.3 Regulation of cell wall lytic enzymes

Cell wall lytic enzymes have critical functions at all stages of *Streptomyces* development. Cell growth requires cleavage of the existing peptidoglycan in order to make room for the incorporation of new cell wall material. However, the action of the cell wall lytic enzymes responsible for this remodeling must be strictly controlled, as they have the capacity to be lethal to the cell: too much peptidoglycan cleavage could severely weaken the cell wall, leading to lysis. Much of this control comes at the transcriptional level, ensuring that these enzymes are only produced when they are needed. Post transcriptional and translational regulation (through the activity of small RNAs and riboswitches), or post translational regulation (through protein-protein interactions, protein modification, or proteolysis) have also been described, and are outlined below. One of the best understood control systems is for the Rpfs, which act both during sporulation and germination.

1.3.1 Transcriptional regulation of cell wall lytic enzymes

The sigma factors directing *rpf* gene expression in the actinobacteria remain poorly characterized throughout growth, and likely differ in different systems. In the best-studied *M. tuberculosis* system, the stress response sigma factor SigE directs the transcription of *rpfC* during exponential growth (Manganelli et al., 2001). *rpfC* expression is also controlled by SigD, an alternative sigma factor upregulated in response to starvation (Raman et al., 2004). SigB, regulated by osmotic stress, directs the transcription of *rpfB* (Lee et al., 2004; Sharma et al., 2015)*,* while SigF, which regulates a number of cell wall associated proteins, controls the expression of many *rpfs* during exponential growth (Williams et al., 2007). SigE and SigB both enhance resistance to antibiotic stress and persister cell formation (Pisu et al., 2017), raising the tantalizing possibility that the *rpfs* could be upregulated during this period and used to remodel the cell wall to enhance resistance. During oxidative stress, SigB indirectly downregulates expression of *rpfC* and *rpfE* through an unknown mechanism (Fontán et al., 2009). These mechanisms allow for the remodeling of the cell wall upon encountering conditions that could damage the cell envelope, or stimulate the entrance into molecular quiescence. In *Streptomyces,* some of these mechanisms are conserved. *sigE* and *rpfA* are both upregulated in response to cell envelope stress (Hesketh et al., 2011). Deleting *sigF*, a sporulation specific sigma factor, results in thin spore walls, suggesting defects in spore maturation (Potúcková et al., 1995).

cyclic AMP (cAMP) and the cyclic AMP receptor protein Crp promote resuscitation of quiescent cells throughout the actinobacteria. In *M. smegmatis*, cAMP triggers resuscitation in response to oleic acid (Shleeva et al., 2013). This process depends on RpfA, whose gene expression increases in response to oleic acid and can be activated by Crp (Kahramanoglou et al., 2014; Shleeva et al., 2013). Crp also positively regulates *rpfD* expression in *M. tuberculosis* (Kahramanoglou et al., 2014). GlxR, the *Corynebacterium glutamicum* homologue of Crp, binds upstream of two *rpf* genes and positively regulates the expression of one of these (Jungwirth et al., 2008, 2013); its effect on the other *rpf* gene is unknown. In *S. coelicolor*, deleting *crp* or the cyclic AMP adenylate cyclase *cya* results in an almost complete inhibition of spore germination (Derouaux et al., 2004; Süsstrunk et al., 1998). This may be in part through the Crp control of *rpfA* and *swlC* (Gao et al., 2012; St-Onge et al., 2015).

Other transcription factors contribute to the controlled expression of the *rpf* genes throughout the actinobacteria. MtrA, the response regulator in the MtrAB two component system represses the expression of *rpfB* in *M. tuberculosis* (Sharma et al., 2015), although this does not seem to be conserved in the streptomycetes (Zhang et al., 2017). Many of the other genes regulated by MtrA are involved in the transition to aerial hyphae (Zhang et al., 2017), suggesting that *rpfB* expression is inversely correlated with developmental progression. In *Corynebacterium*, the global transcription factor RamA directly activates *rpf2* expression while another global transcription factor, RamB, directly inhibits it (Jungwirth et al., 2008). While homologues of these transcription factors exist in *S. coelicolor,* it is not known if they regulate *rpf* gene expression.

1.3.2 Post transcriptional regulation of cell wall lytic enzymes

Small RNAs are typically *trans*-acting regulatory factors, where they are encoded at sites distinct from their target genes. They affect the expression of their target genes through a variety of mechanisms, including transcription factor sequestration, altered mRNA stability, or altered mRNA translatability (reviewed in Gottesman and Storz, 2010). Small RNAs were previously identified in *S. coelicolor* using bioinformatic analyses and cloning (such as in (Swiercz et al., 2008)), and more recently using RNA sequencing (Moody et al., 2013; Vockenhuber et al., 2015). A convergently transcribed small RNA is expressed downstream of *rpfA* in *S. coelicolor,* and promotes *rpfA* mRNA stability through a yet-to-be-established mechanism (St-Onge and Elliot, 2017).

In contrast to the *trans*-acting small RNAs, riboswitches are *cis*-acting regulatory elements typically residing in the 5' untranslated region of mRNAs. Riboswitches undergo conformational changes in response to small molecules or ions, and modulate the transcription or translation of the downstream gene. A riboswitch motif known as the *ydaO* riboswitch, is often associated with cell wall lytic enzyme-encoding genes in the actinobacteria (Block et al., 2010; Haiser et al., 2009; Nelson et al., 2013), including *rpfA* in the streptomycetes (Haiser et al., 2009). This riboswitch responds to cyclic di-AMP, and downregulates the transcription of its associated gene (Nelson et al., 2013; St-

Onge and Elliot, 2017; St-Onge et al., 2015). Consequently, there is an inverse correlation between cyclic di-AMP levels and *rpfA* expression: cyclic di-AMP levels decrease throughout the *Streptomyces* life cycle, and this is accompanied by a concomitant increase in expression of *rpfA* during sporulation (St-Onge and Elliot, 2017).

1.3.3 Post-translational regulation of Rpfs

While the bulk of the regulation of cell wall lytic enzymes occurs at the transcriptional/post-transcriptional/translation initiation level, post-translational regulation offers an important layer of control for these highly regulated enzymes. Post-translational regulation can occur through protein modification, protein degradation, and protein-protein interactions. Each of these mechanisms of regulation have been reported for different Rpf enzymes in the actinobacteria, making them an excellent case study for cell wall lytic enzyme regulation. Rpf2 from *C. glutamicum* is glycosylated by Pmt, a protein-O-mannosyltransferase (Hartmann et al., 2004). While the effect of this modification on enzyme activity is unknown, Pmt is conserved throughout the actinobacteria, suggesting that other Rpfs may be modified in a similar manner (Mahne et al., 2006). The activity of Rpf proteins is also regulated through protein-protein interactions. An interaction between RpfB and RipA, an endopeptidase in *M. tuberculosis*, enhances the activity of RpfB (Hett et al., 2007, 2008; Nikitushkin et al., 2015). This interaction is antagonized by the activity of PBP1, potentially serving to balance peptidoglycan synthesis and remodeling (Hett et al., 2010). To date, no other protein partners for the Rpfs have been identified. A RipA homologue does not exist in *Streptomyces*, suggesting that this pattern of post translational regulation is either not conserved or is mediated through diverse protein partners, as there are many endopeptidases encoded by the streptomycetes (Haiser et al., 2009).

In addition to activity modulation of the Rpfs, developmentally-regulated proteolysis of the Rpfs has recently been demonstrated in the streptomycetes (St-Onge et al., 2015). In *S. coelicolor*, proteolysis is stimulated during stationary phase by the production of guanosine tetraphosphate, and indirect evidence suggests that during this time, a secreted metalloprotease acts to promote the turnover of RpfA (St-Onge et al., 2015). A potential candidate protease is SmpA, a metalloprotease that is regulated by guanosine tetraphosphate and is involved in establishing dormancy in *S. coelicolor* (Hesketh et al., 2007; Kim et al., 2013a).

1.4 Bacterial solutions to multicellularity

Dormancy is just one strategy bacteria have adopted to survive stress conditions. Multicellularity is considered to provide a means of better adapting to environmental conditions, like predation or nutrient limitation. Multicellularity simply requires two or more cells becoming associated and communicating with each other (Lyons and Kolter, 2015). The benefits associated with multicellularity include: increased resistance to chemical or physical stressors, improved nutrient harvesting, protection from predators,

enhanced colonization of new environments, and division of labour amongst specialized cell types (Lyons and Kolter, 2015). However, compared with free-living unicellular bacteria, multicellular bacteria have a suite of costs: production costs for adhesion and signaling molecules, physical constraints on movement, and abuse by 'cheaters', or those not producing common goods (Lyons and Kolter, 2015).

There are of course many ways to achieve multicellularity. Filamentous growth, such as seen with the classical *Streptomyces* lifecycle or in cyanobacteria, is one mechanism. This results in branches networks of cells connected through crosswall formation or incomplete cell division. Bacteria can also achieve multicellularity through aggregation. The transition into multicellular growth first requires cells to become associated with each other. This can involve aggregation mediated by extrapolymeric substances, or the formation of tight intercellular junctions (Claessen et al., 2014; Lyons and Kolter, 2015).

1.4.1 Filamentous growth

Filamentous growth involves cross-wall formation or incomplete cell division, leading to chains of cells that share a periplasm or cytoplasm. This is the oldest mechanism for multicellularity, and is the one used by the streptomycetes; however, it first arose in the cyanobacteria 2.5 billion years ago (Schirrmeister et al., 2011; Tomitani et al., 2006). Cells within a cyanobacterial filament undergo differentiation to allow for physical separation of photosynthesis and nitrogen fixation (Rossetti and Bagheri, 2012). Notably, filaments represent a clonal population of cells, and thus the issue of social cheaters is minimized (Rossetti and Bagheri, 2012).

Filamentous growth by the *Streptomyces* involves occasional cross-wall formation in the multi-nucleate vegetative hyphae. Pores have been observed in these cross-walls, and these are presumed to allow the cytoplasm of conjoined cells to flow freely (Celler et al., 2016; Jakimowicz and Van Wezel, 2012). *Streptomyces* also feature patterned multicellularity, where aerial hyphae grow out of the vegetative hyphae and differentiate into spores. The signals controlling this process are described above. *Streptomyces* have recently been shown to employ a second mode of filamentous growth known as 'exploratory growth', which is initiated under high pH and nitrogen conditions, and low glucose conditions (Jones et al., 2017). This type of growth is most consistent with passive, growth- and surfactant-driven sliding motility at the leading edge of the exploring colony (Jones et al., 2017). Exploratory growth appears to involve the growth of non-branching vegetative-like hyphae; however, it also appears to involve unusual cellular aggregation that is not seen in classically growing *Streptomyces* cultures.

1.4.2 Aggregation: temporary multicellularity

Aggregation is a temporary strategy used by bacteria to achieve multicellularity. These cells often are able to grow as free-living cells, in addition to having the potential for forming multicellular units. Aggregations can be unpatterned, like a group of motile swarmer cells or a biofilm, or have distinct patterns, like those occurring in fruiting

bodies. Biofilms and swarms are associated with cell differentiation and specialization, and their formation is tightly regulated (Vlamakis et al., 2013). Biofilm and swarmer formation has been extensively studied, due to their importance in infectious diseases and because these lifestyles are thought to be the way most bacteria exist in their natural environments. Cells in these aggregates are held in association with each other using complex extracellular matrices composed of polysaccharides, proteins and extracellular DNA. Biofilm formation has been linked to increased resistance to a variety of chemical and environmental stressors, including organic acids, antibiotics, and predation (Claessen et al., 2014).

1.5 Aims and outline of thesis

When I began my thesis, little was understood about *Streptomyces* spore germination. At this point, our group had established that several cell wall lytic enzymes were important (SwlA and RpfA), but little else was known about the molecular requirements for germination. To address this knowledge gap, we identified genes encoding proteins belonging to the Rpf family using a bioinformatic screen. We then deleted these genes and looked for defects at all stages of growth, examined the expression profile of these genes throughout development, and tested for interactions between Rpf proteins using a yeast two-hybrid system. The results of this work were published in 2015 (Sexton et al., 2015), and are presented in Chapter 2 of this thesis. Chapter 3 represents further work done to characterize the mechanism by which Rpf proteins promote the resuscitation of dormant streptomycetes. This work was done in collaboration with Dr. Anthony Clarke's lab at the University of Guelph. We used *in vitro* peptidoglycan cleavage assays and liquid chromatography coupled with mass spectrometry to determine that the Rpf domain had lytic transglycosylase activity. Using phenotypic assays, we determined that the Rpf proteins function to make room for new growth at the last stage of *S. coelicolor* spore germination. This work was submitted to the *Journal of Biological Chemistry* in 2017 and resubmission following revision is pending.

Chapter 4 of this thesis focuses on work that was initiated at the John Innes Centre in the summer of 2017. Using cryogenic scanning electron microscopy, we noted that *Streptomyces* explorer cells were encased in what appeared to be an extracytoplasmic substance. We set out to determine whether the composition of this matrix was similar to biofilm matrices produced by other bacteria and fungi. Using genetics, and diagnostic dyes, together with confocal laser scanning microscopy, we are mapping the contents of the matrix, and propose that explorer cells form a biofilm. This work has not yet been published.

Chapter 2

Resuscitation-promoting factors are cell wall lytic enzymes with important roles in the development of *Streptomyces coelicolor*

Danielle L. Sexton, Renée J. St-Onge, Henry J. Haiser, Mary R. Yousef, Lauren Brady, Chan Gao, Jacqueline Leonard, and Marie A. Elliot

The work that follows in this chapter appears as it was published in the *Journal of Bacteriology*, on pages 848-860 of volume 197, issue 5, 2015 and is reprinted with permission. doi:10.1128/JB.02464-14.

Contributions:

With few exceptions, (below), I conducted all experiments and data analysis. I prepared all figures and tables and assisted with manuscript writing. Dr. Renée J. St-Onge (former Ph.D. candidate, Elliot Lab) assisted with sample preparation for germination assays, isolated RNA, and designed and performed RT-qPCR experiments. Dr. Henry J. Haiser (former Ph.D. candidate, Elliot Lab), Dr. Mary R. Yousef (former postdoctoral fellow, Elliot Lab), Dr. Chan Gao (former Ph.D. candidate, Elliot Lab), Lauren Brady (former undergraduate thesis student, Elliot Lab), and Jacqueline Leonard (former undergraduate thesis student, Elliot Lab) generated mutant strains. Marcia Reid (Electron Microscopy Facility, McMaster University) prepared samples for scanning and transmission electron microscopy. Tamiza Nanji (former M.Sc. candidate, Guarné Lab) and Dr. Alba Guarné (Biochemistry and Biomedical Sciences, McMaster University) assisted with running the FPLC to check for RpfB dimerization. All authors contributed, to varying degrees, to experimental design, data interpretation, and manuscript editing.

2.1 ABSTRACT

Dormancy is a common strategy adopted by bacterial cells as a means of surviving adverse environmental conditions. For *Streptomyces* bacteria, this involves developing chains of dormant exospores that extend away from the colony surface. Both spore formation and subsequent spore germination are tightly controlled processes, and while significant progress has been made in understanding the underlying regulatory and enzymatic bases for these, there are still significant gaps in our understanding. One class of proteins with a potential role in spore-associated processes is the so-called resuscitation-promoting factors or Rpfs, which in other actinobacteria are needed to restore active growth to dormant cell populations. The model species *Streptomyces coelicolor* encodes five Rpf proteins (RpfA-E), and here we show these proteins have distinct, but overlapping functions during development. Collectively, the *S. coelicolor* Rpfs are essential for normal spore maturation, and have an important role in promoting spore germination. Previous studies have revealed structural similarities between the Rpf domain and lysozyme, and our *in vitro* biochemical assays revealed varying levels of peptidoglycan cleavage capabilities for each of these five *Streptomyces* enzymes. Peptidoglycan remodeling by enzymes such as these must be stringently governed so as to retain the structural integrity of the cell wall. Our results suggest that one of the Rpfs, RpfB, is subject to a unique mode of auto-regulation, mediated by a domain of previously unknown function (DUF348) located within the N-terminus of the protein; removal of this domain led to significantly enhanced peptidoglycan cleavage.

2.2 INTRODUCTION

Streptomyces species are Gram- positive bacteria that abound in soil environments. They are renowned for their secondary metabolic capabilities; they produce a multitude of compounds that have found utility in both medicine and agriculture, including a vast array of antibiotics, chemotherapeutics, immunosuppressants, and antiparasitic agents (Hopwood, 2007). They are also well known for their complex, multicellular developmental cycle (Flärdh and Buttner, 2009). The *Streptomyces* life cycle can be broadly divided into two stages: vegetative growth and reproductive development. Unlike most bacteria, *Streptomyces* organisms are filamentous, and during the vegetative phase of their life cycle, they grow by hyphal tip extension and branching, ultimately forming an interwoven network of cells known as the vegetative mycelium (Flärdh et al., 2012). Under certain as yet poorly defined stress conditions, vegetative growth ceases, and reproductive growth ensues. Here, unbranched filamentous cells termed aerial hyphae, grow away from the vegetative mycelium and extend into the air. These cells then undergo a synchronous round of chromosome segregation, cell division, and cell wall modification to yield chains of dormant exospores (Elliot and Flardh, 2012). These spores are resistant to a wide variety of environmental insults and can be widely dispersed.

A dormant cell state is not unique to the streptomycetes, and indeed many well-studied bacteria (e.g., *Bacillus*, *Clostridium*, and *Myxococcus*) have adopted sporulation as a means of surviving adverse environmental conditions (Rittershaus et al., 2013). Other bacteria have evolved less extreme dormant states and instead adopt cell states with low metabolic activity such that these cells are better able to tolerate stresses such as antibiotic exposure or immune system assault (Kim et al., 2013b). In addition to low metabolic activity, dormant cells of all types often have a cell wall architecture that differs from that of their vegetative counterparts. For example, *Bacillus* spores possess thick cell walls comprising peptidoglycan with altered cross-linking compared with that of vegetative cells (Meador-parton and Popham, 2000). Similarly, latent or dormant *Mycobacterium tuberculosis* cells display a different cell wall structure relative to that of actively growing cells (Seiler et al., 2003).

While a thick wall constitutes an effective protective barrier, it can also be refractory to cell growth. Consequently, cell wall remodeling must be integral to restoring dormant cells to an active growth state. In the actinobacteria, a group that includes both the mycobacteria and the streptomycetes, a protein family dubbed the resuscitation-promoting factors (Rpfs) has been implicated in the cleavage of dormant cell walls and subsequent promotion of growth and metabolic reactivation (Keep et al., 2006a). The first Rpf protein was identified in *Micrococcus luteus*, an actinobacterium that forms dormant cells following prolonged starvation. In an elegant set of experiments, Mukamolova and colleagues found that picomolar concentrations of this secreted protein were sufficient to convert dormant *Micrococcus* cells into actively growing cells (Mukamolova et al., 1998, 2002a). Intriguingly, the Rpf protein in *M. luteus* is essential for viability (Mukamolova et al., 2002a), suggesting that its function may extend beyond dormant cell resuscitation. Subsequent studies have focused on the Rpf proteins in *Mycobacterium*; *M. tuberculosis* encodes five Rpf (Rpf_{MTB}) proteins (Mukamolova et al., 2002b). These proteins share some functional redundancy (Tufariello et al., 2004), and while it is possible to delete all five *rpf* genes without affecting viability, the corresponding mutant is unable to exit dormancy and is further compromised in its ability to initiate/establish infections in mouse models (Kana et al., 2008; Russell-Goldman et al., 2008; Tufariello et al., 2006). Several Rpfs in the mycobacteria appear to act as part of a larger peptidoglycan cleavage complex, associating with RipA, an essential enzyme with endopeptidase activity (Hett et al., 2007, 2008).

The mechanistic basis underlying Rpf-mediated emergence from dormancy has not been fully elucidated. An important step toward understanding Rpf activity came with the solution structure of the Rpf domain from RpfB of *M. tuberculosis*, which revealed a protein fold with similarity to both lysozyme and lytic transglycosylases (Cohen-Gonsaud et al., 2005). These results suggested that proteins with an Rpf domain may cleave within the polysaccharide backbone of the peptidoglycan. Given this predicted activity, two—not mutually exclusive— hypotheses have been put forward to explain how Rpf proteins could promote exit from dormancy: (i) Rpf activity relieves the physical

constraints imposed by the altered cell wall structure that had otherwise inhibited growth of the dormant cell; (ii) Rpf activity serves as a signal (or generates a signal) that is, in turn, sensed by the cell, and this signal stimulates the resumption of growth (Keep et al., 2006a).

Like *M. tuberculosis*, the best-studied streptomycete, *Streptomyces coelicolor*, encodes five Rpf (Rpf_{SC}) proteins (Ravagnani et al., 2005). Generally speaking, these proteins are not orthologous to the *M. tuberculosis* proteins, with only one of the five (RpfB) sharing a similar domain organization. Here, we probe the role of these proteins in the growth and development of *S. coelicolor*, compare their peptidoglycan cleavage capabilities and interaction potential, and uncover an intriguing modulatory role for a domain of unknown function associated with RpfB.

2.3 MATERIALS AND METHODS

2.3.1 Bacterial strains and culture conditions

Bacterial strains used or created in this work are detailed in Table 2.1. *Streptomyces coelicolor* A3(2) strain M145 and its derivatives were grown at 30˚C on R5, mannitol soya flour (MS), Difco nutrient agar (DNA) or Lysogeny Broth (LB) agar medium supplemented with antibiotics to maintain selection where appropriate, or in new minimal medium supplemented with phosphate (NMMP) or a 50:50 mixture of tryptone soy broth (TSB)-yeast extract-malt extract (YEME) liquid media as described by Kieser *et al.* (Kieser et al., 2000) . All *Escherichia coli* strains were grown at 37˚C on LB or DNA agar plates, or in LB or super optimal broth (SOB) liquid medium, supplemented with antibiotics where appropriate, with the exception of BW25113, which was grown at 30˚C. All *Saccharomyces cerevisiae* strains were grown at 30˚C in yeast peptone dextrose adenine (YPDA) liquid medium or on YPDA or synthetic defined (SD) amino acid drop out agar plates to maintain selection where appropriate.

Table 2.1: Plasmids and *Streptomyces coelicolor, Escherichia coli* and *Saccharomyces cerevisiae* strains

Strain	Genotype , characteristics and/or use	Reference or Source
***Streptomyces coelicolor* A3(2)**		
M145	$SCP1^-$, $SCP2^-$	(Kieser et al., 2000)
E104a (Δ*rpfA*)	M145 Δ*SCO3097*	(Haiser et al., 2009)
E110 (Δ*rpfC*)	M145 *SCO3098::aac(3)IV*	This study
E111 (*ΔrpfB*)	M145 *SCO3150*::*vph*	This study
E112 (*ΔrpfD*)	M145 *SCO0974*::TOPO 2.1	This study
E113 (*ΔrpfE*)	M145 *SCO7458*::*aac(3)IV*	This study
E114 (Δ*rpfAB*)	M145 *SCO3097-3098::aac(3)IV*	This study

E114a	M145 Δ*SCO3097-3098*	This study
E115 (*ΔrpfA, rpfB, rpfC*) (3× mutant)	M145 Δ*SCO3097-3098 SCO3150*::*vph*	This study
E116 (*ΔrpfA, rpfB, rpfC, rpfE*) (4× mutant)	M145 Δ*SCO3097-3098 SCO3150*::*vph ΔSCO7458*	This study
E117 (*ΔrpfA, rpfB, rpfC, rpfD, rpfE*) (5× mutant)	M145 Δ*SCO3097-3098 SCO3150*::*vph ΔSCO7458 SCO0974::*TOPO 2.1	This study
***Escherichia coli* strains**		
DH5α	Used for routine cloning	
ET12567(pUZ8002)	*dam dcm*; with transmobilizing plasmid pUZ8002	(MacNeil et al., 1992; Paget et al., 1999)
Rosetta 2(DE3)	Protein overexpression	Novagen
BW25113	Construction of cosmid-based knockouts	(Datsenko and Wanner, 2000)
BT340	DH5α-carrying pCP20, used for FLP-recombinase-mediated removal of disruption cassettes	(Datsenko and Wanner, 2000)
***Saccharomyces cerevisiae* strains**		
Y2H Gold	*MATa, trp1-901, leu2-3, 112, ura3-52, his3-200, gal4Δ, gal80Δ, LYS2 : : $GAL1_{UAS}$–$Gal1_{TATA}$–His3, $GAL2_{UAS}$–$Gal2_{TATA}$–Ade2 URA3 : : $MEL1_{UAS}$–$Mel1_{TATA}$ AUR1-C MEL1*	Clontech
Y187	*MATα, ura3-52, his3-200, ade2-101, trp1-901, leu2-3, 112, gal4Δ, gal80Δ, met–, URA3 : : $GAL1_{UAS}$–$Gal1_{TATA}$–LacZ, MEL1*	Clontech
Plasmids		
StE41	Cosmid used for knockout of *rpfA* and *rpfB*	(Redenbach et al., 1996)
StE87	Cosmid used for knockout of *rpfC*	(Redenbach et al., 1996)
St5C11	Cosmid used for knockout of *rpfE*	(Redenbach et al., 1996)
pIJ82	pSET152 derivative, *hyg* replacing	Gift from H.

	aac(3)IV	Kieser
pMC175	pIJ82 + r*pfD*	This work
pMC176	pIJ82 + *rpfE*	This work
pET15b	Overexpression of His_6-tagged proteins	Novagen
pMC177	pET15b + *rpfA*	(Haiser et al., 2009)
pMC178	pET15b + *rpfB*	This work
pMC179	pET15b + *rpfBΔDUF348*	This work
pMC180	pET15b + *rpfC*	This work
pMC181	pET15b + *rpfD*	This work
pMC182	pET15b + *rpfE*	This work
pGAD T7 AD	Used to generate transcriptional fusions to the GAL4 transcriptional activation domain	Clontech
pMC183	pGAD + *rpfA*	This work
pMC184	pGAD + *rpfB*	This work
pMC185	pGAD + *rpfBΔDUF348*	This work
pMC186	pGAD + *rpfC*	This work
pMC187	pGAD + *rpfD*	This work
pMC188	pGAD + *rpfE*	This work
pGBK T7 BD	Used to generate transcriptional fusions to the GAL4 DNA binding domain	Clontech
pMC189	pGBK + *rpfA*	This work
pMC190	pGBK + *rpfB*	This work
pMC191	pGBK + *rpfBΔDUF348*	This work
pMC192	pGBK + *rpfC*	This work
pMC193	pGBK + *rpfD*	This work
pMC194	pGBK + *rpfE*	This work
pFLUX	Integrative transcriptional reporter vector; *ori* (pUC18) *oriT* (RK2) *int* ΦBT1 *attP* ΦBT1 *luxCDABE* (promoterless) *aac(3)IV*	(Craney et al., 2007)
pFLUX-Pos	pFLUX carrying the *ermE** promoter	This work
pMC195	pFLUX carrying the *rpfA* promoter	This work
pMC196	pFLUX carrying the *rpfB* promoter (upstream of *SCO3152*)	This work
pMC197	pFLUX carrying the *rpfC* promoter	This work
pMC198	pFLUX carrying the *rpfD* promoter	This work
pMC199	pFLUX carrying the *rpfE* promoter	This work

2.3.2 Total RNA isolation

S. coelicolor M145 was grown at 30°C on MS agar plates overlaid with cellophane discs. At different developmental stages (vegetative growth, aerial development, and early and late sporulation), biomass was harvested using a sterile spatula. M145 was also grown at 30°C in TSB-YEME, and cells were recovered from culture aliquots by centrifugation. Samples were frozen at -80°C for 3-6 days. Total RNA was extracted by mechanical disruption, and co-extracted DNA was digested using TURBO DNase (Ambion), as previously described by Moody *et al*. (Moody et al., 2013). Total RNA was quantified using a NanoDrop ND-1000 and RNA integrity was confirmed by size-fractionating 2 µg of total RNA on an agarose gel. RNA extract purity was verified by measuring the A_{260}/A_{280} and A_{260}/A_{230} ratios; these ranged from 1.88-2.03, and 2.18-2.38, respectively.

2.3.3 Primer design for RT-qPCR analyses

The predicted *rpfA* (*SCO3097*), *rpfB* (*SCO3150*)*, rpfC* (*SCO3098*), *rpfD* (*SCO0974*) and *rpfE* (*SCO7458*) coding sequences were retrieved from the *Streptomyces* annotation server StrepDB (http://strepdb.streptomyces.org.uk/). Gene-specific PCR primers, generating products of 50-150 nt, were designed using Primer-BLAST (http://www.ncbi.nlm.nih.gov/tools/primer-blast/) (Table 2.2). Standard-desalted primers were purchased from Integrated DNA Technologies.

The specificity of each primer pair to its intended target was tested *in silico* by searching the *S. coelicolor* genome for potential product-generating annealing sites. Generation of a single amplicon was confirmed by PCR. Briefly, 20 µL reactions contained 1× *Taq* reaction buffer, 200 µM each dNTP, 5%$_{v/v}$ dimethylsulfoxide, 300 nM each primer (Table 2.2), 0.125 U/µL *Taq* DNA polymerase and 1 ng/µL *S. coelicolor* M145 genomic DNA. Nuclease-free water was used as template for the negative control reactions. The following amplification conditions were used: initial denaturation at 95°C for 3 min; 35 amplification cycles [consisting of denaturation at 95°C for 30 sec; annealing for 30 sec (temperatures were optimized for each primer pair; Table 2.2), and extension at 72°C for 45 sec]; followed by a final extension step at 72°C for 5 min.

Table 2.2: RT-qPCR primers and reaction conditions.

Gene	Primers [a]	Sequence (5′ → 3′)	Product location [b]	Product length (bp)	Annealing temperature (°C)	PCR efficiency [c]
rpfA	rpfAF rpfAR	GAGTCCGGCGGCAACTGGTC GCTGGGACTTGCTCGCCTGG	+160 to +292	133	61	1.020 ± 0.023
rpfB	SCO3098F SCO3098R	AGTACGGCGGTCTGGACTA CTTATCTGCTGGGAGCGACT	+236 to +296	61	57	1.057 ± 0.029

rpfC	SCO3150F SCO3150R	GGCTCTACCAGTTCGACTCC TGCGCACGTAGAGCTTCTG	+1220 to +1330	111	60	N/A
rpfD	SCO0974F SCO0974R	GTTCGTACGGCTACCAGGTG GTCCGCTCTTCACGGAGAT	+1079 to +1168	90	60	1.054 ± 0.038
rpfE	SCO7458F SCO7458R	ACCGGCAACGGCTACTAC CATCCCCTGCAGACGGG	+199 to +345	147	66	N/A

[a] Forward and reverse primers are denoted with letters F and R, respectively.
[b] Nucleotide sites are numbered relative to the start codon.
[c] Values are presented as mean ± standard deviation.

2.3.4 Reverse transcription (RT) and real-time PCR

rpfA, *rpfB*, *rpfC*, *rpfD* and *rpfE* transcripts were reverse transcribed using SuperScript III reverse transcriptase (Invitrogen). An initial reaction containing 167 ng/µL total RNA, 167 nM each reverse primer (Table 2.2) and 833 µM each dNTP (Fermentas or Invitrogen) was heated at 95°C for 5 min and immediately cooled on ice. Each reaction was then supplemented with a second solution containing 2.5× First-Strand Buffer (Invitrogen), 12.5 mM dithiothreitol, 5 U/µL RNaseOUT (Invitrogen) and 25 U/µL SuperScript III reverse transcriptase (Invitrogen). Transcripts were reverse transcribed at 55°C for 60 min, prior to heat-inactivating the enzymes at 70°C for 15 min. To verify the absence of undigested genomic DNA, "no RT" controls were conducted as described above, only omitting RNaseOUT and SuperScript III reverse transcriptase. The resulting cDNA samples were stored at -20°C for no more than 5 days.

cDNAs were quantified using real-time PCR. Triplicate 20 or 25 µL singleplex reactions were carried out in 1× PerfeCTa SYBR Green SuperMix (Quanta Biosciences), together with 300 nM of each gene-specific primer (Table 2.2) and 8 ng/µL reversely transcribed total RNA. "No template" negative controls, in which cDNA was replaced with an equal volume of nuclease-free water, were included in each PCR run. Reactions were performed in clear 96-well PCR plates (Bio-Rad) with a CFX96 Touch Real-Time PCR Detection System (Bio-Rad) using the following conditions: initial denaturation at 95°C for 3 min, followed by 50 amplification cycles consisting of denaturation at 95°C for 15 sec and annealing/extension at a primer-specific temperature (Table 2.2) for 45 sec. Fluorescence was measured during each extension step. A melt curve analysis (65-95°C with 5 sec fluorescence reads every 0.5°C increase) was also conducted immediately following product amplification.

Fluorescence data were baseline-corrected using the CFX Manager software v2.1 (Bio-Rad). Transcript levels were then calculated using the DART-PCR 1.0 workbook (Peirson,

2003). Starting fluorescence values (R_0), which are proportional to initial template quantities, were calculated for each sample using the average midpoint and amplification efficiency for a given primer pair, as described by Peirson *et al*. (Peirson, 2003). Expression levels of each gene were normalized to total RNA mass and PCR product length.

2.3.5 Luciferase assays

To monitor *rpf* expression during germination, the promoter regions for each *rpf* gene were cloned into the BamHI and KpnI sites of pFLUX (Table 2.1; see also Table 2.3 and Fig. 2.1), and these constructs, together with pFLUX alone (negative control) and pFLUX plus the *ermE** promoter (positive control, where *ermE** is a constitutive, highly active promoter) (Table 2.1), were conjugated into wild type *S. coelicolor* M145. Equal numbers of spores were inoculated into 150 µl of TSB-YEME liquid medium in white 96-well plates (Thermo-Fisher). Plates were then incubated at 30°C with shaking, and luminescence was measured (integration time of 4,000 ms) every 10 min for 12 h using a Tecan Ultra Evolution plate reader. Luminescence levels of the negative control were subtracted from those of the *rpf* fusions and positive control. Eight biological replicates were prepared, and experiments were conducted at least twice.

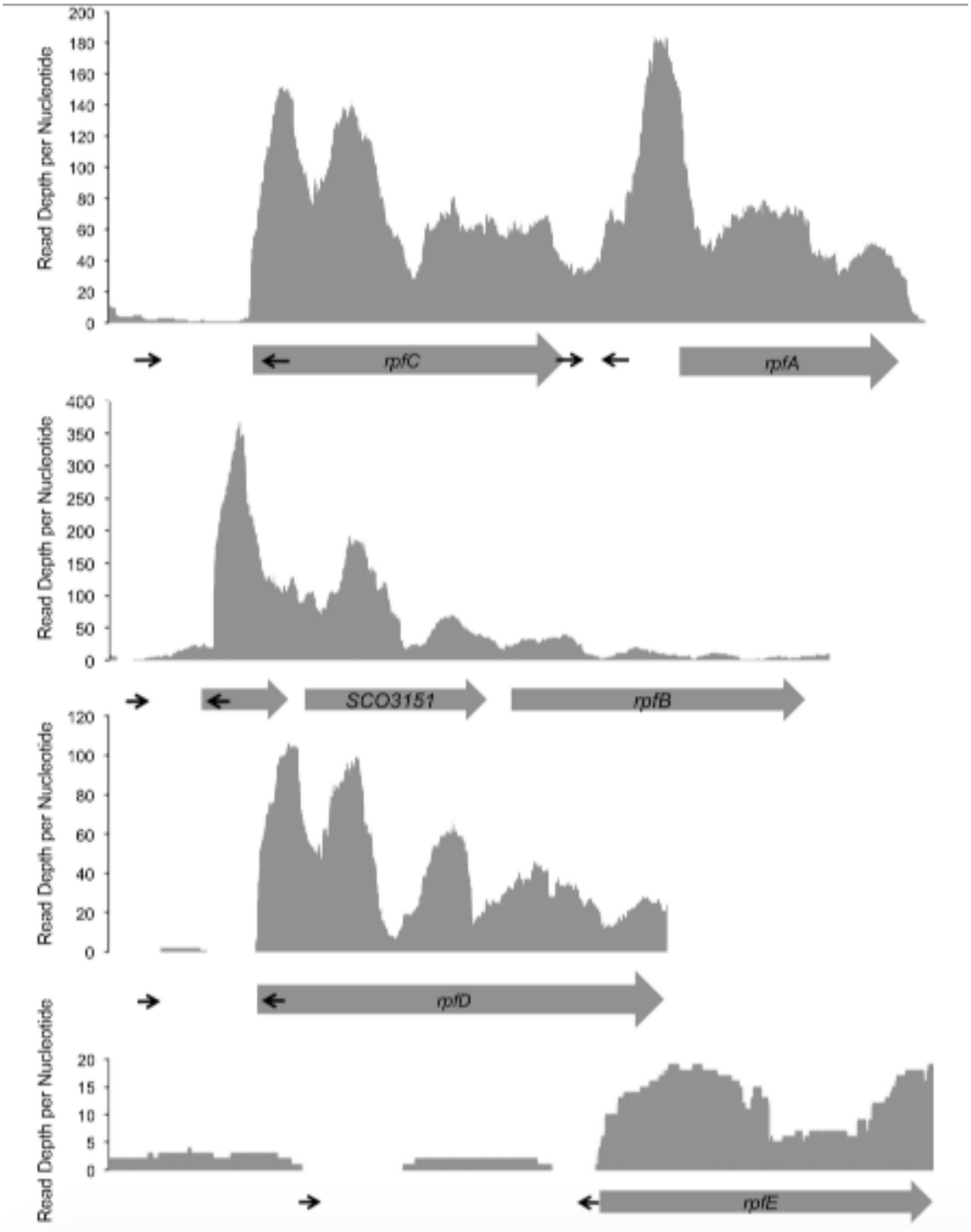

Figure 2.1: Primer locations for luciferase assays. Primers for luciferase assays were positioned to amplify the promoter region for each *rpf* gene, based on previously published RNA sequencing data (Moody et al., 2013). Graphs show the number of reads at each nucleotide for both the protein-coding sequence and region upstream of each *rpf*. Protein coding sequences are indicated with grey arrows. Primer locations are indicated with black arrows.

2.3.6 *rpf* mutant strain construction

Single null mutations were made in *rpfB, rpfC,* and *rpfE* using ReDirect technology (Gust et al., 2003); the *rpfA* mutation had been created previously (Haiser et al., 2009). *rpfB* was replaced with a viomycin resistance (*vph*) cassette on cosmid StE87, whereas *rpfC* and *rpfE* were each replaced with apramycin resistance [*aac(3)IV*] cassettes on cosmids StE41 and St5C11, respectively (see Table 2.1 for plasmid and strain information, and Table 2.3 for primer information). For mutation of *rpfD,* the typical ReDirect gene replacement protocol was unsuccessful due to spurious cosmid recombination, and instead *rpfD* was disrupted in the chromosome. A 700 bp region encompassing the Rpf domain of *rpfD* was amplified and cloned into the TOPO vector (Invitrogen). The kanamycin resistance gene on the TOPO vector backbone was then replaced with an *aac(3)IV-oriT*-containing DNA fragment using the ReDirect protocol (Gust et al., 2003).

Mutant cosmids/disruption plasmids were introduced into the non-methylating *E. coli* strain ET12567/pUZ8002 prior to conjugation into *S. coelicolor* M145. Resulting exconjugants were subsequently screened for double cross over recombinants (or in the case of the *rpfD* disruption, selected for single crossover recombinants). Correct replacement of each *rpf* gene with the appropriate antibiotic resistance cassette or for *rpfD,* disruption of the coding sequence was confirmed using diagnostic PCRs with mutant chromosomal DNA as template, alongside wild type chromosomal DNA and mutant cosmids (where appropriate) as negative and positive controls, respectively. These reactions were conducted to confirm that the cosmids/plasmids had recombined at the appropriate positions in the chromosome, and that the wild type gene was no longer present or intact (see Table 2.3 for primer combinations).

To create markerless mutants and to permit recycling of the *aac(3)IV* resistance marker when creating multiple mutations, the apramycin resistance cassette was removed from the *rpfA, rpfC* double mutant cosmid, and from the *rpfE* single mutant cosmid using the temperature sensitive FLP recombination plasmid in *E. coli* DH5α (strain BT340) (Table 2.1). Cosmids were introduced into these cells and grown non-selectively at 42˚C to stimulate expression of the FLP recombinase. To identify colonies carrying cosmids in which the antibiotic resistance marker had been excised by FLP recombinase, colonies were tested for kanamycin resistance and apramycin sensitivity. Diagnostic PCR using primers specific for regions upstream and downstream of the Rpf coding sequences (Table 2.3) was used to confirm appropriate removal of the apramycin cassette from the cosmid. These cosmids were then re-introduced into their corresponding marker-containing *S. coelicolor* mutant strain by protoplast transformation. The resulting transformants were screened for double cross-over recombination and loss of the apramycin resistance marker in the chromosome; this was further confirmed by PCR.

To create a multiple *rpf* mutant strain, we used the approach detailed in the schematic diagram in Figure 2.2 The double *rpfA, rpfC* mutant was created by replacing both genes (which are adjacent on the *S. coelicolor* chromosome) with the *aac(3)IV* resistance gene

on cosmid StE41. This resistance gene was then removed, and the *rpfB::vph* mutant cosmid was next introduced, followed by screening and confirmation of the *rpfB* mutation as described above. Next, the *rpfE::aac(3)IV* mutant cosmid was introduced, and the *rpfE* mutation was confirmed, before the apramycin resistance cassette was removed from *rpfE* as outlined previously. Finally, the *rpfD* disruption construct was introduced into the 4× *rpf* mutant strain, selected for integration into *rpfD* in the chromosome and confirmed by PCR.

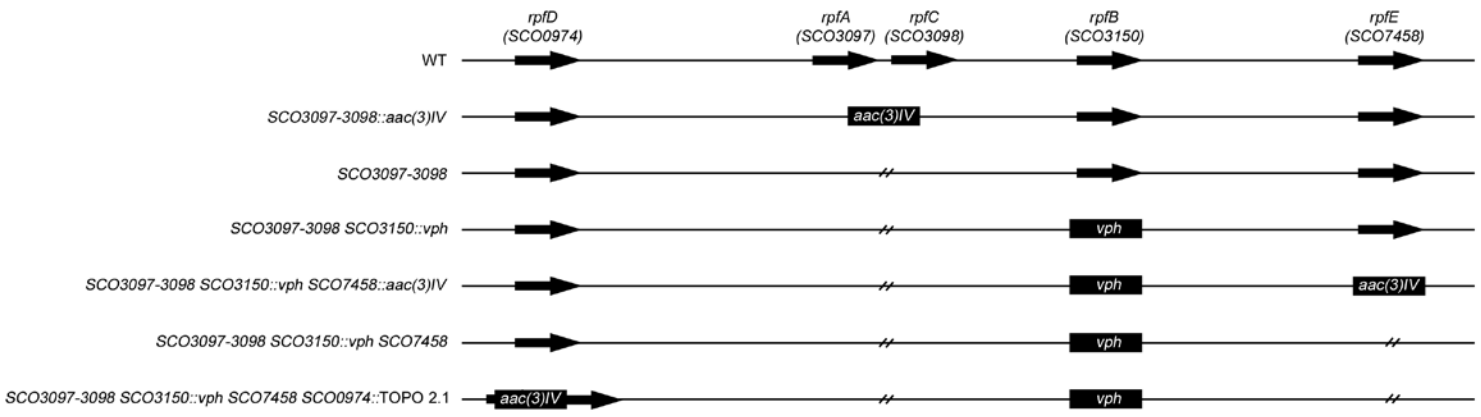

Figure 2.2: Construction of multiple *rpf* mutants. *rpf* genes were replaced with antibiotic resistance cassettes in the order shown. Double diagonal lines represent 'scar' sequences left after removal of the antibiotic resistance cassettes. Abbreviations:: *aac(3)IV*, apramycin resistance cassette; *vph*, viomycin resistance cassette.

Table 2.3: Oligonucleotides used in this study

Primer name	Sequence (5' – 3')	Function
SCO0974 F	GGCACCGCCGGTATCAGCCGAACA	Disruption of *rpfD*
SCO0974 R2	GCTGCTGCTCGTCCTGCCGTCTTCC	Disruption of *rpfD*
SCO0974 up	AGTGCTCATTGGGTTGGCTC	*rpfD* complementation and disruption confirmation
SCO0974 down	CAGGTGATACCGGCGAGTG	*rpfD* complementation and disruption confirmation
SCO3097FWD	CAGCTCACCTCGCAGGCGTCGGTGAGGGGATCAA CCATGATTCCGGGGATCCGTCGACC	*rpfA* knockout
SCO3097REV	CACGCACCGGGGCGGGAGTCACGGGACCGCCGCC GCTTATGTAGGCTGGAGCTGCTTC	*rpfA* and *rpfA/C* knockout
SCO3098FWD	CCGCGTGGTCCCCGTCGTCTTGTGAAAGGTCGTC GCATGATTCCGGGGATCCGTCGACC	*rpfC* and *rpfA/C* knockout
SCO3098REV	GGGACATACGGTCTCTAACCGTGACGCGAACTCC CTCTATGTAGGCTGGAGCTGCTTC	*rpfC* knockout
SCO3098 up	CGTGATCTGCGCGGCATGAAC	*rpfC* knockout confirmation
SCO3098 int	GCAGGCCGCCGTAGTACC	*rpfC* knockout confirmation
SCO3150FWD	CTGGGGGCCCGATCGGGACCCCTGGAGCGTGTGG GCGTGATTCCGGGGATCCGTCGACC	*rpfB* knockout
SCO3150REV	GCTCACCCCGCAAGAGTAGCCGGGGGCCGGGCGG CCTCATGTAGGCTGGAGCTGCTTC	*rpfB* knockout
3150 up	TTCAAGAACGCCCAGAACCTG	*rpfB* knockout confirmation
3150 down	ACCGTGTTGGCGTCGATGAC	*rpfB* knockout confirmation
3150 internal	AGCAGTTCACTCACGTCGTC	*rpfB* knockout confirmation
SCO7458FWD	GGGCGACCGGTGGTCACCTGGTGTAACAGTCTTC TTATGATTCCGGGGATCCGTCGACC	*rpfE* knockout
SCO7458REV	GTCAACCCGGCGCGGCCGGGGCCCGGTTTGGCAC CGTCATGTAGGCTGGAGCTGCTTC	*rpfE* knockout
7458 up	ACAAGGAGGCGGTCCACG	*rpfE* complementation and knockout confirmation
7458 down	GTTGGTCGGCCTACTCGG	*rpfE* complementation and knockout confirmation
7458 internal	CGACATCCCCTGCAGACG	*rpfE* knockout confirmation
SCO0974PP 5'	CAGTACCATATGGCCGACGCGCGACCTGGGAC	Overexpression of RpfD
SCO0974PP 3'	CAGTACGGATCCTCAGATCCTGACGCCGCCGGC	Overexpression of RpfD
SCO3097PP 5'	CAGTACCATATGGCCACCGCGTCCGAGTGGGAC	Overexpression of RpfA
SCO3097PP 3'	CGAAGTGGATCCTTACTTCAGGTGCAGCTGCTG	Overexpression of RpfA
SCO3098PP 5'	CAGTACCATATGGCCGACTCCACGAACTGGGAC	Overexpression of RpfC
SCO3098PP 3'	CAGTACGGATCCCTACTTTTCGCCCGATTCGCC	Overexpression of RpfC

SCO3150ΔDUFPP5'	CAGTACCATATGGCGACCGGCTTCCCGC	Overexpression of RpfBΔDUF348
SCO3150PP 5'	CAGTACCATATGGCCAAGGACAAGGCGGTCGAG	Overexpression of RpfB
SCO3150PP 3'	CAGTACGGATCCTCATTCCCGCAGCCGGGCGCC	Overexpression of RpfB
SCO7458PP 5'	CGAAGTCATATGGCGCCCTCGGCGCC	Overexpression of RpfE
SCO7458PP 3'	CGAAGTGGATCCTCAGGCGCAGCCCC	Overexpression of RpfE
SCO3096R-B	GCACTGGATCCCCTCGGGAGTCCAGGATTT	Cloning *rpfA* promoter
SCR3097R-K	GCACTGGTACCGGGACTTTTCATGTTCCGC	Cloning *rpfA* promoter
SCO3152 pFlux Fwd	TGATGAGGATCCTCTGAGGGGATCCATAGGGC	Cloning *SCO3152* promoter
SCO3152 pFlux Rev	TGATGAGGTACCTCCTTGGTTCGTTCTGCTCC	Cloning *SCO3152* promoter
SCO3098 pFlux Fwd	TGATGAGGATCCGCATCCACTACTGCCTCGG	Cloning *rpfC* promoter
SCO3098 pFlux Rev	TGATGAGGTACCAGGGAGATCATCGCTTGTCA	Cloning *rpfC* promoter
rpfD pFlux Fwd	TGATGAGGATCCCCTAGTGACCTTGGTGTCCG	Cloning *rpfD* promoter
rpfD pFlux Rev	AAGAAGGGTACCCACCAGGTGACCGTCAGGAG	Cloning *rpfD* promoter
rpfE pFlux Fwd	TGATGAGGATCCCCGTGTCCATCGTCTCCAC	Cloning *rpfE* promoter
rpfE pFlux Rev	TGATGAGGTACCAAGAAGACTGTTACAGGTGAC	Cloning *rpfE* promoter
ermEF-B	GCACTGGATCCAGCCCGACCCGAGCACGCGC	Cloning *ermE** promoter
ermER-K	GCACTGGTACCGATCCTACCAACCGGCACGA	Cloning *ermE** promoter

2.3.7 *rpf* mutant strain complementation

Within the single *rpf* mutations, the greatest phenotypic effects were seen for *rpfA*, *rpfD* and *rpfE* mutant strains, with the *rpfA* mutant phenotype having been complemented previously (Haiser et al., 2009). To ensure that the mutant phenotypes associated with Δ*rpfD* and Δ*rpfE* were due to loss of their respective Rpf protein, complementation clones were generated. The *rpfD* coding sequence was amplified, together with sufficient upstream and downstream sequence so as to encompass all necessary regulatory elements (325 nt upstream and 244 nt downstream sequence). This fragment was then cloned into the integrating plasmid pIJ82 (Table 2.1) and the integrity of the resulting construct confirmed by sequencing. The plasmid was subsequently introduced into the Δ*rpfD* mutant strain, where hygromycin resistant colonies were selected. Complementation of *rpfE* followed a similar scheme, only the complementing fragment extended 175 bp upstream of the translation start site, and 237 bp downstream of the stop codon. Empty plasmid vectors were also introduced into each mutant strain as a control for any plasmid-specific effects. Complementation was confirmed by comparing germination profiles of plasmid alone-containing mutant and wild type strains, with the complemented mutant strain, as described below.

2.3.8 Scanning and transmission electron microscopy and light microscopy

Wild type and mutant strains were grown on MS agar at 30˚C for 7 days before being examined by scanning and transmission electron microscopy, and light microscopy. Samples for light microscopy were obtained by taking coverslip impressions. Individual colonies were prepared for scanning electron microscopy (SEM) as detailed in Haiser *et al*. (Haiser et al., 2009) and examined with a TESCAN SEM. Transmission electron microscopy (TEM) and light microscopy were performed as described by Haiser *et al*. (Haiser et al., 2009). Images were processed using Adobe Photoshop Elements 11 Editor. Cell wall thickness and spore lengths/widths were measured using ImageJ software (Schneider et al., 2012). When evaluating spore wall thickness from TEM images, a minimum of 25 spores were measured for each strain, whereas a minimum of 200 spores were measured when assessing spore lengths and widths using light microscopy images.

2.3.9 Spore germination assay

Mutant and wild type spores were plated on MS agar overlaid with cellophane discs and incubated at 30˚C for up to 12 h. At intermediate time points, a 1 cm square was excised from the cellophane disc and was examined using phase contrast microscopy to score germinated spores (those possessing at least one germ tube) versus non-germinated spores. A minimum of 200 spores were counted per strain per time point, in at least three independent experiments.

2.3.10 Antibiotic sensitivity assays

Equal numbers of mutant and wild type spores were dispersed over 500 µL of MS agar containing the indicated amounts of bacitracin (Bioshop Canada) or D-cycloserine (Sigma-Aldrich) in 48 well microplates (Thermo). Plates were incubated for 4 days at 30˚C. For overlay experiments, spores were inoculated on 500 µL of MS agar in 48 well microplates and incubated at 30˚C for 16 h to allow for germination of dormant spores. Wells were then overlaid with the indicated amounts of bacitracin or D-cycloserine. Plates were incubated for an additional 3 days at 30˚C. All assays were conducted in three independent replicates.

2.3.11 Protein overexpression and purification

To assess the enzymatic activity of each Rpf, the sequence encoding the extracellular domain of each protein [excluding the SignalP-predicted signal peptide sequence (Petersen et al., 2011)] was amplified from *S. coelicolor* M145 chromosomal DNA using the primers described in Table 2.3. The amplified products were sequentially digested with BamHI and NdeI and ligated with pET15b (Novagen), which had been digested with the same enzymes and dephosphorylated prior to ligation. All constructs were verified by sequencing, using the T7 promoter and terminator primers (Table 2.3). All constructs were introduced into chemically competent *E. coli* Rosetta 2 cells (Novagen), and the resulting colonies were grown overnight in 5 mL cultures supplemented with ampicillin

and chloramphenicol. These overnight cultures were used to inoculate 500 mL of LB medium containing ampicillin and chloramphenicol, and cultures were grown at 37˚C to an OD_{600} of 0.8 before isopropyl ß–D-thiogalactopyranoside (IPTG) was added in the amounts indicated in Table 2.4 to induce protein overexpression. Cultures were incubated for the times indicated in Table 2.4 before the cells were collected by centrifugation.

Cell pellets were resuspended in 10 mL lysis buffer (50 mM NaH_2PO_4, 300 mM NaCl, 10 mM imidazole, 1 mg/mL lysozyme, pH 8.0) containing one cOmplete Mini EDTA-free protease inhibitor pellet (Roche) and incubated on ice for 30 min. The cell suspension was sonicated on ice for 6 × 10 s, before being treated with 40 µg RNase A and 20 U Turbo DNase (Ambion) for 15 min on ice. The lysate was then centrifuged at 10,000 × *g* for 30 min at 4˚C. The supernatant was removed and incubated with 1 mL of Ni-NTA slurry (Qiagen) for 1.5 hr at 4˚C before being applied to a PolyPrep chromatography column (Bio-Rad). The column was washed with buffer (50 mM NaH_2PO_4, 300 mM NaCl, pH 8.0) containing increasing concentrations of imidazole (4 mL each of wash buffer containing 20 mM imidazole, 50 mM imidazole and 70 mM imidazole) before His_6-tagged proteins were eluted with imidazole-containing buffer at concentrations optimized for each protein (Table 2.4). Purified proteins were applied to an Ultra Centricon centrifugal unit (Amicon), which allowed for exchange of the imidazole-containing buffer with protein storage buffer (50 mM NaH_2PO_4, 300 mM NaCl, pH 8.0). Protein purification was assessed following separation of purified proteins (and their accompanying washes) on a 12% SDS-PAGE polyacrylamide gel and staining with Coomassie Brilliant Blue. Protein concentrations were determined using a Bradford assay (Bradford, 1976), with bovine serum albumin as a standard.

Table 2.4: Conditions for Rpf protein over expression and purification.

Protein	Size (kDa)*	[IPTG] (mM)	Induction time (h)	Induction temperature (˚C)	[Imidazole] (mM) for elution
RpfA	21.7	1	2.5	30	250
RpfB	36.6	0.25	14	16	250
RpfBΔDUF348	21.5	0.25	14	16	250
RpfC	40.0	1	14	16	150
RpfD	42.6	1	14	16	70
RpfE	10.2	1	2.5	30	250
sIHF	13.3	1	14	16	250

*Calculated excluding the signal peptide but including the 6 × His tag from pET15b.

2.3.12 Cell wall cleavage assays

The EnzChek Lysozyme Assay kit (Molecular Probes) was used to assess the ability of Rpfs to cleave fluorescein labeled *Micrococcus lysodeikticus* cell wall material *in vitro*. One nanomole of purified Rpf was added to each reaction and the volume was brought to 50 µL with 1 × reaction buffer (100 mM sodium phosphate, 100 mM NaCl, pH 7.5) before adding 50 µL of the fluorescein labeled *M. lysodeikticus* peptidoglycan substrate to each reaction. One nanomole of the DNA-binding protein sIHF (Swiercz et al., 2013) was used as a negative control. Assays were performed in black 96 well plates (Thermo-Fisher). The amount of fluorescein released was measured every hour over the course of 8 h using a Synergy 4 Microplate Reader (BioTek), with an excitation wavelength of 494 nm and an emission wavelength of 521 nm. Each assay was conducted using at least three independently isolated protein samples, with each protein activity assessed in triplicate.

2.3.13 Rpf interactions

To probe the potential for Rpf-Rpf protein interaction, mature Rpf sequences were excised from their corresponding pET15b plasmid (Table 2.1) using NdeI and BamHI, and cloned into both pGAD T7 AD (activating domain) and pGBK T7 BD (binding domain) vectors (Clontech) digested with the same enzymes. Conveniently, these vectors contain antibiotic selection markers to facilitate cloning in *E. coli* (ampicillin and kanamycin, respectively), and prototrophic markers for selection in yeast (Leu biosynthesis and Trp biosynthesis, respectively). pGAD T7 AD-Rpf and pGBK T7 BD-Rpf constructs were transformed into *S. cerevisiae* strains Y187 and Y2H Gold (Clontech), respectively, following the TRAFO high-efficiency transformation protocol (Gietz and Schiestl, 2008). Transformants were isolated on SD medium lacking Leu (Y187) or Trp (Y2H Gold) following incubation at 30°C for 3 days. To test for Rpf-Rpf interactions, single colonies (2-4 mm in diameter) of Rpf construct-containing Y2H Gold and Y187 strains were picked from 3 day old plates and were mixed together in 1 mL 2× YPDA for mating. Cultures were incubated overnight at 30˚C, after which cells were collected by centrifugation and plated on SD lacking both Trp and Leu. Single colonies were patched onto SD plates lacking Trp and Leu to confirm the viability of the mated strains, and on SD plates lacking Trp, Leu, adenine and His to test for protein-protein interactions. Plates were examined for growth after two days incubation at 30˚C.

2.3.14 Gel filtration chromatography

Purified RpfB and RpfBΔDUF348 were separated on a Superdex 75 column (GE Healthcare) pre-equilibriated with storage buffer (300 mM NaCl, 50 mM NaH_2PO_4, pH 8) to remove protein aggregates. Pure protein was applied to the column and eluted with storage buffer at a flow rate of 0.4 mL/min at 4˚C. The absorbance of the eluate at 230 nm was recorded to confirm protein presence. Standards for column calibration (and assessment of protein oligomeric status) included ribonuclease A (13.7 kDa),

chymotrypsinogen A (25 kDa), ovoalbumin (43 kDa) and albumin (67 kDa). Peak fractions were pooled and separated on a 12% SDS-PAGE polyacrylamide gel stained with Coomassie Brilliant Blue to confirm the presence of RpfB/RpfBΔDUF348.

2.4 RESULTS

2.4.1 Bioinformatic analysis of the Rpfs in *S. coelicolor*

S. coelicolor encodes at least 60 proteins having domains with predicted peptidoglycan cleavage capabilities, and of these, seven possess an Rpf-like domain (Haiser et al., 2009; Ravagnani et al., 2005). Of these seven, two (SCO2326 and SCO5029) appeared to be more distantly related to the well-characterized Rpf domains from *Micrococcus* and *Mycobacterium* (Ravagnani et al., 2005) and lacked key catalytic residues (Fig. 2.3); these were not considered further. The remaining five proteins (SCO0974, SCO3097, SCO3098, SCO3150, and SCO7458) bore domains that were highly similar to the crystallized *M. tuberculosis* RpfB protein (Rpf_{MTB}) and contained both critical catalytic amino acids and important substrate binding residues (Fig. 2.4A). Of these five proteins, SCO3150 showed the greatest sequence divergence relative to Rpf_{MTB} (Fig. 2.4A) but shared a similar domain architecture, with its Rpf domain positioned at the extreme C-terminal end of the protein, where it was preceded by a G5 domain having potential *N*-acetylglucosamine-binding activity (Bateman et al., 2005) and three DUF348 domains whose functions are unknown (Fig. 2.4B). We have therefore designated this protein $RpfB_{SC}$. For all other *S. coelicolor* Rpf proteins, the Rpf domain was immediately adjacent to the signal peptide at the N-terminal end. SCO3097 (RpfA), SCO3098 (RpfC), and SCO0974 (RpfD) each also carried a downstream LysM peptidoglycan-binding domain, like the first characterized Rpf from *M. luteus* (Fig. 2.4B), while RpfD possessed an additional domain with predicted peptidase activity at its C-terminal end. SCO7458, or RpfE, in its mature form comprised solely an Rpf domain (Fig. 2.4B).

Within the streptomycetes, four of the five Rpf proteins were broadly conserved (RpfA, RpfB, RpfC, and RpfD), while the smallest protein, RpfE, was not encoded by any of the other well characterized *Streptomyces* species (Table 2.5). Instead, *Streptomyces venezuelae* and *Streptomyces avermitilis* encoded additional LysM containing Rpfs that lacked equivalent orthologues in *S. coelicolor* and *Streptomyces griseus* (Table 2.5).

Figure 2.3: Alignment of distantly related Rpf-like domains from SCO2326 and SCO5029 with RpfB from *Mycobacterium tuberculosis* and the more closely related Rpfs from *S. coelicolor*. Identical amino acid residues are highlighted in black, while similar residues indicated in grey. The red asterisk marks the key catalytic residue, while the blue asterisks mark important substrate-binding residues.

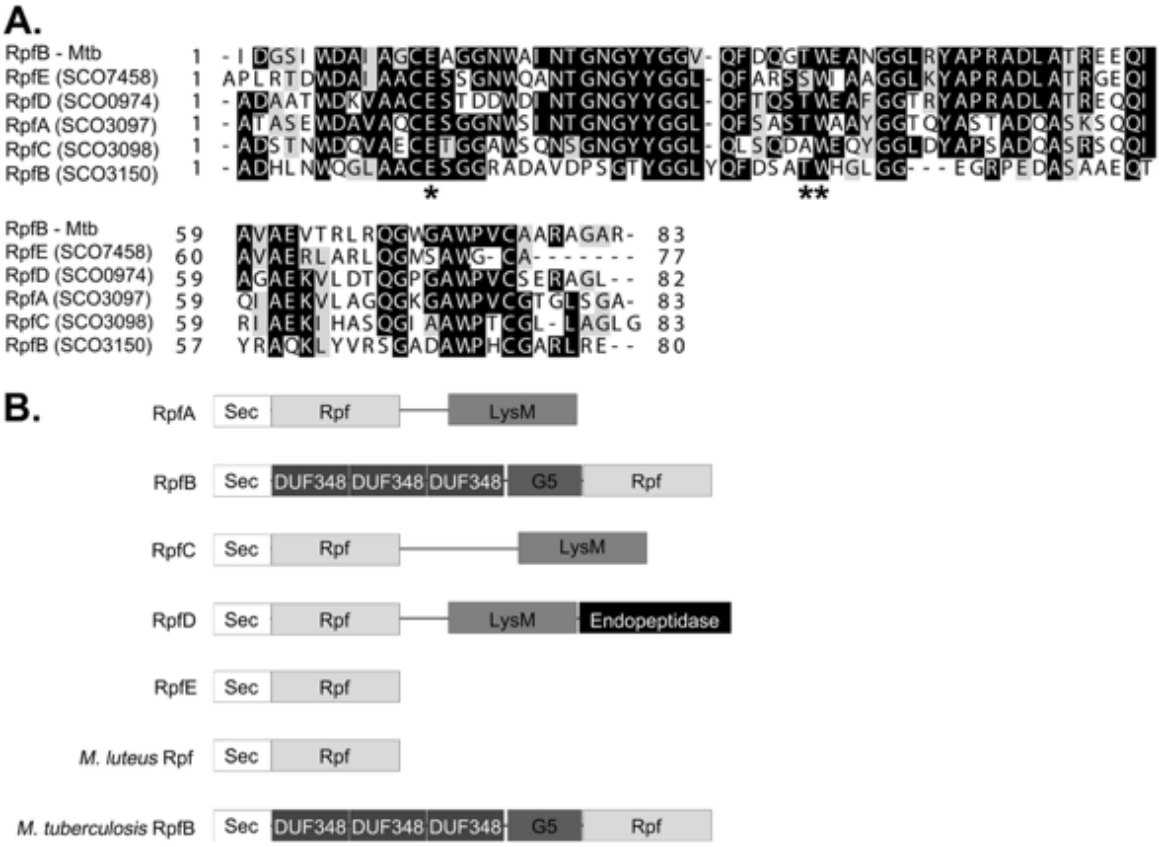

Figure 2.4: Sequence analysis of five Rpf homologues. (A) Multiple-sequence alignment of the Rpf domain from the five predicted Rpf proteins in *S. coelicolor*, together with RpfB from *Mycobacterium tuberculosis* ($RpfB_{MTB}$). Identical residues are highlighted in black. Similar residues are indicated in gray background. Key catalytic (Glu) and substrate-binding residues (Ser/Thr and Trp) are indicated with asterisks. (B) Schematic representation of the functional domain organization of the predicted Rpf proteins, along with *M. luteus* Rpf and $RpfB_{MTB}$. Sec, general secretion signal; Rpf, resuscitation-promoting factor domain; LysM, lysin motif; DUF348, domain of unknown function 348; G5, peptidoglycan-binding domain. Mtb, *M. tuberculosis*.

Table 2.5: Rpf domain-containing proteins in *S. coelicolor, S. avermitilis, S. venezuelae,* and *S. griseus*

	Orthologues in		
S. coelicolor	*S. avermitilis*	*S. venezuelae*	*S. griseus*
RpfA (SCO3097)	SAV3534	SVEN2900	SGR4438
RrfB (SCO3150)	SAV3588	SVEN2970	SGR4355
RpfC (SCO3098)	SAV3535	SVEN2901	SGR4437
RpfD (SCO0974)	SAV7250	SVEN6803	SGR745
RpfE (SCO7458)	X	X	X

2.4.2 Temporal expression of *rpf* genes during solid and liquid culture growth

As an initial characterization step, we monitored the transcription profiles of the five *rpf* genes to determine when these genes were expressed and whether their expression was coordinately regulated. RNA was harvested from plate-grown cultures during vegetative growth (24 h), aerial hyphae formation (48 h), and early and late sporulation (72 and 96 h). Transcript levels were then assessed using RT-qPCR. We could detect expression for only three of the *rpf* genes (*rpfA*, *rpfC*, and *rpfD*), with the levels of *rpfB* and *rpfE* being too low to obtain transcript profiles. For the detectable *rpf* genes, expression was highest during vegetative growth before levels dropped at the onset of aerial development (Fig. 2.5A). Similar profiles were observed for *rpfA* and *rpfC* when transcripts extracted from liquid-grown cultures were examined. Note that *S. coelicolor* does not differentiate in liquid culture, and thus these profiles reflect expression in vegetatively growing cells (Fig. 2.5A). A different pattern was detected for *rpfD*, however, where initial transcript levels were relatively low before rising during entry into stationary phase (40 h) (Fig. 2.5A). As was the case for our solid culture samples, *rpfB* and *rpfE* transcripts were below the level of reliable detection.

Given the importance of *rpf* gene products in resuscitating dormant cells in *Mycobacterium* and *Micrococcus* (Mukamolova et al., 1998, 2002a), we were interested in monitoring *rpf* transcription during spore germination. We were unable to do this using RT-qPCR (we could not isolate sufficient levels of RNA), so instead we constructed *rpf* promoter fusions to the *lux* reporter genes (Craney et al., 2007) and followed luminescence at 10 min intervals for the first 12 h of growth in liquid culture (spore germination was first seen at 4 h under these growth conditions). We found that *rpfB* transcription began almost immediately and continued through the first 5 h of growth/germination (a similar expression pattern was occasionally seen for *rpfC* as well, although it was not consistently observed), while *rpfA* expression was first detected at 3

h, increased to maximal levels from 5 to 6 h, and then dropped back to a low steady-state level (Fig. 2.5B). Expression from the other *rpf* promoters was below the detectable limit of the luminometer during this time course.

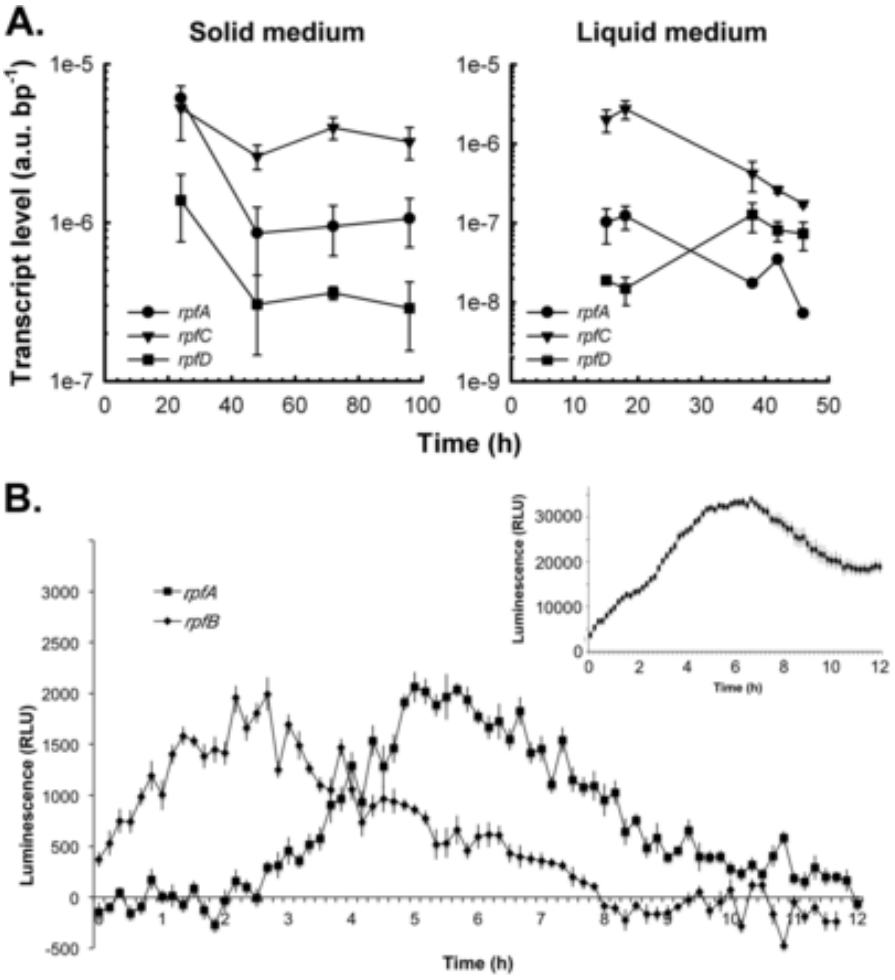

Figure 2.5: Transcript levels of Rpf-encoding genes in *S. coelicolor* throughout growth and development. (A) The *S. coelicolor* wild type strain M145 was grown at 30°C on MS agar medium and TSB-YEME liquid medium. At the times indicated, total RNA was extracted from cells, and transcripts bearing the *rpfA*, *rpfC*, and *rpfD* coding regions were quantified using RT-qPCRs. Transcript levels were normalized to total RNA mass and PCR product length. The quantification cycle value of each no-RT control was greater than that of the RT samples by at least 10 cycles. Quantification cycle values of all no-template controls were consistently greater than 40 cycles. All data are presented as means standard errors (*n* = 1 to 3). au, arbitrary units. (B) *rpf* promoter activities were monitored in TSB-YEME liquid medium for 12 h post inoculation using a luminescence-based reporter. The inset panel (positive control) represents the activity of the strong constitutive *ermE** promoter fused to the *lux* genes over the same 12-h time course. Data are presented as means ± standard errors (*n* = 8). RLU, relative light units.

2.4.3 Rpfs are important for initiating germination

Given the early transcription of *rpfA* and *rpfB* (and sometimes *rpfC*) and the resuscitation-associated function of the Rpfs as a whole, we sought to determine whether the Rpfs played a role in spore germination, the "dormant cell resuscitation" equivalent in *Streptomyces*. We first constructed strains bearing individual *rpf* deletions (*rpfA*, *rpfB*, *rpfC*, and *rpfE*) or disruptions (*rpfD*). As peptidoglycan lytic enzymes are notoriously redundant in their activities (Typas et al., 2012), we also generated strains with deletions in increasing numbers of *rpf* genes (deletions of two, three, four, and five *rpf* genes) with the goal of gaining a clearer picture as to the role of Rpf domain-containing proteins in *S. coelicolor* germination, growth, and development.

Spore germination for single and multiple *rpf* mutant strains was monitored over a 12 h time course, with spores being scored for the presence of one or more germ tubes using light microscopy (Fig. 2.6A). We found that, generally, loss of individual *rpf* genes was correlated with a delay in the onset of germination. The most significant delays were observed for *rpfA* and *rpfE* single mutants, and subtle but reproducible germination delays were seen for the *rpfD* mutant; loss of *rpfB* had no effect on spore germination, whereas *rpfC* mutants occasionally took longer than the wild type to initiate germination. Somewhat surprisingly, we found that the initial delay in germination did not translate into a longer time frame needed for complete germination to occur: all spores (mutant and wild type) were fully germinated by 12 h. The germination defect for the *rpfA* mutant has been complemented previously (Haiser et al., 2009), and here we were able to partially complement the defect observed for the *rpfD* and *rpfE* mutants with a wild type copy of their respective genes (see Fig. 2.7). The strain with deletions of *rpfA* through *rpfE* (5× *rpf* mutant) showed the greatest impairment in germination: germ tubes had emerged from fewer than 40% of spores after 9 h although, as was seen for the single mutants, germination was complete by 12 h (Fig. 2.6A). Collectively, the delay in initiating germination seen for the *rpf* mutants indicates that these proteins play an important (although not essential) role in promoting spore germination.

Delayed germination in these strains could stem directly from the lack of Rpfs, which may be needed to remodel the spore peptidoglycan during germination and/or release a germination-promoting signal. Alternatively, the germination defects could stem from Rpf-dependent changes in spore peptidoglycan architecture such that the spore wall is less amenable to germ tube emergence. Indeed, deleting peptidoglycan hydrolases has been associated with increased cell wall thickness in *Bacillus subtilis* (Fan and Beckman, 1971; Fan et al., 1972). To determine whether this was a possibility, we probed spore wall thickness for those *rpf* mutants exhibiting germination delays and found that there was no correlation between spore wall thickness and germination rate. Of the single mutants, the *rpfA* strain exhibited the greatest germination defect, yet *rpfA* mutant spores had the thinnest walls of all strains tested (Haiser et al., 2009) (Fig. 2.6B and C). In

contrast, the spore walls of the 5× mutant were at least as thick as those of the wild type, and this mutant showed the greatest delay of all strains (Fig. 2.6B and C). While these experiments do not preclude the possibility that altered cell wall structure contributes to delayed germination, they do indicate that wall thickness alone cannot be used as a surrogate for germination competence.

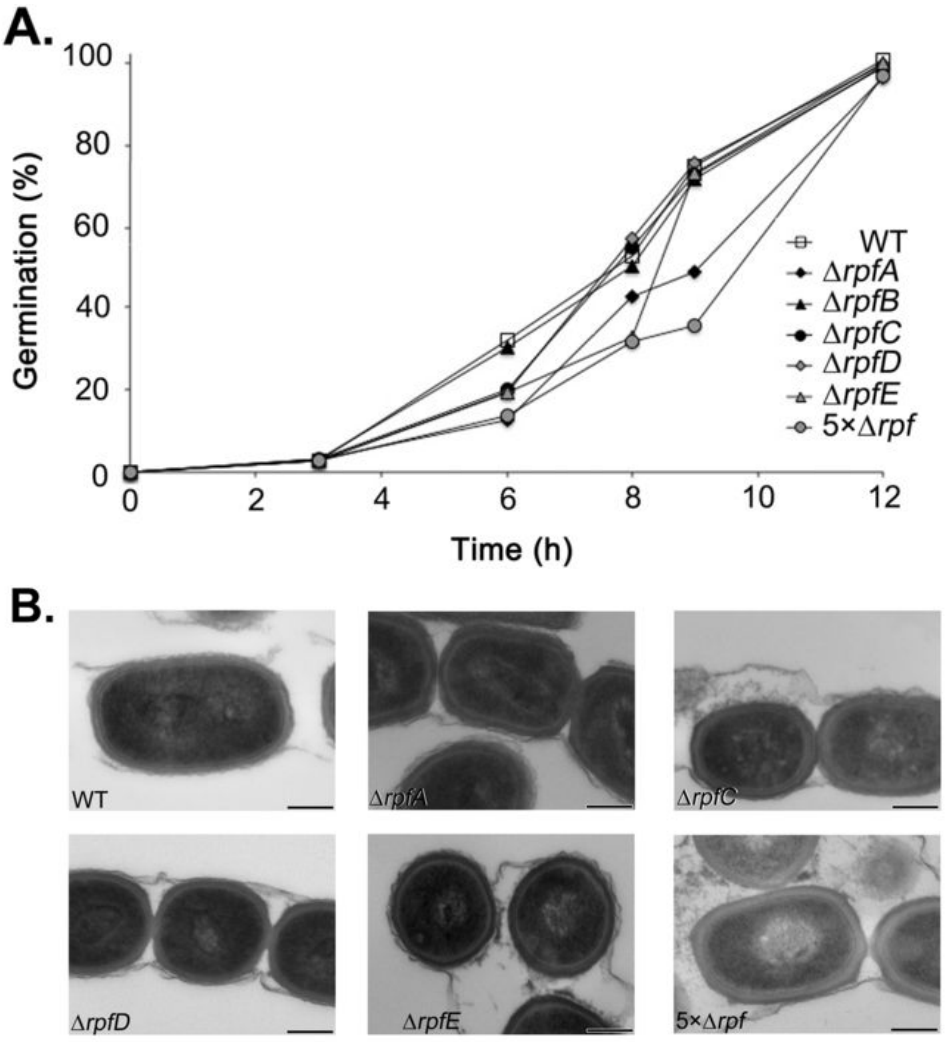

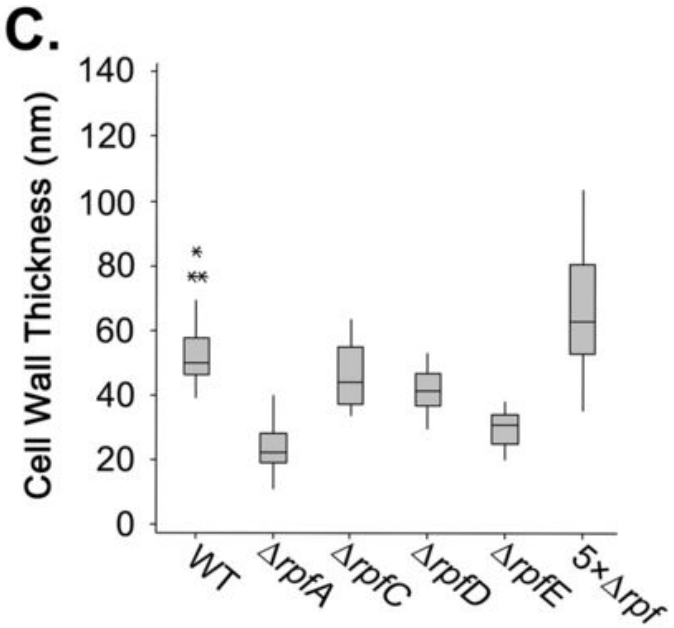

Figure 2.6: Rpfs are involved in initiating germination of *S. coelicolor* spores. (A) Wild type (WT), individual *rpf* mutants, and 5×Δ*rpf* mutant spores were monitored for germination using light microscopy over 12 h. The proportion of germinated spores was determined for each strain at the indicated time points. Data are representative of three independent trials (*n* = 100 spores for every time point, for every strain). (B) Transmission electron micrographs (TEMs) of wild type, individual *rpf* mutants, and 5× *rpf* mutant strains. Scale bar, 250 nm. (C) Wall widths of spores (*n*=25) from the samples shown in panel B were determined from TEMs. Box plots indicate the median (center band), the 25th and 75th percentiles (lower and upper limits of the box, respectively), and the 5th and 95th percentiles (lower and upper whiskers, respectively). Asterisks indicate outliers.

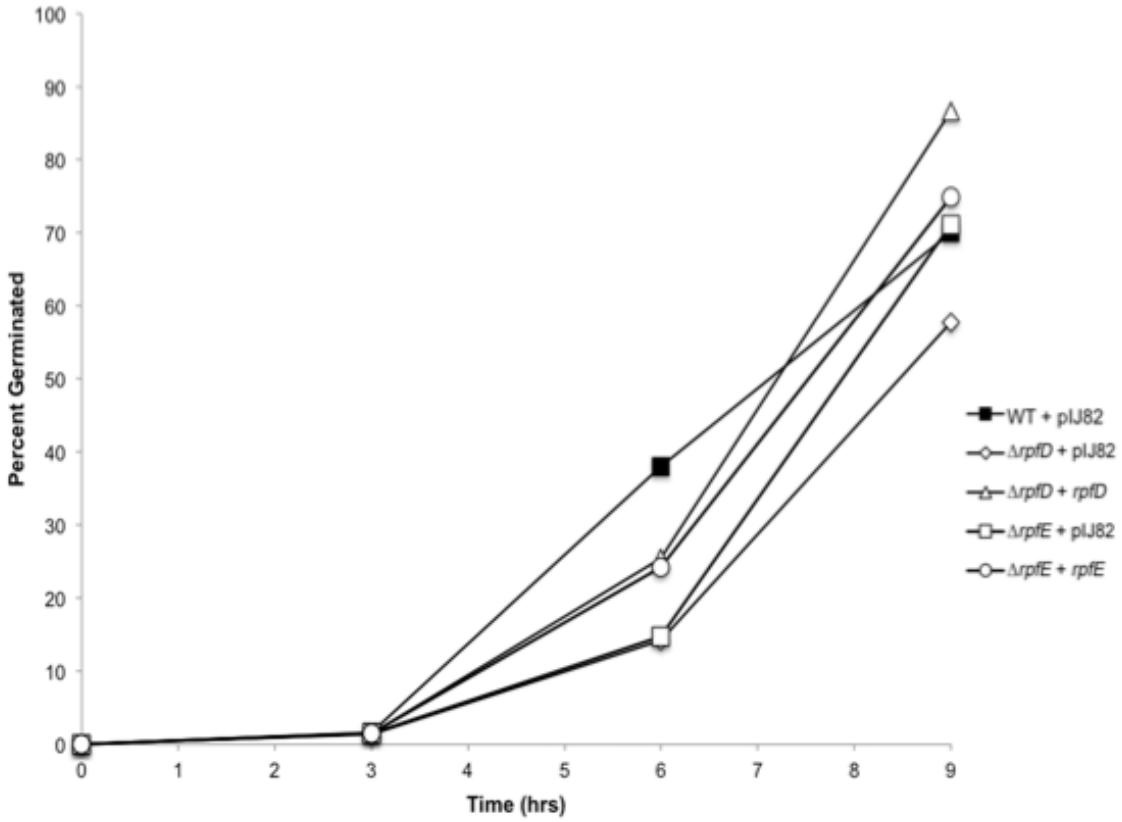

Figure 2.7: Partial complementation of Δ*rpfD* and Δ*rpfE* confirmed by examining germination profiles. Spores of complemented and vector alone-containing *rpf* mutants were plated on MS agar overlaid with cellophane discs. Spores were monitored for the presence or absence of germ tubes at the indicated time points. Data are representative of three independent trials (n > 100 per time point per strain). WT, wild type.

2.4.4 Germinating spores lacking Rpfs are more sensitive to cell wall-specific antibiotics

To determine whether the germination defects and heterogeneous spore wall thickness of the different *rpf* mutants might reflect altered cell wall properties, we tested the different mutants for their sensitivity to antibiotics targeting the cell wall. Mutant and wild type spores were plated on MS agar containing increasing amounts of D-cycloserine (inhibitor of DAla–D-Ala ligase) (Fig. 2.8A) and bacitracin (inhibitor of C_{55}-bactoprenol pyrophosphate dephosphorylation) (Fig. 2.8B). As a control, we also tested all strains for their sensitivity to hygromycin, an antibiotic targeting protein synthesis. Relative to the wild type, all *rpf* mutants showed increased sensitivity to D-cycloserine and bacitracin, with the *rpfA*, *rpfD*, and the 5× *rpf* strains being the most sensitive. To determine if the increased *rpf* mutant sensitivity reflected a germination-specific defect, mutant and wild

type spores were spread on MS agar and grown for 16 h to allow for complete germination. The vegetatively growing cells were then overlaid with increasing amounts of D-cycloserine (Fig. 2.8C) or bacitracin (Fig. 2.8D). In contrast to our previous results, the *rpf* mutant strains were resistant to all concentrations of both antibiotics. This suggested that Rpf activity alters the spore wall— or that of the initial germ tubes—such that Rpf-deficient strains display enhanced sensitivity to antibiotics that block cell wall synthesis.

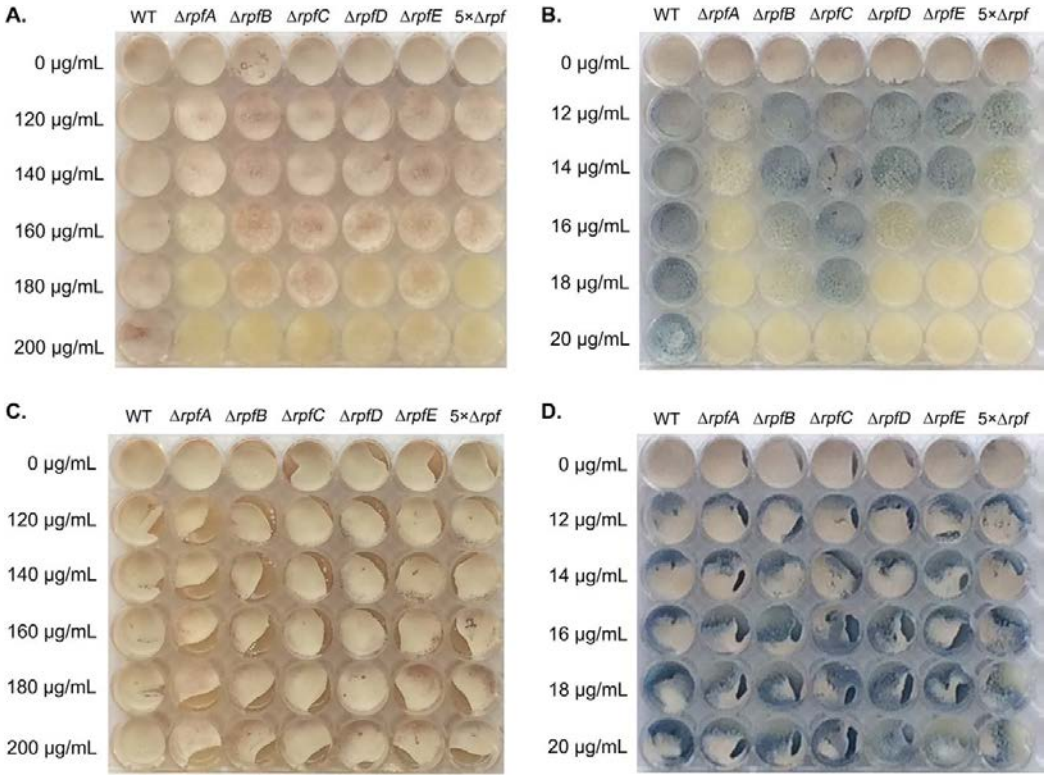

Figure 2.8: Rpf deletion enhances antibiotic sensitivity during germination. Equal numbers of mutant and wild type (WT) spores were spread on MS agar containing the indicated amounts of D-cycloserine (A) or bacitracin (B) or were inoculated onto MS agar and allowed to germinate for 16 h before being overlaid with the indicated amounts of D-cycloserine (C) or bacitracin (D). Plates were incubated for 4 days at 30°C. Images are representative of three independent replicates.

2.4.5 Deleting *rpf* genes impacts vegetative growth in liquid culture

To further probe the biological role of the Rpf proteins in *S. coelicolor*, we followed the growth and development of the individual and multiple *rpf* mutant strains on solid agar plates (sporulation-specific [MS] and rich [R5] media). After 2 days, the majority of *rpf* mutants appeared largely wild type (Fig. 2.9A).

For the *rpf* genes whose expression was detectable, transcript levels were generally highest during germination and vegetative growth, with the exception of the level of *rpfD* in liquid culture. To determine whether any of the *rpf* mutations had an effect on vegetative growth, we followed colony growth over a 24 h time course on solid medium (Fig. 2.9B). We did not observe any delays in the growth of the *rpfA* or *rpfB* mutant, but the growth of *rpfC*, *rpfD*, and *rpfE* mutants was slightly retarded at 12 h. Intriguingly, the 5× *rpf* mutant failed to form a detectable colony after 12 h, and its growth was detectable only by 18 h (Fig. 2.9C). It is conceivable that these growth delays simply reflected slower germination rates; however, this cannot be the only explanation as the *rpfC* strain had largely normal germination but showed delayed vegetative growth, while the *rpfA* mutant had a significant germination delay but exhibited robust vegetative growth.

As defects in vegetative growth may be more pronounced in liquid culture, we followed the growth profile of the 5× *rpf* mutant relative to its wild type parent strain in rich and minimal media. In rich medium, the growth curve of the 5× *rpf* mutant was virtually indistinguishable from that of the wild type strain prior to stationary phase, at which point the 5× *rpf* mutant showed better growth than the wild type (Fig. 2.9D). In contrast, in minimal medium, the 5×Δ*rpf* mutant grew far less robustly than the wild type at all time points, suggesting that the Rpfs confer a distinct competitive advantage during growth under nutrient-limiting conditions.

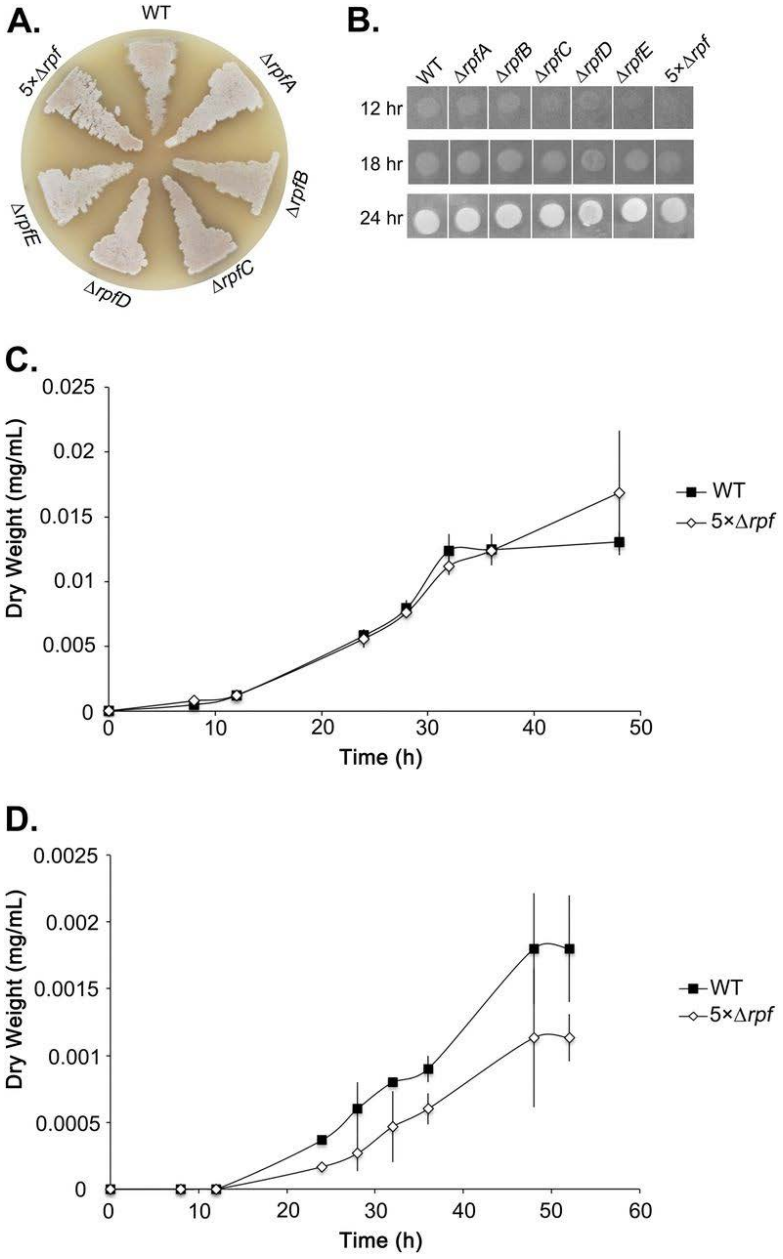

Figure 2.9: Phenotypic analyses of *rpf* mutant strains. (A) Colony morphology of the wild type, individual *rpf* mutants, and 5×Δ*rpf* deletion strains after 2 days growth on MS agar medium. (B) A total of 2×10^5 mutant and wild type spores were plated on LB agar medium (a low-Mg^2 medium used to exacerbate any cell wall defects). Pictures were taken at the indicated time points and are representative of three independent trials. (C and D) Growth profile of the 5×Δ*rpf* mutant compared to the wild type during liquid culture in TSB-YEME medium (C) and NMMP medium (D). Values are presented as means ± standard errors (*n* = 3). WT, wild type.

2.4.6 *In vitro* activity assays of each Rpf protein reveal widely varying levels of peptidoglycan cleavage capabilities

To begin probing the biochemical basis for Rpf function, we set out to assess the ability of each of these enzymes to cleave purified peptidoglycan. As a substrate, we opted to use commercially available and fluorescently labeled peptidoglycan from the close *Streptomyces* relative *M. luteus*. The fluorescein labeling density was sufficiently high that fluorescence was quenched; this quenching could be alleviated through cleavage of the labeled peptidoglycan, with increased fluorescence being directly proportional to cleavage activity. We overexpressed and purified each of the five Rpf enzymes and monitored their activity over 8 h. While all Rpfs were significantly less active than lysozyme (positive control), there were considerable differences in their activity levels. RpfE was the most active enzyme, followed by RpfA and RpfD. RpfB and RpfC had the lowest activities, with their levels always being less than half that of any other enzyme (Fig. 2.10). sIHF, a cytoplasmic DNA-binding protein from *S. coelicolor*, was also overexpressed, purified, and subjected to the cleavage assay to ensure that any activity observed was not due to contaminating *E. coli* proteins. These results indicate that all of the *S. coelicolor* Rpfs have some level of peptidoglycan cleavage capability and thus would be able to remodel *Streptomyces* cell walls.

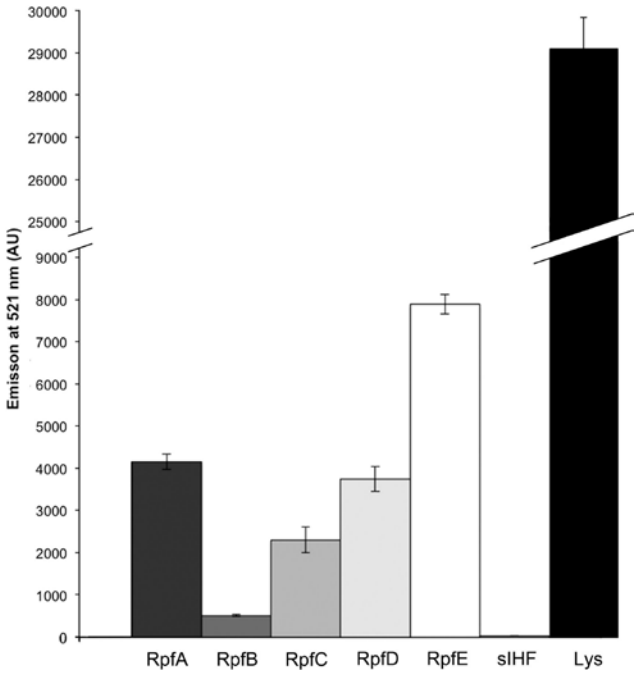

Figure 2.10: Rpf proteins cleave peptidoglycan *in vitro*. One nanomole of pure protein (as indicated) was mixed with fluorescein-labeled *M. luteus* cell walls. Data represent the average emission at 521 nm after 8 h of incubation of three trials ± standard error. Negative control, cytoplasmic DNA binding protein sIHF; positive control, lysozyme (Lys). AU, arbitrary units.

2.4.7 Rpf interactions: RpfB forms a dimer

Previous work in *Mycobacterium* has suggested that several Rpfs interact with other cell wall-lytic enzymes (Hett et al., 2007). In particular, the RipA endopeptidase interacts with $RpfB_{MTB}$, and this association results in synergistic activity. RipA further interacts with RpfE, an enzyme like RpfE in *S. coelicolor* that lacks an obvious means of associating with the peptidoglycan (Hett et al., 2007, 2008). There is no RipA homologue encoded by the streptomycetes, and thus we wondered whether RpfD, with its endopeptidase domain, might interact with RpfB and whether any of the LysM domain-containing Rpfs (RpfA, RpfB, or RpfD) might associate with RpfE, helping to anchor it to the cell wall. To test this hypothesis we examined interactions between each Rpf protein (excluding their signal peptides) using a yeast two-hybrid system. Rpf interactions were tested in a pairwise fashion, with each mating pair spread on diagnostic medium such that only the strains with an interacting Rpf pair would be capable of growing. We found that RpfB associated with itself, based on the robust growth observed for this mating pair on selective medium, in contrast to all other Rpf pairs, which were unable to interact in this system (Fig. 2.11A).

To further test the oligomerization capabilities of RpfB, we overexpressed and purified mature RpfB and followed its oligomeric status using gel filtration chromatography. We found that RpfB eluted at a volume that was most consistent with a dimer form (molecular mass of the His-tagged fusion protein was 36.6 kDa), with no detectable monomer species observed (Fig. 2.11B), supporting our yeast two-hybrid observations.

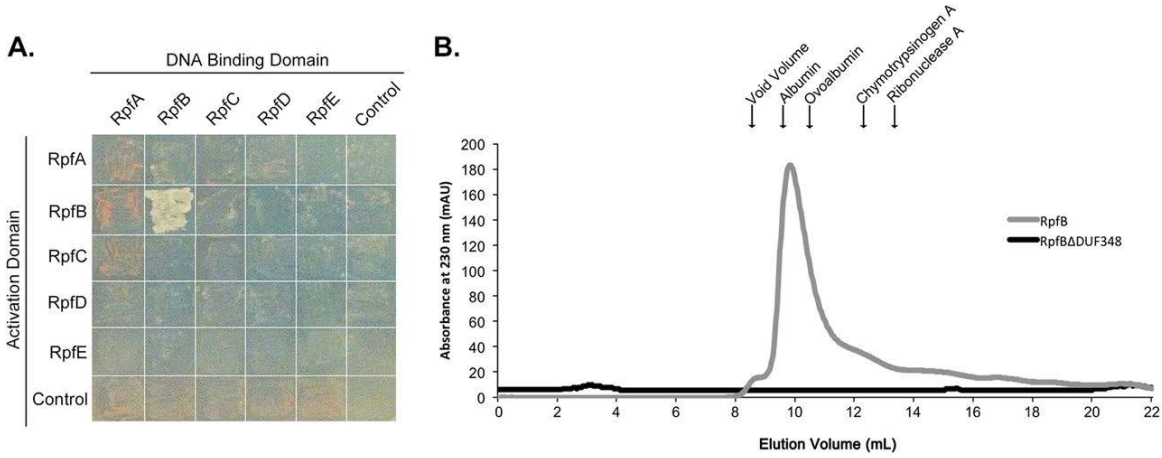

Figure 2.11: RpfB forms dimers. (A) Yeast two-hybrid analysis of interactions between Rpf proteins. Pictures were taken after 2 days of incubation at 30°C. Growth on selective medium indicates an interaction between bait (DNA-binding domain)- and prey (activation domain)-associated proteins. (B) Purified RpfB and RpfBΔDUF348 were separated on a Sephadex 75 gel filtration column. The peak at 9.4 ml represents likely RpfB dimers. RpfBΔDUF348 dimers were expected to elute at 12 ml. The molecular mass and elution volume, respectively, of each of the standards indicated above the figure are as follows: albumin, 67 kDa and 9.6 ml; ovalbumin, 43 kDa and 10.4 ml; chymotrypsinogen A, 25 kDa and 12.4 ml; and RNase A, 13.7 kDa and 13.3 ml.

2.4.8 Removal of the DUF348 domains from RpfB impacts dimerization and enhances enzyme activity

RpfB does not possess any obvious protein interaction domains (Fig. 2.4B): its G5 domain is predicted to promote peptidoglycan binding (Bateman et al., 2005), while the Rpf domain failed to promote dimerization in any of the other Rpf protein combinations tested here. DUF348 domains are frequently associated with proteins functioning at the cell wall (Bateman et al., 2005; Ravagnani et al., 2005), but, as their name implies, their function is unknown; these domains therefore seemed the most likely candidates for mediating dimerization. To test the role of the DUF348 sequences in RpfB dimerization, we constructed a truncated version of RpfB in which the three DUF348 domains were removed (RpfB DUF348). We found that RpfB DUF348 failed to interact as robustly with itself as it did with the full-length mature RpfB protein, and its ability to interact with RpfB differed, depending on the vector system (Fig. 2.12A). To further probe the role of DUF348 domains in dimerization, we again conducted gel filtration chromatography. While RpfB appeared to elute predominantly as a dimer, no dimers were observed for RpfB DUF348 (molecular mass of the His-tagged fusion was 21.5 kDa) (Fig. 2.11B). Instead, it did not elute as a discrete peak, suggesting that it had a very different conformation than full-length RpfB.

Given this observation, we sought to determine whether the DUF348 domains influenced RpfB activity. We tested the peptidoglycan cleavage activity of RpfBΔDUF348 in our fluorescent substrate assay and found its activity to be far greater than that of the full-length RpfB, suggesting that these domains may function to modulate enzyme activity (Fig. 2.12B).

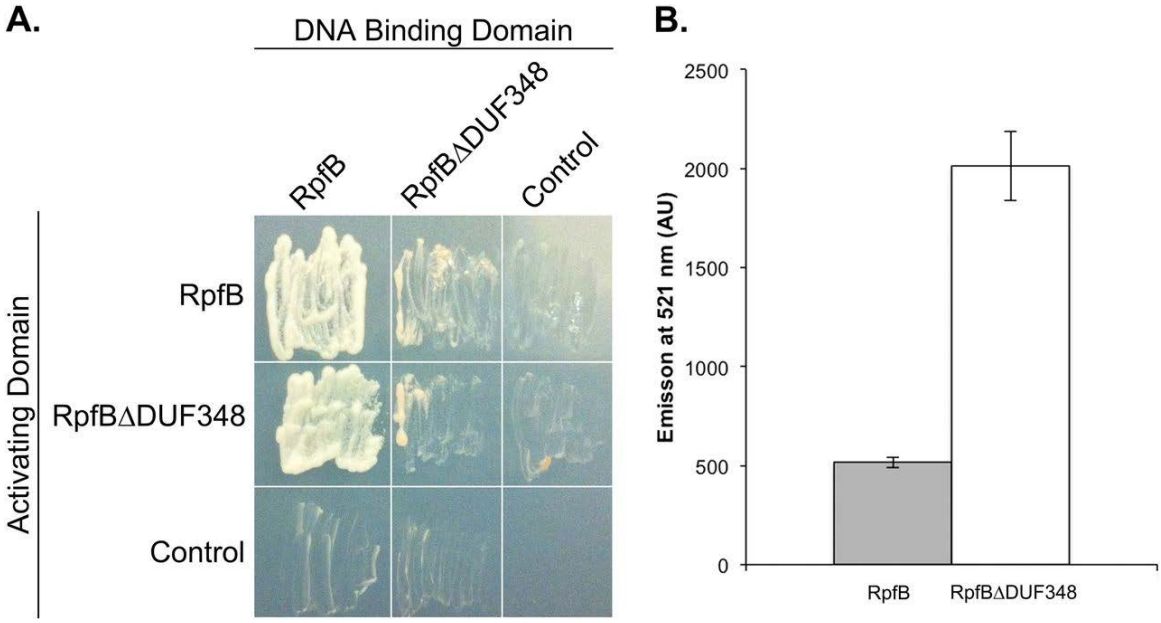

Figure 2.12: The DUF348 domains in RpfB are required for dimerization and inhibit RpfB activity. (A) Yeast two-hybrid analysis of interactions between full-length and truncated RpfB proteins, as described in the legend to Fig. 2.10. Pictures were taken after 2 days of incubation at 30°C on selective medium. The level of growth is correlated with the strength of the protein interaction. (B) One nanomole of pure protein was incubated with fluorescein-labeled *M. luteus* cell wall for 8 h. Fluorescence emitted at 521 nm was quantified. Data are presented as means ± standard errors (n = 3).

2.5 DISCUSSION

2.5.1 Rpfs and their role in resuscitation

Rpf enzymes were originally defined on the basis of their resuscitation-promoting activities in *Micrococcus* and, later, in *Mycobacterium*. Our results support a role for the Rpfs in spore germination in *S. coelicolor*; however, they do not all contribute equivalently, and the fact that germination can proceed (albeit without wild type kinetics) in the complete absence of Rpfs suggests that they must function in conjunction with other factors. Of the individual Rpfs, *rpfA* mutants had the most severe

germination defect, with *rpfB* and *rpfC* mutants behaving most like the wild type. For the *rpfB* mutant, this could be explained in part by the fact that RpfB reproducibly exhibited the lowest *in vitro* cleavage activity of all the Rpfs. In contrast, *rpfC* was not routinely transcribed during germination, and we expected that it may have little to no enzymatic activity because, unlike the other Rpfs, it lacks a key substrate binding residue, having an Ala in place of a Ser/Thr residue (Cohen-Gonsaud et al., 2005) (Fig. 2.4A). Surprisingly, we found it to have intermediate levels of activity, suggesting that this residue is not critical for substrate recognition and binding. In examining the sequence of the RpfC orthologues in other streptomycetes, this particular residue varied considerably, with everything from Leu (*Streptomyces* sp. strain S4) and Asn (*S. avermitilis* and *Streptomyces scabies*) through to the expected Ser (*S. venezuelae*) and Thr (*S. griseus* and *Streptomyces clavuligerus*) residues found at this position (Fig. 2.13).

The germination defect observed for the *rpfE* mutant was surprising, given that *rpfE* transcripts were undetectable. It is possible that low levels of expression are all that are required for its function; this would be consistent with previous observations in *M. luteus*, where the lone Rpf could restore active growth at extremely low (picomolar) concentrations (Mukamolova et al., 1998).

The 5× *rpf* mutant exhibited the most severe defect in germination and subsequent vegetative outgrowth. These defects did not dramatically impact the growth of this strain under nutrient rich conditions; however, in minimal medium, growth of this strain was severely attenuated compared with that of the wild type. This suggests that for *Streptomyces* species growing in a nutrient poor soil environment, the lack of Rpf enzymes may confer a profound fitness cost, analogous to that seen for other bacteria (Segev et al., 2013).

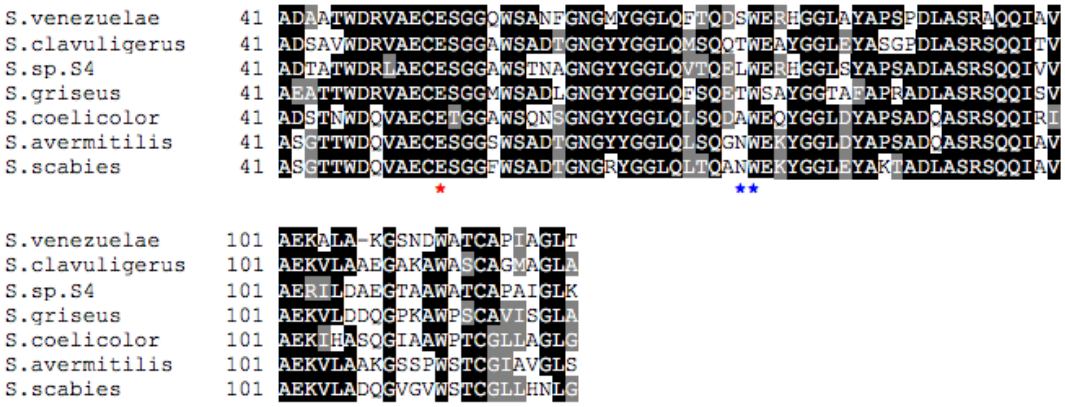

Figure 2.13 Alignment of the Rpf domain of RpfC orthologues from diverse *Streptomyces* species. The key catalytic residue is indicated with a red asterisk, while important substrate-binding residues are marked with blue asterisks.

2.5.2 Rpf redundancy in the Streptomycetes.

Within the *Actinobacteria*, *M. luteus* encodes a single Rpf enzyme that is essential for viability. In contrast, *Streptomyces* and *Mycobacterium* species encode four or more Rpf domain-containing enzymes, and at least in a laboratory environment, these Rpf-encoding genes can all be deleted without compromising viability. In *M. tuberculosis*, studies have suggested that deleting $rpfB_{MTB}$ (homologous to *rpfB* in *S. coelicolor*) delays *M. tuberculosis* resuscitation in a chronic tuberculosis model (Tufariello et al., 2006) although single deletions of any other *rpf* gene had no obvious effect. Combining mutations led to more severe phenotypic consequences, with double and triple *rpf* mutants attenuated in their ability both to resuscitate dormant cells *in vitro* and to establish chronic infections *in vivo*(Biketov et al., 2007; Downing et al., 2005; Russell-Goldman et al., 2008).

In *S. coelicolor*, we found that individual *rpf* deletions conferred modest germination defects, with differing levels of severity. This suggested that these enzymes make distinct contributions to germination and vegetative outgrowth, a possibility supported by the fact that individual Rpfs possessed distinct functional domains, and were expressed at various levels and, in some cases, at different times. We did not, however, observe directly additive phenotypic effects when multiple *rpf* genes were deleted, suggesting that there is some level of functional redundancy shared by these enzymes. Notably, in strains lacking all Rpfs, spore germination was still complete by 12 h, despite the marked delay in germination initiation. This suggests that the resuscitation process in *Streptomyces* is more complex than that in either *Mycobacterium* or *Micrococcus* and that the Rpfs may function as part of a larger peptidoglycan remodeling network.

2.5.3 Rpf interactions

In considering the Rpf proteins encoded by *Streptomyces* and *Mycobacterium*, only RpfB shared full-length similarity. Previous work in *Mycobacterium* had shown that while the *rpfB* mutation had phenotypic consequences, *in vitro* assays revealed RpfB to have little activity on its own (Cohen-Gonsaud et al., 2005), a phenomenon we also observed in our *in vitro* assays here. Subsequent investigations revealed a key interaction between RpfB and the endopeptidase RipA and synergistic peptidoglycan cleavage by the two enzymes (Hett et al., 2007, 2008).

The dimerization capability of RpfB had not been previously recognized, as the screen that led to RipA identification included only the Rpf domain of RpfB (Hett et al., 2007), and the Rpf domain does not appear to promote dimerization, based on the lack of interaction seen for all other Rpfs. Our results suggest that, instead, the DUF348 domains found at the N terminus of RpfB facilitate dimerization and inhibit RpfB enzyme activity. It is tantalizing to speculate that the RipA-RpfB association in *Mycobacterium* may lead to a conformational change in RpfB, alleviating the DUF348-mediated inhibition of enzyme activity. DUF348 domains are found in proteins throughout the *Actinobacteria* and *Firmicutes* and in most cases are found together with both G5 and peptidoglycan cleavage-associated domains (in *S. coelicolor*, these domains are not present in any protein but RpfB). Our results indicate that DUF348 domains may serve as a means of controlling the activity of peptidoglycan-cleaving enzymes.

Given the potentially destructive nature of cell wall-lytic enzymes like the Rpfs, it is critically important that their activity be tightly controlled. Increasingly, protein-protein interactions are being found to contribute to this regulation. In *M. tuberculosis*, RpfB-RipA activity is negatively influenced by interactions with penicillin binding protein 1 (PBP1) (Hett et al., 2010), while in *E. coli*, two amidases responsible for cell separation are controlled by peptidoglycan-binding enzymes that confer spatial and temporal regulation (Uehara and Bernhardt, 2011). Notably, the two regulatory proteins in *E. coli* were initially classified as having peptidoglycan cleavage activity themselves, specifically, endopeptidase activity. It will be interesting to see whether equivalent proteins control any of the Rpf enzymes in *S. coelicolor*.

2.6 ACKNOWLEDGEMENTS

We would like to thank Tamiza Nanji and Dr. Alba Guarné for their assistance with the gel-filtration chromatography experiments. This work was supported by a Vanier Canada Graduate Scholarship to R.J.S-O.; an Ontario Graduate Scholarship to H.J.H.; the Canada Research Chairs program (to M.A.E.); and a grant from the Canadian Institutes for Health Research (to M.A.E.; grant no. MOP-93635).

Chapter 3

Peptidoglycan cleavage and the molecular mechanisms underlying Rpf-mediated cellular resuscitation in *Streptomyces* bacteria

Danielle L. Sexton, Francesca A. Herlihey, David A. Crisante, Anthony J. Clarke, and Marie A. Elliot

The work that follows in this chapter appears as it was submitted to the *Journal of Biological Chemistry* in June 2017. This work is presently undergoing revision before resubmission for publication.

Contributions: Initial conceptualization of the project was by D.L.S. and M.A.E. D.L.S. performed the experiments and analyzed the data associated with the experiments presented in Figures 1 (in conjunction with D.A.C.), 4 and 5; F.A.H. performed the experiments and both F.A.H. and A.J.C. analyzed the data in Figures 2 and 3. Project oversight was provided by A.J.C. and M.A.E. The manuscript was written by D.L.S., F.A.H., A.J.C. and M.A.E., with input from D.A.C. All authors reviewed and approved the final version of the manuscript.

3.1 ABSTRACT

Bacterial dormancy can take many forms, including *Bacillus* endospores, *Streptomyces* exospores, and metabolically latent *Mycobacterium*. In the actinobacteria, including the streptomycetes and mycobacteria, the rapid resuscitation from a dormant state requires the action of a family of cell wall lytic enzymes called the resuscitation promoting factors (Rpfs). Whether Rpf activity promotes resuscitation by generating muropeptide signaling molecules, or by simply remodeling the dormant cell wall, has been the subject of much debate. To address this question, we first sought to gain broader insight into the biochemical function of the Rpf enzymes. Rpfs come in many forms, and we showed that the associated LysM and LytM domains enhance Rpf enzyme activity. We further demonstrated that the Rpfs function as endo-acting lytic transglycosylases, cleaving within the peptidoglycan backbone. Unlike in other systems, Rpf activity in the streptomycetes was not correlated with peptidoglycan-responsive Ser/Thr kinases, and the germination of *rpf* mutant strains could not be stimulated by the addition of known germinants. Collectively, these results suggest that in *Streptomyces*, Rpf function is more structural than signaling, and that in the actinobacteria, any signaling function must require the activity of additional – yet to be identified – enzymes.

3.2 INTRODUCTION

Bacteria are masters of survival. When faced with unfavourable growth conditions, many bacteria have evolved the ability to enter a non-replicative state, allowing them to survive a wide range of adverse conditions. These non-replicating states include everything from persister cells and viable but not culturable (VNBC) bacteria, through to specialized dormant spores (Oliver, 2010; Swiercz and Elliot, 2011; Wood et al., 2013). Despite the different forms adopted by these non-replicating cells, they all share reduced metabolic activity compared with their vegetative counterparts, and often have an altered (thicker) cell wall.

A major constituent of the cell wall – in both vegetative and dormant cells – is peptidoglycan. Peptidoglycan polymers are defined by their glycan backbones, composed of alternating *N*-acetylmuramic acid (Mur*N*Ac) and *N*-acetylglucosamine (Glc*N*Ac) residues, and by short peptides extending from the lactyl groups of the Mur*N*Ac residues. The peptide stems of different glycan strands can in turn be joined together either directly or by amino acid linkers of varying lengths. These peptide bridges crosslink parallel strands together, yielding a rigid structure that serves to maintain the integrity of the cell membrane (Cava and De Pedro, 2014). In dormant cells, the peptidoglycan is relatively inert, whereas in actively growing cells it is highly dynamic (Cava and De Pedro, 2014).

Cell wall cleavage is a critical component of cell growth, being required for the insertion of new peptidoglycan. Muralytic enzymes target the glycan strands of peptidoglycan, and are classified as either hydrolases or lytic transglycosylases. Hydrolases, including the lysozymes and β-*N*-acetylglucosaminidases, hydrolyse β-(1-4) linkages in the glycan (Vollmer et al., 2008b). In contrast, lytic transglycosylases cleave the same bond as lysozymes (between Mur*N*Ac and Glc*N*Ac), but they do not require water and instead generate Glc*N*Ac and 1-6 anhydroMur*N*Ac products (Scheurwater et al., 2008). All of these enzymes can be further subdivided into exo- or endo-acting enzymes, depending on whether they cleave at the ends of glycan strands, or within strands, respectively.

For many dormant cells, resuming active growth requires the breakdown of the thick, protective cell wall, and different bacteria have evolved distinct strategies to achieve this. Within the actinobacteria, dormant cells employ a common degradative enzyme that promotes the resumption of vegetative growth. The so-called 'resuscitation promoting factor' (Rpf) enzymes, share structural homology with lysozyme and lytic transglycosylases (Cohen-Gonsaud et al., 2005), and have muralytic activity (Cohen-Gonsaud et al., 2004; Haiser et al., 2009; Hett et al., 2008; Mukamolova et al., 2006; Ruggiero et al., 2009; Sexton et al., 2015; Telkov et al., 2006). In *Micrococcus luteus*, a single Rpf enzyme is required for the resuscitation of metabolically quiescent cells (Mukamolova et al., 1998). Most other actinobacteria encode multiple Rpfs (Machowski et al., 2014; Ravagnani et al., 2005), and these collectively stimulate the growth of dormant cells (Downing et al., 2005; Hartmann et al., 2004; Kana et al., 2008; Russell-

Goldman et al., 2008; Sexton et al., 2015). In *Streptomyces coelicolor*, the products of five *rpf* genes (*rpfA*-*E*) promote the rapid germination of dormant spores, and can influence both vegetative growth and sporulation (Haiser et al., 2009; Sexton et al., 2015). Deleting individual *rpf* genes results in modest germination defects in some instances (Haiser et al., 2009; Sexton et al., 2015), while deleting all five has the greatest impact on germination (Sexton et al., 2015).

Resuscitation is a complex process, and how the Rpfs promote resuscitation is not fully understood. Two models have been put forth to explain Rpf function during the escape from dormancy: 1) Rpf activity liberates peptidoglycan-derived signaling molecules that activate a regulatory cascade needed for growth resumption, and 2) Rpf activity relieves the physical constraints imposed by dormant cell walls, allowing cell growth to resume (Keep et al., 2006a). While these proposals are not mutually exclusive, investigations to date appear to favour a signaling-type of mechanism (Nikitushkin et al., 2013).

Resuscitation from dormancy has been best studied in *Bacillus*, which forms highly resistant endospores (Dworkin and Shah, 2010; Setlow, 2014)and encodes an Rpf-like enzyme (Keep et al., 2006b). *Bacillus* spore germination can be promoted by the addition of peptidoglycan fragments (muropeptides) (Shah et al., 2008). These muropeptides bind to PrkC, a eukaryotic-like Ser/Thr kinase located in the spore membrane, initiating a signaling cascade that triggers spore germination(Shah et al., 2008). PrkC contains tandem PASTA (penicillin-binding protein and Ser/Thr kinase associated) domain repeats, and these domains can recognize both nascent peptidoglycan and muropeptides (Mir et al., 2011; Shah et al., 2008; Squeglia et al., 2011; Turapov et al., 2015; Yeats et al., 2002). A similar situation may exist in *Mycobacterium*, where emergence from latency can be stimulated by muropeptide binding to the PrkC homologue, PknB (Mir et al., 2011). It is worth noting, however, that mycobacterial resuscitation via this route is not robust, and the major function of muropeptide binding appears to be in directing the subcellular localization of PknB (Mir et al., 2011). The molecular basis for *Streptomyces* resuscitation, and the contribution made by the Rpf proteins to this process, remains to be determined.

There is considerable diversity in Rpf enzyme architecture, and a clear understanding of Rpf function requires not only a full characterization of the enzymes themselves, but also a systematic assessment of the contributions made by the different domains. Here, we show that Rpf accessory domains make critical contributions to enzyme activity. We establish that the Rpfs function as endo-acting lytic transglycosylases, and further demonstrate that their activity is independent of known signaling cascades associated with germination in other systems. Unexpectedly, our data are most consistent with a cell wall remodeling role for the Rpfs in *Streptomyces* spore germination.

3.3 MATERIALS AND METHODS

3.3.1 Bioinformatic analysis

Rpf domain configurations were identified using CDART (Geer et al., 2002). The HMMER webserver (Finn et al., 2015) was used to search the UniProtKB database to identify homologues of each Rpf configuration.

3.3.2 Bacterial strains and growth conditions

Bacterial strains used or created in this work are outlined in Table 3.1. *S. coelicolor* A3(2) strain M145 and its derivatives were grown at 30˚C on solid minimal medium (MM) or mannitol soya flour (MS) agar, with antibiotics to maintain plasmid selection where appropriate, or in new minimal medium with phosphate (NMMP), as described by Kieser *et al*. (Kieser et al., 2000). All *Escherichia coli* strains were grown at 37˚C on LB or nutrient agar (NA) plates (Kieser et al., 2000), or in LB or super optimal broth (SOB) liquid medium (Bertani and G, 1951; Hanahan, 1983) supplemented with antibiotics where appropriate to maintain plasmid selection.

3.3.3 Spore germination assay

To assess the germination efficiency of the different strains, spores were plated on MS agar overlaid with cellophane discs and incubated at 30˚C for up to 12 h. At the indicated time points, a 1 cm by 1 cm square was excised from the cellophane disc and examined using light microscopy. Images were acquired at 1000× magnification using a Nikon Eclipse E600 microscope fitted with DS-Fi1 camera. Image capture was performed using Nikon NIS-Elements software. Spore germination was then assessed, scoring germinated spores (those possessing at least one germ tube) versus non-germinated spores, with a minimum of 200 spores being assessed per strain, at each time point, in at least three independent trials. Spore scoring was performed using the cell counter plugin for ImageJ (Schneider et al., 2012). To test the effects of Ca^{2+} on germination, spores were plated on minimal medium (Kieser et al., 2000) with and without 10 mM $CaCl_2$. Spore germination assays were then conducted as described above.

3.3.4 Protein overexpression and purification

The sequence encoding the extracellular domain of each RpfA and RpfD variant [excluding the SignalP predicted signal peptide sequence (Petersen et al., 2011)] was amplified using the primers outlined in Table 3.2. Overlap extension PCR (Heckman and Pease, 2007) with the primers described in Table 3.2 was used to generate *rpfDΔLysM*. Other mutants were truncations of either RpfA or RpfD and were generated with the primers indicated in Table 3.2. Digested PCR products were cloned into the BamHI and NdeI restriction sites of pET15b (Novagen) (Table 3.1). Construct integrity was confirmed by sequencing using the T7 promoter and terminator primers (Table 3.2). Each plasmid was freshly transformed into *E. coli* Rosetta 2 cells (Table 3.1) prior to overexpression. Transformants were grown overnight at 37˚C in 5 mL of LB liquid medium supplemented

with ampicillin and chloramphenicol. These overnight cultures were used to inoculate 500 mL of LB medium, again supplemented with ampicillin and chloramphenicol. Cultures were grown at 37˚C until they reached an optical density at 600 nm (OD_{600}) of 0.6-1.0 (depending on the Rpf variant), at which point 1 mM isopropyl-β-D-thiogalactopyranoside (IPTG) was added to induce protein overexpression. Conditions for overexpression are summarized in Table 3.3. Overexpression of RpfDΔLysM was attempted at an initial OD_{600} of 0.4-1.2, using 0.25-2 mM IPTG, and induced cultures were grown for 1.5 h to overnight at 16, 30 or 37˚C. Overexpression was also attempted using *in vitro* translation with the PURExpress kit (New England Biolabs) following manufacturer's recommendations. None of the conditions tested yielded the desired protein.

For those proteins where overexpression was observed, cell pellets were resuspended in 5 mL of lysis buffer (50 mM NaH_2PO_4, 300 mM NaCl, 10 mM imidazole, pH 8.0) containing Complete Mini EDTA-free protease inhibitor (Roche) and lysed using the Constant Systems TS-2 0.75kW cell disruptor. The lysate was centrifuged at 10,000 × *g* for 20 min at 4˚C to remove insoluble debris. The clarified lysate was incubated with 1 mL of Ni-nitriloacetic acid (Ni-NTA) agarose (Thermo) for 1 hr at 4˚C before being applied to a chromatography column. The column was washed twice with 5 mL buffer (50 mM NaH_2PO_4, 300 mM NaCl, pH 8.0) containing 20 mM and 50 mM imidazole before His_6 tagged proteins were eluted sequentially with buffers containing 100 mM, 250 mM and 500 mM imidazole. The success of protein overexpression and the quality of protein purification was assessed by separating purified proteins (and their accompanying washes and crude soluble and insoluble fractions) on a 12% tricine polyacrylamide gel (Schägger, 2006) and staining with Coomassie Brilliant Blue. Protein concentrations were determined using a Bradford assay (Bradford, 1976) with bovine serum albumin as a standard. Each Rpf was dialyzed into storage buffer (50 mM NaH_2PO_4, 10% glycerol, pH 8) overnight to remove imidazole. Proteins were stored at 4˚C for a maximum of 24 h before all assays.

3.3.5 Enzyme activity assays

3.3.5.1 Quantitative Rpf activity assays

The EnzChek lysozyme assay kit (Molecular Probes) was used to assess the ability of the different RpfA and RpfD variants to cleave fluorescein-labelled *M. luteus* cell walls, as described previously (Sexton et al., 2015). Briefly, one nanomole of purified Rpf protein was added to each reaction, and the volume was brought to 50 µL with storage buffer before adding 50 µL of fluorescein-labelled *M. luteus* cell wall substrate. One picomole of lysozyme was used as a positive control, while a reaction without protein served as a negative control. Reactions were set up in black 96 well plates (Thermo). Fluorescein release was measured after 1 h using a Cytation 5 plate reader (BioTek) with an excitation wavelength of 494 nm and emission wavelength of 521 nm. Assays were conducted in technical triplicate, using at least two independent protein preparations.

These assays are currently being repeated using purified *Streptomyces* peptidoglycan (purified as described below for *M. luteus*).

3.3.5.2 Isolation and purification of peptidoglycan

Insoluble peptidoglycan for use in the enzymatic assays was isolated from *M. luteus* using the boiling SDS protocol and purified by enzyme treatment (amylase, DNase, RNase, and Pronase) as described by Clarke (Clarke, 1993); as Gram- positive bacteria, both *M. luteus* and *S. coelicolor* produce PG with limited 1,6-anhydromuramoyl content (Desmarais et al., 2013). O-acetyl groups were removed by incubating peptidoglycan in 20 mM NaOH at room temperature overnight and insoluble PG was isolated by centrifugation (9,000 × *g*, 30 min, room temperature) and washed with water at least three times. Teichoic acids were removed by extracting the peptidoglycan with 10% TCA overnight at room temperature and peptidoglycan was washed four times in water, frozen, lyophilized and stored at -20 °C.

3.3.5.3 [^{18}O]H_2O -based assay to differentiate between hydrolases and lytic transglycosylases

The [^{18}O]H_2O-based assays were conducted as described by Herlihey *et al*. (Herlihey et al., 2014) using *M. luteus* peptidoglycan as substrate. *M. luteus* peptidoglycan was resuspended to a final concentration of 1.4 mg/mL in [^{18}O]H_2O and briefly sonicated to homogenize the suspension. To start reactions, 1 nmol of purified Rpf protein was mixed with 100 µL of *M. luteus* peptidoglycan in [O^{18}]H_2O, and the reaction was brought to 200 µL with Rpf storage buffer. Reactions were incubated at 37˚C for 9.5 h with gentle shaking and then stopped by rapid freezing. Mutanolysin (1.1 nmol) was used as a positive control, while reactions without added protein were used as negative controls. Reaction mixtures were thawed and soluble reaction products were separated from insoluble peptidoglycan by centrifugation (15,000 × *g*, 15 min, 4 °C) prior to analysis by LC-Q-TOF-MS. The insoluble fractions were washed four to five times with 200 µL volumes of water and recovered each time by centrifugation (15,000 × *g*, 6 min, room temperature). The washed peptidoglycan pellets were resuspended in 0.1 mM potassium phosphate buffer, pH 6.2 and solubilized by mutanolysin (1.1 µmol, final concentration) prior to LC-Q-TOF-MS analysis. LC-Q-TOF-MS was performed by injecting samples into an Agilent 1260 Infinity liquid chromatograph interfaced to an Agilent 6540 UHD accurate Mass Q-TOF mass spectrometer as described previously (Herlihey et al., 2014). Mass spectrometry analysis was conducted at the Mass Spectrometry Facility at the University of Guelph.

Table 3.1: Plasmids and *Streptomyces coelicolor* and *Escherichia coli* strains

Strain or plasmid	Genotype, characteristic(s) and/or use	Reference or source
***Streptomyces coelicolor* A3(2) strains**		
M145	SCP1$^-$ SCP2$^-$	(Kieser et al., 2000)
E117	Δ*rpfA-E* (*rpf* null)	(Sexton et al., 2015)
J3385	3×Δ*PASTA*	(Hempel et al., 2012)
***Escherichia coli* strains**		
DH5α	Routine cloning	
ET12567(pUZ8002)	*dam dcm*; with transmobilizing plasmid pUZ8002	(MacNeil et al., 1992; Paget et al., 1999)
Rosetta 2(DE3)	Protein overexpression	Novagen
Plasmids		
pET15b	Overexpression of His_6 tagged proteins	Novagen
pMC177	pET15b carrying *rpfA*	(Haiser et al., 2009)
pMC200	pET15b carrying *rpfAΔLysM*	This study
pMC181	pET15b carrying *rpfD*	(Sexton et al., 2015)
pMC201	pET15b carrying *rpfDΔLytMΔLysM*	This study
pMC202	pET15b carrying *rpfDΔLysM*	This study

Table 3.2: Oligonucleotides used in this study

Primer Name	Sequence (5'- 3')[1]	Use
0974 PP 5'	CAGTACCATATGGCCGACGCGCGACCTGGGAC	Overexpression of RpfD
0974 PP 3'	CAGTACGGATCCTCAGATCCTGACGCCGCCGGC	Overexpression of RpfD
0974ΔlytM PP 3'	CATCATGGATCCCCGGGTGGTCCCCTGCCCGC	Overexpression of RpfDΔLytM
SCO0974ΔlysM rev	TGCTCTTGCTTCTGCTCTTTCAGTCCGGCCCGCTCCGAGCA	RpfDΔLysM overexpression
SCO0974ΔlysM fwd	AAAGAGCAGAAGCAAGAGCA	RpfDΔLysM overexpression
0974ΔlytMΔlysM PP3'	CATCATGGATCCTCCGGCCCGCTCCGAGCACA	Overexpression of RpfDΔLytM ΔLysM
3097 PP 5'	CAGTACCATATGGCCACCGCGTCCG	Overexpression of RpfA
3097 PP 3'	CGAAGTGGATCCTTACTTCAGGTGCAGCTGCTG	Overexpression of RpfA
3097ΔlysM PP 3'	CATCATGGATCCTCAGCCGGTGCCGCA	Overexpression of RpfAΔLysM
T7 promoter	TAATACGACTCACTATAGGG	Sequencing
T7 terminator	GCTAGTTATTGCTCAGCGG	Sequencing

[1]Introduced restriction sites are underlined

Table 3.3: Conditions for protein overexpression

	Induction OD_{600}	[IPTG] (mM)	Induction time (hr)	Induction temperature (˚C)	Molecular weight (kDa)[1]
RpfA	0.8	1	2.5	30	22.8
RpfAΔLysM	0.6	1	2.5	30	10.0
RpfD	0.8	1	5	30	42.6
RpfDΔLysM	0.8	1	16	16	30.3
RpfDΔLysMΔLytM	1	1	2.5	30	10.9

[1] Calculated without the SignalP predicted signal peptide and with the 6×His tag

3.4 RESULTS

3.4.1 Rpf domain diversity in the actinobacteria

The Rpf domain is found in proteins throughout the actinobacteria, in association with a variety of different protein domains (Machowski et al., 2014; Ravagnani et al., 2005). How these accessory domains influence the biological and biochemical function of different Rpfs remains unclear. To prioritize different architectures for investigation, we searched for Rpf domain-containing proteins in the streptomycetes, mycobacteria, micrococci and other actinobacteria (Table 3.4). We found the 'short Rpf' protein, comprising only a signal peptide and Rpf domain, was the most wide-spread in the actinobacteria. This configuration was, however, not widely conserved within any specific genus (Table 3.4).

Outside of the short Rpfs, there were interesting phylogenetic distributions associated with other common Rpf domain architectures. Within the mycobacteria, Rpf domains were most frequently found in conjunction with uncharacterized N- or C-terminal extensions, as observed for RpfA and RpfC-E in *M. tuberculosis* (Machowski et al., 2014; Ravagnani et al., 2005) (Table 3.4). These extended regions lacked any obvious functional domains, and were confined to Rpf-associated proteins in the mycobacteria. The corynebacteria also encoded a distinct subset of Rpf proteins associated with an uncharacterized DUF3235 domain (Ravagnani et al., 2005) (Table 3.4).

In addition to these genus-specific subsets, Rpfs were also associated with other functional domains, with two configurations being most highly represented: the RpfB sub-group, and the LysM-containing group (Table 3.4). Members of the RpfB group were found in a range of actinobacterial species, and contained a G5 domain and tandem repeats of the DUF348 domain. Recent structural studies on an RpfB variant from *M. tuberculosis* revealed an interesting ubiquitin-like fold for the DUF328 domain, and a close physical association between these domains and the G5 domain (Ruggiero et al., 2016, 2017). G5 domains bind to Glc*N*Ac residues and are thought to promote peptidoglycan binding (Bateman et al., 2005), while the DUF348 domains facilitate RpfB dimerization, and appear to negatively affect RpfB cleavage activity (Sexton et al., 2015). In contrast to the RpfB group, the LysM-containing group of Rpfs is the predominant

form in the streptomycetes and micrococci. The LysM domain, like the G5 domain from the RpfB subfamily, binds Glc*N*Ac residues (Mesnage et al., 2014), and is proposed to enhance Rpf binding to its peptidoglycan substrate. In the streptomycetes, many LysM domain-containing Rpfs also possess a LytM domain (Pfam: M23 metallopeptidase), which is expected to have endopeptidase activity and thus the potential to cleave either within peptide stems or peptide cross-bridges (reviewed in Firczuk and Bochtler, 2007; Grabowska *et al.*, 2015).

Table 3.4: Prevalence of Rpf configurations in the actinobacteria[1]

	Number in streptomycetes[2]	Number in mycobacteria[2]	Number in micrococci[2]	All actinobacteria[2]
$RpfA_{SC}$ (Rpf domain and LysM)	233 (60.2%)	0	5 (71.4%)	370 (27.9%)
RpfB (Rpf, G5, DUF348)	27 (7%)	101 (37.9%)	0	425 (32.1%)
RpfD (Rpf, LysM, LytM)	88 (22.7%)	0	0	89 (6.7%)
Short Rpfs	38 (9.8%)	60 (22.6%)	2 (28.6%)	209 (15.7%)
$RpfA_{Mtb}$	0	40 (15.0%)	0	40 (3.0%)
$RpfC_{Mtb}$	0	34 (12.8%)	0	34 (2.6%)
$RpfD_{Mtb}$	0	24 (9.0%)	0	24 (1.8%)
$RpfE_{Mtb}$	0	7 (2.6%)	0	7 (0.2%)
Rpf DUF3235	0	0	0	95 (7.2%)
Rpf, PG binding 1	1 (0.3%)	0	0	25 (1.9%)
Peptidase Rpf, SLT/GEWL	0	0	0	9 (0.7%)
Total	387	266	7	1327

[1] Based on bioinformatics analyses conducted on April 4, 2016
[2] Numbers in brackets are % of all Rpfs in each genera

3.4.2 LysM and LytM domains enhance Rpf activity

There is currently nothing known about how the Rpf-associated LysM and LytM domains contribute to Rpf activity. Given that the vast majority (>80%) of *Streptomyces* Rpf proteins possess one or both of these domains, we sought to determine how they influenced the biochemical activity of the Rpfs. To probe the functional contributions made by these domains, we created a truncated version of RpfA lacking the LysM domain (RpfAΔLysM), alongside two RpfD variants: one missing the LysM domain (RpfDΔLysM), and one lacking both the LysM and LytM domains (RpfDΔLysMΔLytM). We overexpressed and purified these proteins, along with their full length counterparts [minus their SignalP-predicted secretion signals (Petersen et al., 2011)], and evaluated the enzyme activity of each using a fluorescence-based peptidoglycan cleavage assay. The assay employs fluorescein-labelled *M. luteus* peptidoglycan as a substrate, where the fluorescein labelling is sufficiently dense so as to quench the fluorescent signal.

Peptidoglycan cleavage results in the release of fluorescein molecules, leading to increased fluorescence.

Mature versions of the full length and truncated RpfA and RpfD enzymes were added in equimolar concentrations to the fluorescein-labelled substrate. For both RpfA and RpfD, we found that enzymes lacking the LysM domain had 65-70% the activity of the full length variants (Fig. 3.1A). This suggested that peptidoglycan targeting by the LysM domain may help position the Rpfs on their substrate and enhance their cleavage capabilities. We observed that removal of the LytM domain from RpfD led to a further decrease in activity; RpfD lacking both LysM and LytM domains had only ~30% the activity of the full length enzyme (Fig. 3.1A).

The contribution of the LytM domain to RpfD activity may be enzymatic, as this domain typically has metallopeptidase activity, or it could provide an additional substrate specificity determinant. LytM peptidase activity requires a Zn^{2+} co-factor, and thus we tested the activity of all RpfD variants in the presence and absence of EDTA, which would be expected to chelate any associated Zn^{2+} ions. Unexpectedly, we found that EDTA had no effect on RpfD activity, irrespective of whether the LytM domain was present or not (Fig. 3.1B). This suggested that the RpfD-associated LytM domain may not function as an enzyme, and may instead provide additional targeting specificity for RpfD. We checked to see whether the LytM domain was lacking any of the key Zn^{2+}-binding or active site residues, as is the case for EnvC and NlpD in *E. coli*. However, all critical residues appeared to be present (Fig. 3.2), suggesting that the lack of enzyme activity is not due to the inability to bind the Zn^{2+} co-factor, nor to a degenerate active site.

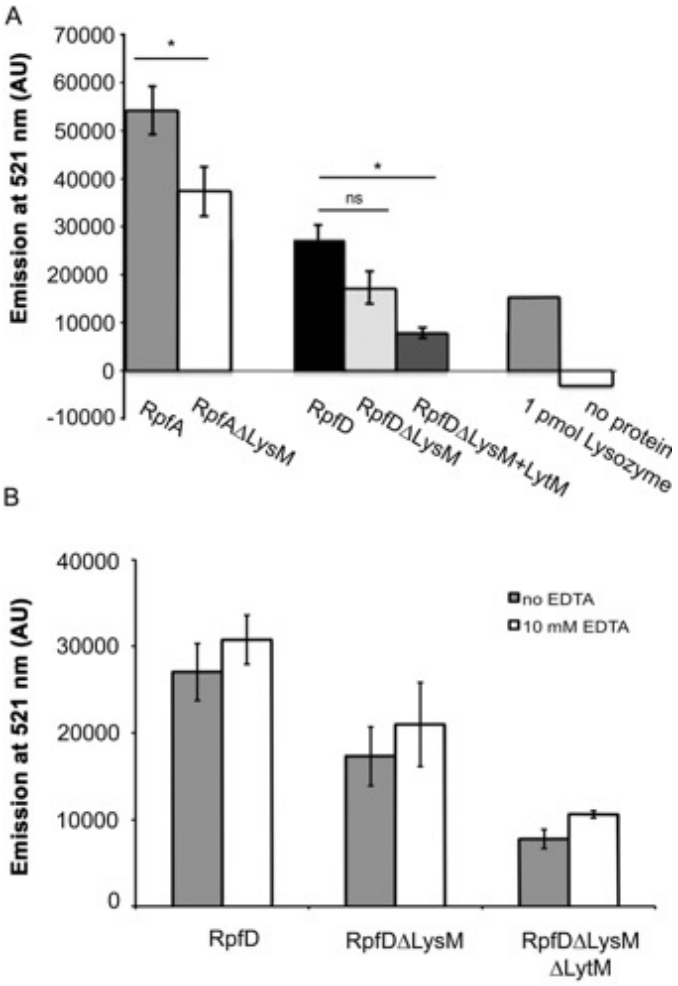

Figure 3.1: LysM and LytM domains contribute to Rpf activity. A fluorescence-based assay was used to quantify the activity of Rpf proteins. Purified protein was mixed with fluorescein-labelled cell walls and incubated at 37˚C for 1 h. Cleavage of the substrate allows for release of fluorescein, which can be detected by measuring the emission at 521 nm. **(A)** One nanomole of each protein (or 1 pmol of lysozyme) was mixed with fluorescein labelled *M. luteus* cell wall material. **(B)** As described for (A), only purified protein was incubated in storage buffer with or without 10 mM EDTA for 1 h at room temperature prior to setting up the peptidoglycan cleavage assays. For both (A) and (B), bars represent the average emission at 521 nm for of three independent biological replicates (two for RpfA), each of which is the average of three technical replicates, ± standard error. Statistical significance was assessed using the Student's *t*-test (* denotes $p < 0.01$; ns denotes not significant).

```
NlpD      -NKGIDIAGSKGQAIIATADGRVVYAGNALRG-YGNLIIIKHNDDYLSAYAHNDTMLVRE   58
RpfD      -HTGVDFPVPTGTSVKSVADGRVVSAGWGGSYGYQV-V-VRHGDGRYSQYAHLSAISVKS   57
LytM      AHYGVDYAMPENSPVYSLTDGTVVQAGWSNYGGGNQVTIKEANSNNYQWYMHNNRLTVSA   60
           . *:*        : : :** ** ** .           .  .   . * * . : *

NlpD      QQEVKAGQKIATMGSTGTSS-TRLHFEIRYKGKSV-----  92
RpfD      GQSVGVGQRLGRSGSTGNVTGPHLHFEVRTGPGFGSDVDP  97
LytM      GDKVKAGDQIAYSGSTGNSTAPHVHFQRMSGG--------  92
           :.* .*:::.  ****. :  ::**:
```

Figure 3.2: Catalytic residues in the LytM domain of *S. aureus* LytM are conserved in RpfD. Alignment of the amino acid sequence of LytM domains from *E. coli* NlpD, *S. aureus* LytM and RpfD from Clustal Omega. LytM catalytic residues are highlighted in grey. Asterisks denote residues that are conserved, colon denotes conservation of residues with strongly similar properties, and period denotes conservation of residues with weakly similar properties at a specific position.

3.4.3 Rpf domain functions as an endo-lytic transglycosylase

Having established that the LysM and LytM domains impact Rpf activities *in vitro*, we next set out to investigate the mechanistic basis underlying peptidoglycan cleavage by the various Rpf enzymes. We opted to study all five Rpfs from *S. coelicolor* (RpfA-E), as these enzymes represented four different structural classes (Rpf alone, RpfB, Rpf+LysM and Rpf+LysM+LytM). For this, we used the assay of Herlihey et al. (Herlihey et al., 2014) taking advantage of the fact that hydrolases require water to break their cognate glycosidic bonds. Thus, in the presence of water labelled with the stable isotope ^{18}O, hydrolase products would have an $[^{18}O]OH^-$ incorporated at the C-1 position, altering the isotopic distribution of products detected using mass spectrometry, relative to those produced in the presence of unlabelled water. In contrast, lytic transglycosylases do not use water in breaking the glycosidic bond in the peptidoglycan backbone, and as a result their muroglycan products would have an unaltered isotopic distribution.

M. luteus peptidoglycan, suspended in ^{18}O -labelled water, was thus used as a substrate for RpfA-E, and for the control hydrolytic enzyme mutanolysin. Being a highly active and efficient hydrolase, mutanolysin completely solubilized the peptidoglycan and we detected a variety of muroglycans by LC/MS analysis (Fig. 3.3). As expected, a number of these muroglycans were enriched with ^{18}O. Subsequent MS/MS analysis confirmed the association of this ^{18}O with only muramoyl residues (Fig. 3.4). In contrast, we detected very few soluble muroglycan products from each of the reactions involving RpfA, RpfB, RpfC and RpfE, while none were produced by RpfD (Fig. 3.3A). MS analyses

indicated that the few soluble muroglycans released did not contain ^{18}O. These data suggested that the Rpfs did not function as either muramidases or β-*N*-acetylglucosaminidases. Instead, tandem MS analysis revealed that the released soluble muroglycans contained Glc*N*Ac-1,6-anhydroMur*N*Ac (peptides) (Table 3.5), indicating that each of RpfA/B/C/E function as lytic transglycosylases.

We wondered if the lack of soluble product in reactions with RpfD, and the minimal amount produced by the other Rpf proteins, was due to a predominant endo-type lytic activity associated with each, where reaction products would remain crosslinked to the insoluble peptidoglycan sacculus. To analyze the insoluble fraction for any evidence of lysis, we washed the recovered insoluble peptidoglycan products and digested them with mutanolysin; any initial hydrolytic products of Rpf activity would retain their ^{18}O enrichment, if present, following this secondary digestion. As seen in Fig. 3.3B, the muroglycan profiles of peptidoglycan incubated with each of the Rpfs, including RpfD, followed by mutanolysin digestion (traces b-f), were distinct from the control reaction with mutanolysin alone (trace a). Tandem MS analysis of the unique muroglycan fractions revealed that none were enriched with ^{18}O and that the majority were linear oligomers terminating with an anhydromuramoyl residue (Table 3.5). These data thus suggested that each of the Rpfs function as endo-acting lytic transglycosylases.

Unexpectedly, the muroglycan profiles for each of the five Rpfs were similar, and any specificity for glycan chain length, peptide stem composition or cross-linking was not observed in the soluble or insoluble fractions. This suggested that the different domains associated with the Rpf proteins did not confer any obvious substrate specificity with respect to PG cleavage. However, it is important to note that the peptidoglycan compositions, specifically the variation of the third amino acid and interpeptide bridge, of *S. coelicolor* and *M. luteus* are different (Schleifer and Kandler, 1972).

Given the potential peptidase activity associated with the LytM domain of RpfD, we also closely examined the cleavage products for any hydrolytic activity not associated with the muroglycan backbone, but none were detected. These results were consistent with our *in vitro* analyses, suggesting that the LytM domain promoted RpfD functioning in ways that did not require peptidase activity.

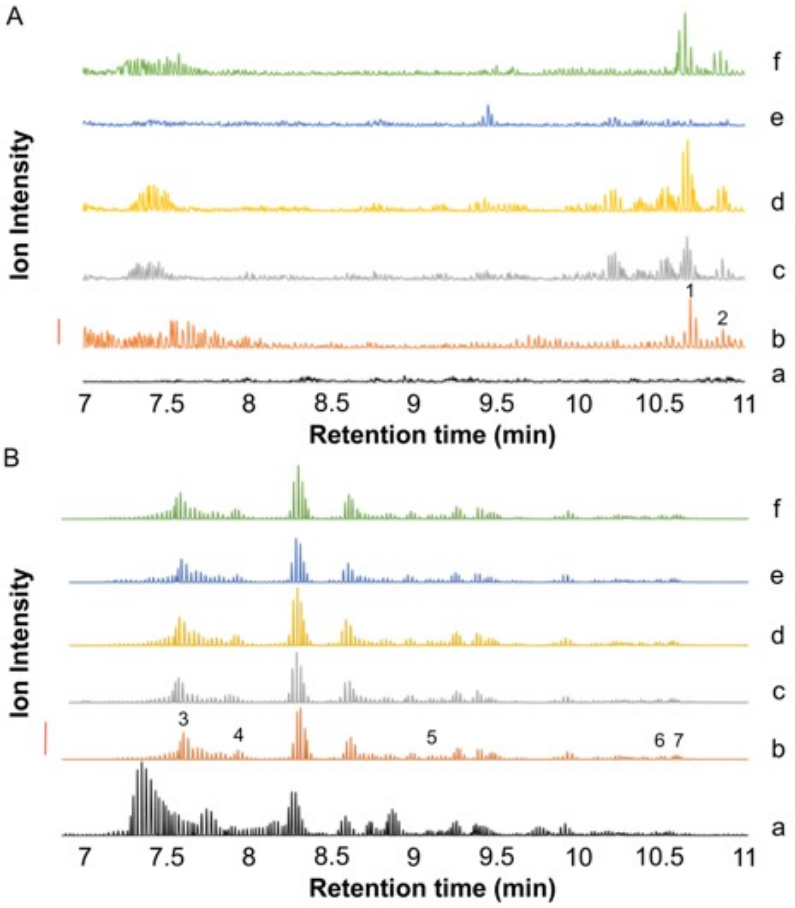

Figure 3.3: Characterization of RpfA-E as endo-lytic transglycosylases by LC-Q-TOF MS analysis of their reaction products. Samples of *M. luteus* peptidoglycan suspended in [^{18}O]H_2O to a final concentration of 1.4 mg·mL^{-1} were incubated separately with 1 nM Rpf or 1.1 µM mutanolysin (positive control). After incubation at 37°C for 9.5 h, soluble reaction products were separated from insoluble material by centrifugation. The insoluble peptidoglycan pellets from the Rpf digestions were washed with water and then resuspended in 0.1 mM potassium phosphate buffer, pH 6.2 for solubilization by 1.1 µM mutanolysin. Soluble muropeptides from this secondary digestion were recovered by centrifugation. Each soluble and secondary-soluble fraction was subjected to LC-Q-TOF MS analysis. **(A)** Analysis of soluble fraction from peptidoglycan alone (PG), and reactions with 1 nM of RpfA-E, as indicated. **(B)** Analysis of insoluble products following secondary mutanolysin digestion from reaction with 1.1 µM mutanolysin (Mut; positive control); or 1 nM of RpfA-E, as indicated. The identities of the numbered muropeptide fractions are listed in Table 3.4. The solid vertical bar to the left denotes 10,000 and 200,000 intensity units, for panel *A* and *B*, respectively.

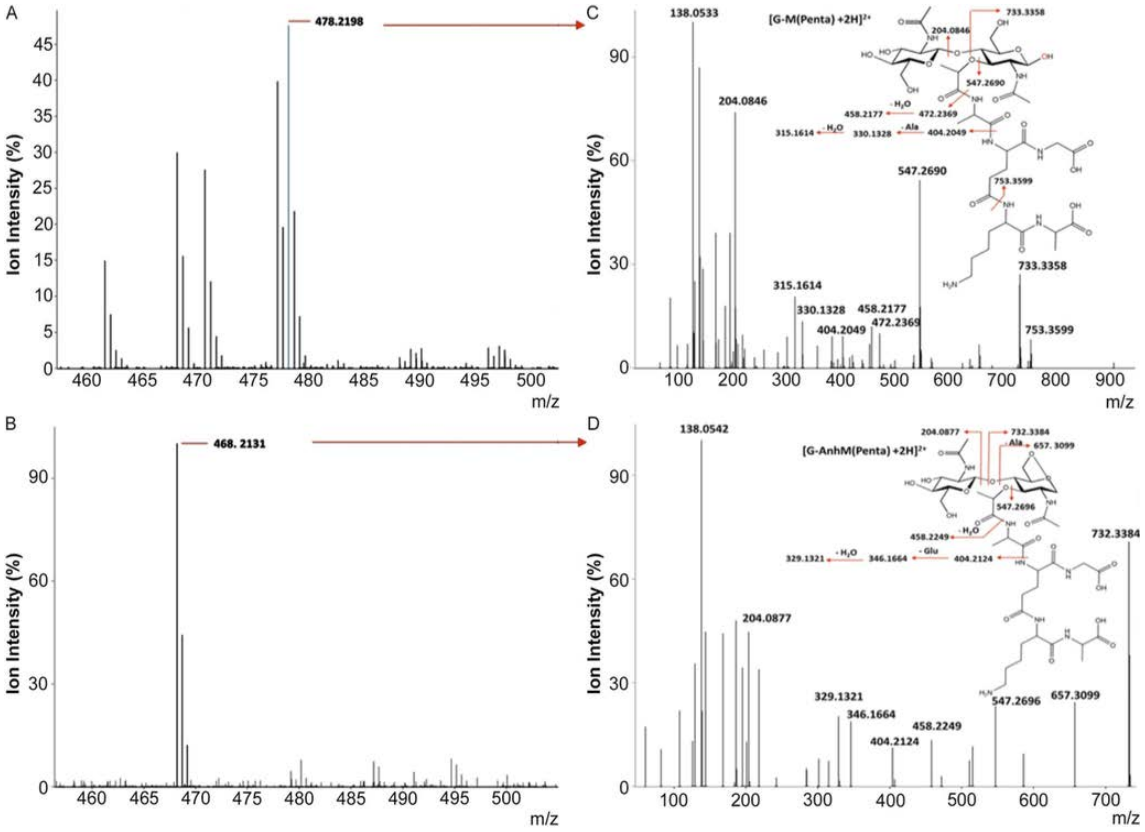

Figure 3.4: Tandem Q-TOF MS analysis of select muropeptides. Example MS analysis of parent ions for muropeptides recovered from (A) mutanolysin (positive control) and (B) soluble RpfA digests of *M. luteus* peptidoglycan by LC-MS as described in the legend of Figure 2. (C) and (D), Tandem Q-TOF MS analysis of denoted parent ions from corresponding panels (A) and (B). The blue spectral line in the MS spectrum of panel (A) denotes the ^{18}O-containing isotope of the respective muropeptide. The monoisotopic masses $(M+2H)^{2+}$ are presented for each of the identified fragments.

Table 3.5: ESI MS analysis of select muropeptides released from insoluble PG by RpfA-E

Fraction[1] No.	Annotation[2]	m/z Expected	m/z Observed RpfA	RpfB	RpfC	RpfD	RpfE	z
Rpf soluble reaction products								
1	G-$_{Anh}$M(Penta)	468.2050	468.2131	468.2112	468.2103	-	468.2121	2
2	G-$_{Anh}$M(Penta-Ala)	503.7250	503.7322	503.7326	503.7330	-	503.7309	2
Rpf insoluble reaction products								
3	G-$_{Anh}$M(Penta)	468.2050	468.2118	468.2117	468.2120	468.2137	468.2123	2
4	G-$_{Anh}$M(Penta-Ala)	503.7250	503.7300	503.7309	503.7300	503.7320	503.7306	2
5	G-M*-G-M(Penta)-G-$_{Anh}$M	616.6200	616.9644	616.6293	616.9655	616.6328	616.6308	3
6	G-M-G-M(Penta)-G-$_{Anh}$M(Penta)	782.0300	782.0290	782.0266	782.0266	782.0297	782.0269	3
7	G-M-G-M-G-$_{Anh}$M(Penta-Ala)	979.9350	979.9418	979.9393	979.9386	979.9434	979.9394	2

1. The muropeptide fractions correspond to those of the RP-HPLC separation presented in Fig. 3.1.
2. Identification of each muropeptide was made by tandem Q-TOF-MS analysis of each parent ion
G, GlcNAc; M, MurNAc; $_{Anh}$M, 1,6-anhydroMurNAc; Penta, $_{L}$-Ala-$_{D}$-Glu-(Gly)-$_{L}$-Lys-$_{D}$-Ala; *, O-acetylation

3.4.4 PASTA domain-containing Ser/Thr kinases in *S. coelicolor* inhibit germination and vegetative outgrowth

One hypothesis put forward to explain the role of Rpfs in cell resuscitation involves the release of muropeptide signals, which activate a regulatory cascade leading to the reactivation of metabolism. Such a model would be most consistent with exo-activity of the Rpfs, as this would promote the release of muropeptides; however, our results indicated that the Rpfs were endo-acting lytic transglycosylases.

In *Bacillus,* and to a lesser extent in *Mycobacterium,* the resuscitation-promoting signaling cascade is mediated through PASTA domain-containing Ser/Thr kinases (Mir et al., 2011; Shah et al., 2008). We considered two possibilities that could accommodate both the endo-activity of the Rpfs, and a role for Ser/Thr kinase signaling. In the first, the PASTA domain-containing kinases in *S. coelicolor* may recognize the ends of cleaved peptidoglycan rather than a defined muropeptide. The second involved Rpf-cleaved products serving as a substrate for other cell wall lytic enzymes, resulting in the release of germination-stimulating muropeptides that are recognized by these kinases.

S. coelicolor encodes three PASTA domain-containing protein kinases, and we obtained a triple mutant strain, here dubbed the 3×Δ*PASTA* strain (Table 3.1) (Hempel et al., 2012). We expected that this strain would have similar germination rates to that of an *rpf* null mutant if the Rpfs were involved in generating appropriate peptidoglycan ends or germination-promoting muropeptides that were recognized by these kinases. We measured germination rates of the triple mutant strain, and compared these to the wild type and *rpf* null strains. We found that germination of the 3×Δ*PASTA* strain was

consistently more rapid than either the wild type or the *rpf* null strain (Fig. 3.5A). This suggested that that the three PASTA domain-containing Ser/Thr kinases in *S. coelicolor* were not involved in recognizing a product produced directly or indirectly by the Rpfs. Instead, the rapid germination of these strains implied that the activity of these kinases may inhibit germination. We also assessed the growth of the 3×Δ*PASTA* strain in liquid minimal medium, to determine if it exhibited defects in vegetative growth compared to wild type and the *rpf* null strain. Consistent with our germination results, growth of the 3×Δ*PASTA* strain was faster than either comparator strain (Fig. 3.5B). These results suggested that these Ser/Thr kinases may function to delay germination/growth, given the enhanced rates of both processes in the absence of these enzymes, and further indicated that Rpf-dependent muropeptide signaling did not promote germination or impact the rate of vegetative growth of *S. coelicolor*, at least through the PASTA domain-containing Ser/Thr kinases.

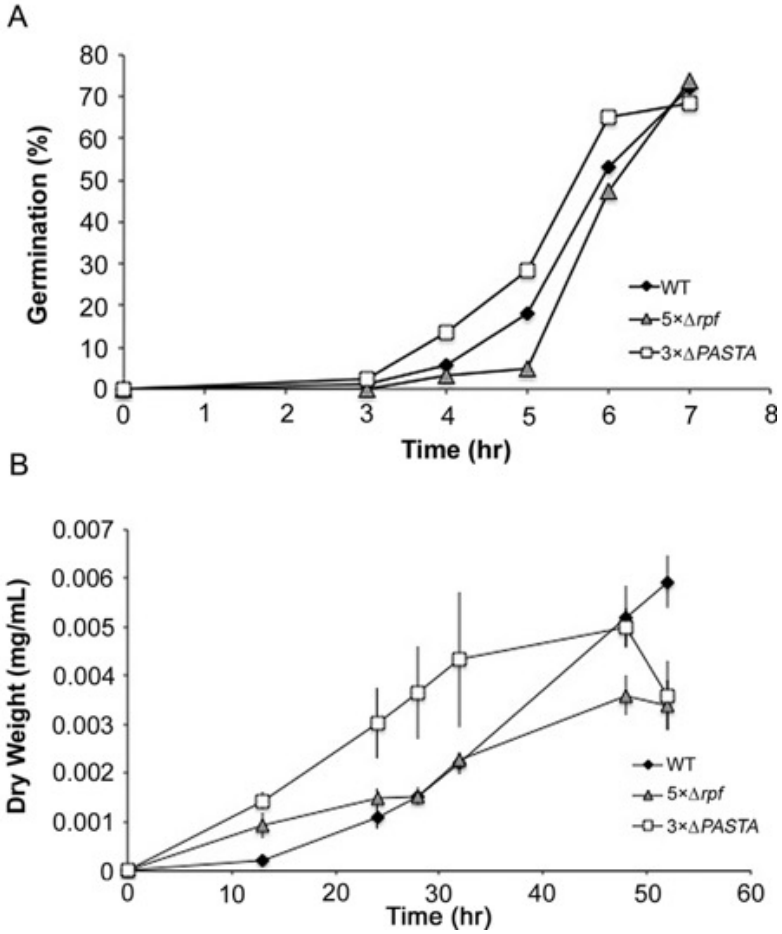

Figure 3.5: PASTA domain Ser/Thr protein kinases function independently of the Rpfs to affect spore germination and growth. (A) Wild type (WT), *rpf* null (5×Δ*rpf*) and PASTA Ser/Thr kinase null (3×Δ*PASTA*) spores were monitored for germination using light microscopy over the course of 8 h. Data are representative of three independent replicates ($n \geq 200$ spores per strain per time point). (B) Growth profiles of the wild type, *rpf* null and Ser/Thr PASTA kinase null strains in NMMP liquid medium. Data presented are the average of three independent replicates ± standard error.

3.4.5 Rpf activity is required for germination with alternative germinants

An alternative hypothesis to explain how Rpf enzymes promote germination is that their cell wall cleavage activities provide cells with an opportunity to insert new peptidoglycan, thus permitting cell expansion and growth. We predicted that if the role of the Rpfs was a physical one, we should be able to stimulate germination of the wild type strain – but not an *rpf* mutant – by adding a known germinant. To test this, we incubated spores on minimal medium in the presence or absence of germination-promoting calcium chloride (Eaton and Ensign, 1980). We followed germination over an

8 h time course, and found that calcium chloride effectively stimulated wild type spore germination but had little effect on the *rpf* null strain (Fig. 3.6). This supported the proposal that germination is inhibited at the outgrowth step in the *rpf* null strain.

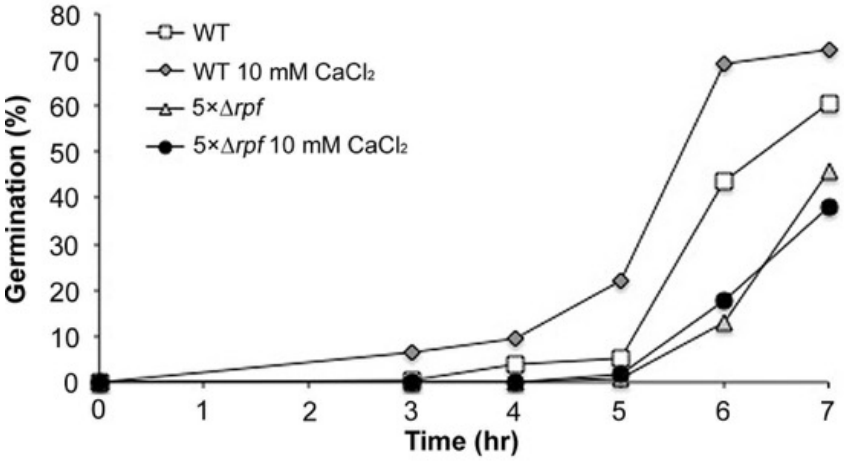

Figure 3.6: Germination of the *rpf* null strain cannot be stimulated by a known germinant. Germination of the wild type (WT) and *rpf* null (5×Δ*rpf*) strains on minimal medium with and without 10 mM calcium chloride was monitored over the course of 7 h using light microscopy. Data presented are representative of three independent replicates. ($n \geq 200$ spores per strain per time point).

3.5 DISCUSSION

Here, we demonstrated that Rpfs were endo-acting lytic transglycosylases, and their function was enhanced by a variety of associated domains. In the streptomycetes, we found Rpf function was not tied to an obvious signaling cascade. Instead our data were most consistent with a physical mechanism, structurally altering the germinating spore wall.

3.5.1 Role of LysM and LytM domains in Rpf activity

LysM-containing Rpfs represent one of the largest Rpf protein configurations in the actinobacteria, but the role of LysM domains in cell wall lytic enzymes is not universally conserved: some enzymes require these domains for activity, while others do not (Eckert et al., 2006; Mukamolova et al., 2002a; Steen et al., 2005; Wong et al., 2014). In the case of RpfA and RpfD, deleting the LysM domains decreased their cell wall lytic activity *in vitro*. LysM domains do not have catalytic activity of their own, and thus we suggest that the LysM domain, through its Glc*N*Ac binding, increases the affinity of Rpf

proteins for peptidoglycan, thereby enhancing enzyme activity. In their natural environments, LysM domains may further serve to anchor the Rpf proteins to the cell wall, thereby preventing indiscriminate peptidoglycan cleavage by these enzymes, and ensuring that the Rpfs remain a 'private good' rather than a shared product in mixed microbial communities. LysM domains have reduced affinity for peptidoglycan with longer peptide stems, which are common in spore peptidoglycan (van der Aart et al., 2018; Mesnage et al., 2014). Longer peptide stems in spore peptidoglycan could be a mechanism to reduce the activity of cell wall lytic enzymes, by reducing the affinity of the enzymes for their substrate. It remains to be seen if the Rpfs require the action of an endopeptidase or amidase to reduce peptide stem length to increase their activity during germination. Intriguingly, other peptidoglycan modifications that are commonly used to regulate the activity of cell wall lytic enzymes, such as deacetylation and *O*-acetylation, are not common in *Streptomyces* spore peptidoglycan (van der Aart et al., 2018; Vollmer, 2008).

In contrast to the LysM domains, LytM domains are expected to have catalytic activity, and function in cleaving stem/cross-bridge peptides. Intriguing, the RpfD-associated LytM domain does not appear to have peptidoglycan cleavage capabilities, at least in the assays conducted here. Despite the lack of LytM enzyme activity, removing the LytM domain, in conjunction with the LysM domain, significantly reduced the activity of RpfD beyond what had been observed by simply deleting the LysM domain. This implies that the LytM domain must contribute to RpfD function in some other way. It is possible that the LytM domain further enhances the affinity of RpfD for peptidoglycan through its peptide binding. Alternatively, it may serve to increase Rpf enzyme activity through allosteric activation, similar to the activation of AmiA, AmiB and AmiC by EnvC and NlpD in *E. coli* (Uehara et al., 2010).

Unlike EnvC and NlpD, however, the RpfD LytM domain has retained all active site and Zn^{2+}-binding residues, suggesting that it may still be enzymatically competent. Some LytM metallopeptidases require additional processing for activation (Firczuk et al., 2005; Odintsov et al., 2004). It is conceivable that such processing may occur upon secretion of RpfD to the *Streptomyces* cell surface, where the LytM domain then makes an enzymatic contribution to RpfD activity. Alternatively, this domain may be functionally silent when in the context of the RpfD polypeptide, but may be processed in such a way that it acts independently of RpfD. RpfD is unusual amongst the Rpfs in *S. coelicolor*, in that its expression peaks later in development, as opposed to during germination as is the case for all other Rpfs with detectable transcript levels (Sexton et al., 2015). It is therefore possible that its function, and that of its LytM domain, is more important at later stages of development than the other Rpfs in *S. coelicolor*. This would be consistent with the observation that LytM-containing Rpf proteins are found exclusively in the streptomycetes, and thus may function in aspects of development unique to these bacteria.

3.5.2 Revising the model of Rpf function during germination

How Rpfs promote resuscitation/germination is still being debated, 20 years after the discovery of these proteins. Do they function to liberate a signaling molecule that acts as a germinant? Or is their role more structural, where they permit cell expansion and new peptidoglycan incorporation through their cell wall cleavage activities?

Three lines of evidence support a peptidoglycan remodeling role for the *Streptomyces* Rpfs. One, we demonstrated that peptidoglycan-binding kinases, known to influence germination through a muropeptide-mediated signal transduction cascade in *Bacillus* (Shah et al., 2008), and to a lesser extent in *Mycobacterium* (Mir et al., 2011), are not associated with Rpf function in *S. coelicolor*. Instead, these kinases appear to negatively influence germination, based on the rapid germ tube outgrowth observed in their absence. Two, the endo-acting lytic transglycosylase activity of the Rpfs is more compatible with an architectural role than with a signaling role. Finally, a known germinant for *Streptomyces* (calcium chloride) stimulated germination of wild type spores, but had no effect on the germination of an *rpf* null strain. The fact that alternative germinants could not substitute for the lack of Rpfs, suggests that the Rpfs may be universally required for efficient germination. Notably, in *M. tuberculosis,* the equivalent experiment (treating dormant cells with both an Rpf inhibitor and oleic acid - a known germinant) led to metabolic reactivation (based on uracil uptake from the environment) but delayed cellular outgrowth (Demina et al., 2009; Shleeva et al., 2013), again suggesting that the Rpf role may be more structural. Taken together, the simplest explanation for these results would be that the Rpfs function to remodel the cell wall and promote cell expansion and growth after metabolic reactivation.

Our findings do not, however, definitively rule out an additional signaling role for the Rpfs. Indeed, a wide variety of muropeptides clearly enhance the resuscitation of *Mycobacterium* (Nikitushkin et al., 2013, 2015; Turapov et al., 2015). In *M. tuberculosis,* RpfB acts synergistically in association with the endopeptidase RipA (10), and a product of their activity (a peptidoglycan-derived disaccharide-dipeptide) has been proposed to promote mycobacterial resuscitation (Nikitushkin et al., 2015). It would seem, however, that additional glycosidic enzymes must be required, as the endo-lytic activity of the Rpfs would not allow for the generation of a disaccharide molecule. We suggest that muropeptide release may be a secondary effect of Rpf activity, and this could be accomplished either directly through the cleavage activity of Rpfs and any associated enzymes, or indirectly through cell growth and the associated peptidoglycan shedding that accompanies this process.

3.6 ACKNOWLEDGEMENTS

We thank Dr. Mark Buttner for the gift of the 3×PASTA mutant strain, and Dr. Dyanne Brewer of the University of Guelph Mass Spectrometry Facility for helpful discussions.

This work was supported by a grant from the Canadian Institutes for Health Research to M.A.E. (grant no. MOP-93635) and a grant from the Natural Sciences and Engineering Research Council to A.J.C. (RGPIN 03965). D.L.S. was supported by a Canada Graduate Scholarship.

3.7 CONFLICT OF INTEREST

The authors declare that they have no conflicts of interest with the contents of this article.

Chapter 4

Streptomyces explorers are biofilms

Danielle L. Sexton, Stephanie E. Jones, David A. Crisante, Matt Zambri and Marie A. Elliot

Chapter 4 contains unpublished work. Aside from the exceptions below, I performed all experiments, analyzed all data, and wrote the manuscript. David Crisante constructed the 5×Δ*chp* strain. Stephanie Jones constructed the Δ*cslA* strain and made the *mcherry* overexpression plasmids. Matt Zambri constructed the Δ*eps* mutant. Marie A. Elliot and I contributed to experimental design, data interpretation, and editing the manuscript.

4.1 ABSTRACT

Under low glucose, high amino acid conditions, *Streptomyces venezuelae* forms rapidly expanding hydrophilic colonies that are dramatically different from the classical *S. venezuelae* growth seen under standard laboratory conditions. Based on phenotypic similarity to biofilms produced by other bacteria, we hypothesized that *S. venezuelae* forms biofilms under these alternative growth conditions. We identified putative components of the extracellular matrix and demonstrated that deleting the genes involved in the production of these components alters the phenotype of these 'explorer' colonies. Based on matrix composition and colony behaviour, we propose that explorer colonies are biofilms.

4.2 INTRODUCTION

Under normal laboratory conditions, *Streptomyces venezuelae* forms hydrophobic, sporulating green colonies. However, under low glucose, high amino acid conditions, *S. venezuelae* enters into a non-branching, rapidly expanding mode of growth termed 'exploratory growth'(Jones et al., 2017). These colonies are dramatically different from 'classically' growing *S. venezuelae*. The colonies do not become hydrophobic, and feature an extremely wrinkled morphology. In addition, the rate of expansion of these colonies is much faster than for those grown under classical conditions. This is appears to be due to a passive, growth driven mode of motility analogous to sliding motility, where sliding motility is a passive means of traversing a substratum, and is facilitated by growth at the colony centre and the use of a surfactant to reduce surface tension (Kearns, 2010). Rather than growth occurring exclusively at the leading edge of explorer colonies, it appears as though growth occurs predominantly in the colony centre, where this serves to push the leading colony edge outward (Jones and Elliot, unpublished). We

hypothesize that a surfactant is secreted from explorer cells and coats the colony-substrate interface, reducing surface tension and increasing motility.

Based on visual similarities to biofilms, we hypothesized that *S. venezuelae* formed a biofilm during exploratory growth. Biofilms are arguably the most common type of microbial growth in the wild. One of the defining features of biofilms produced by bacteria and fungi is the biofilm matrix (Flemming and Wingender, 2010; Mitchell et al., 2016). The matrix promotes cell-cell and cell-surface adhesion, and for pathogenic microbes, may promote host invasion during infection (Flemming and Wingender, 2010; Mitchell et al., 2016). Biofilms are also extremely resistant to antimicrobial compounds. Decreased susceptibility is multifactorial, and includes reduced diffusion of compounds through the biofilm, sequestration of antibiotics by the biofilm matrix, the presence of antimicrobial compound modifying enzymes in the matrix, metabolic quiescence or dormancy of the biofilm cells, increased expression of efflux pumps, modification of the cell surface to reduce drug penetrance, and genomic heterogeneity (reviewed in Hall and Mah, 2017). Biofilm matrices produced by both bacteria and fungi are often composed of four main components: lipids, extracellular DNA (eDNA), extracellular proteins, and polysaccharides (reviewed in Hobley et al., 2015; Mitchell et al., 2016).

Of the major biofilm macromolecules, the least-studied of these are lipids. In fungal biofilms, matrix lipids have similar composition to that of the cell membrane, but feature an increase in the relative amount of polar lipids (Lattif et al., 2011). In bacterial biofilms, the role of lipids in the extracellular matrix remains poorly understood; however, they may play a role in the release of eDNA via membrane vesicles (Schooling and Beveridge, 2006; Schooling et al., 2009). eDNA has also been proposed to be released through cell death, resulting from the lateral pressure exerted on cells within the densely populated regions of the biofilm (Asally et al., 2012). Within the biofilm, eDNA is thought to function in promoting cell-cell adhesion (Flemming and Wingender, 2010).

Biofilm-associated polysaccharides vary considerably in bacteria, both with respect to composition and function. For example, in *Escherichia coli,* cellulose is a major component of the biofilm, whereas in *Bacillus subtilis*, the composition of the extracellular polysaccharide has not been well-characterized, however it has a role in the formation of the wrinkled biofilm architecture (Branda et al., 2004). In contrast, fungal biofilms incorporate polysaccharides that are similar in composition to the fungal cell wall; they are synthesized using similar sugars (Mitchell et al., 2016), but differ in branching patterns and precise composition relative to those used in cell wall synthesis (Mitchell et al., 2016).

In many bacterial biofilms, the major protein components in the matrix are organized into amyoid fibres. Amyloids are self-assembling polymers of proteins with a distinctive cross-β structure once assembled into the polymer. The initial polymerization of proteins into amyloid fibres is slow, until a threshold concentration of protein oligomers is reached, at which point rapid protein polymerization occurs. eDNA is proposed to

function as a nucleator for amyloid fibre assembly, promoting more rapid formation of amyloid aggregates. Amyloid fibres maintain the wrinkled morphology of the biofilm, which is thought to also be affected by cell death within the biofilm (Asally et al., 2012; Romero et al., 2010) Other protein components contribute to biofilm formation, however these are not uniform across model species. Surface appendages, such as pili and flagella, can promote biofilm formation and architecture in a wide variety of organisms (revied in Hobley *et al.*, 2015).

In *E. coli,* curli amyloid fibrils comprise the major protein component of the biofilm, and they help to promote biofilm formation (Chapman *et al.*, 2002; Serra *et al.*, 2013b). Curli facilitate cell-cell adhesion, cell-surface attachment, and host invasion. *E. coli* also produce flagella in biofilms, where the flagella contribute to biofilm architecture (Serra *et al.*, 2013b). Notably, curli and flagella are produced in distinct regions of the biofilm, with curli produced by cells localized to the top and the centre of the biofilm, while flagella are assembled by cells at the bottom and leading edge of the biofilm (Serra et al., 2013b). The middle zone, between the amyloid-rich top and flagellar-focused bottom of the colony, comprises a cellulose rich region (Serra et al., 2013b). Mutational analyses have suggested that each of these components impact the overall biofilm colony architecture (Serra et al., 2013b). For example, curli promote a wrinkled colony morphology, where deletion of the transcriptional activator for the curli operon (*csgD*) resulting in a smooth colony morphology (Serra *et al.*, 2013a). Inactivating the flagellar motor or deleting the main component of the flagellum results in the loss of the ring architecture between the wrinkled core and the periphery of the biofilm (Serra *et al.*, 2013a). eDNA has also been implicated in promoting curli fibre polymerization within the biofilms of *Salmonella enterica* serovar Typhimurium (Gallo et al., 2015).

Within a *B. subtilis* biofilm, the major protein components are amyloid fibrils composed of the TapA and TasA proteins. Wild type *B. subtilis* biofilms have a wrinkled appearance that is due to the presence of these amyloid proteins, alongside an extracellular polysaccharide (Branda et al., 2006). Deleting the gene cluster responsible for the production of either polymer results in a smooth colony phenotype (Branda et al., 2006). Biofilm formation also requires the assembly of a hydrophobic layer on the surface of the biofilm (Hobley et al., 2013). Without this layer, the biofilms are flat (Ostrowski et al., 2011). While eDNA is important during the initial stage of *Bacillus cereus* biofilm formation (Vilain et al., 2009), the role of eDNA in *B. subtilis* biofilms remains undefined. The matrix of the *B. subtilis* biofilm is thought to be uniform throughout, aside from the hydrophobic coating on the surface of the biofilm, in contrast to the stratified nature of the *E. coli* biofilm.

When considering bacterial and fungal biofilms, some common themes emerge. Biofilms are assembled on a substratum, where cells are aggregated into clumps, in the case of single celled organisms, or into multilayered, tightly associated bundles of hyphae, for filamentous organisms (Beauvais et al., 2007; Costa-Orlandi et al., 2017; Harding et al.,

2009). All biofilms have an extracellular matrix, is composed of polysaccharides, proteins, eDNA, and often lipids. The polysaccharide component often includes cellulose, while the protein component often features amyloid fibrils. The matrix as a whole promotes cell-cell and cell-substrate adhesion, and affects colony architecture. Finally, biofilm formation offers protection against antimicrobial compounds or other environmental stresses (reviewed in Hall and Mah, 2017). We unexpectedly discovered that *S. venezuelae* explorer colonies appeared to be encased in a biofilm-like matrix. In following up this initial observation, we sought to determine the composition and general properties of this apparent matrix. Our results raise the intriguing possibility that explorer colonies form motile biofilms.

4.3 MATERIALS AND METHODS

4.3.1 Bacterial strains and culture conditions

Bacterial strains created or used in this work are outlined in Table 4.1. *S. venezuelae* and its derivatives were grown on or in maltose, yeast extract, malt extract (MYM) agar or broth; mannitol, soya flour agar (MS), Difco nutrient agar (NA); Lysogeny Broth (LB) agar or broth; or yeast extract, peptone (YP) agar at 30˚C, supplemented with antibiotics (kanamycin, hygromycin, and apramycin at 50 μg/mL, and viomycin at 30 μg/mL) where appropriate for selection. All *E. coli* strains were grown at 37˚C, with the exception of BW25113 which was grown at 30˚C, on LB agar or NA plates, or in LB or super optimal broth (SOB) liquid medium supplemented with antibiotics as above to maintain plasmid selection where appropriate.

4.3.2 Cryogenic scanning electron microscopy

Seven day old colonies of wild type *S. venezuelae* were mounted on the surface of an aluminum stub with optimal cutting temperature compound (Agar Scientific Ltd., UK), before being plunged into liquid nitrogen slush at -210˚C. Samples were then transferred to the cryostage of an Alto 2500 cryotransfer system (Gatan, England) attached to a Zeiss Supra 55 VP field emission gun scanning electron microscope (Carl Zeiss Ltd., Germany). Surface frost was sublimated at -95˚C for 3 min before sputter coating with platinum for 5 min at 10 mA at below -110˚C. The sample was then moved to the cryostage held at -130˚C in the main chamber of the microscope. Samples were viewed at 3.0 kV.

4.3.2 Deletion of the rodlin genes

The three rodlin genes (*SVEN_4628, SVEN_4631, SVEN_4632*) and two intervening genes (*SVEN_4629, SVEN_4630*) were deleted using ReDirect technology (Gust et al., 2004). Cosmid Sv-5-A10 was checked via digestion with KpnI to ensure cosmid integrity. All five genes were replaced with a viomycin resistance cassette (*vph*) on cosmid Sv-5-10 (see Table 4.1 for plasmids and Table 4.2 for primers). The mutant cosmid was screened using a diagnostic primer pair located up and downstream of the replaced region (*rdl* KO check fwd and *rdl* KO check rev), which allowed for confirmation that the region was

replaced. Mutant cosmids were introduced into *E. coli* ET12567/pUZ8002 prior to conjugation into *S. venezuelae*. Exconjugants were screened for double crossover recombinants and disruption was confirmed using diagnostic PCR with the same set of primers, ensuring that the wild type gene cluster was no longer present. The phenotype was not dramatically different compared to the wild type, and consequently the mutation was not complemented.

4.3.4 *ebosin* cluster deletion and complementation

The ebosin gene cluster was deleted using ReDirect technology (Gust et al., 2004). The twenty genes in the predicted cluster (*SVEN_7180-7200*) were first replaced with a viomycin resistance cassette (*vph*) on cosmid Sv-4-G09 (see Table 4.1 for plasmid information and Table 4.2 for primer information). The cosmid was initially checked via digestion with EcoRI to ensure integrity. The mutant cosmid was screened by PCR using two diagnostic primer combinations, one set flanking the replaced region, and the second with one primer located outside the replaced region and the second located within *SVEN_7200* in the replaced region, which allowed for confirmation that the cassette replaced the desired gene cluster. Mutant cosmids were introduced into *E. coli* ET12567/pUZ8002 prior to conjugation into *S. venezuelae*. Exconjugants were screened for double crossover recombinants and disruption was confirmed using diagnostic PCR with the same two sets of primers as before, ensuring that the wild type gene cluster was no longer present. The phenotype was not dramatically different compared to the wild type, and as for the *rdl* mutants, was not complemented.

4.3.5 Colony surface area determination

1 uL of spore stock was spotted into the middle of a YP agar plate and allowed to air dry. Plates were incubated for 7 days at 30˚C. After 7 days, images of the plates were collected and the area tool in ImageJ (Schneider et al., 2012) was used to trace and calculate the surface area. The diameter of the plate, 10 cm, was used to scale images. Surface area was measured for three independent colonies for wild type and each mutant.

4.3.6 Lectin staining

Wild type *S. venezuelae* or matrix mutants containing the integrating plasmid pMS82 expressing *mcherry* constitutively from the *ermE** promoter, were spotted onto YP agar and grown for 7 days, or streaked onto MYM agar and grown for 24 h at 30˚C. Vegetatively growing colonies were excised from the MYM agar plate and washed onto coverslips using sterile Nanopure water. Explorer colonies were floated off the agar surface and onto coverslips using an excess of Nanopure water. Colonies were stained with 20 µg/mL of lectin fluorescein conjugates (Vector Labs, Canada) in phosphate buffered saline (PBS) pH 7.4 for 20 min. Colonies were washed ten times with PBS, after which they were mounted for imaging in 100 µL PBS.

4.3.7 TOTO-3 staining for extracellular DNA and DNase treatment

Wild type *S. venezuelae* containing pMS82 expressing *mcherry* constitutively from the *ermE** promoter was spotted onto YP agar and grown for 7 days at 30˚C. To assess the eDNA composition of the apparent explorer colony matrix, colonies were either treated with DNase, or with DNase buffer (negative control). For the DNase treatment, 20 µL of 2 U/µL of Turbo DNase (Ambion, United States of America) were applied to the colony surface (40 U in total) after 7 days growth, and incubated at 30˚C for 3 h. To examine eDNA composition during classical development, wild type *S. venezuelae* was grown on MYM for 24 hrs. Explorer and classically growing colonies were then transferred to coverslips using an excess of Nanopure water and stained with 20 µg/mL TOTO-3 (Molecular Probes, United States of America) in PBS for 20 min at room temperature. Colonies were washed ten times with 1 mL PBS prior to mounting for imaging in 100 µL PBS.

4.3.8 Chaplin cysteine labelling and maleimide staining

To visualize chaplin amyloids, and the location of specific chaplin proteins/fibres within the explorer colonies, we created cysteine-labelled variants of multiple chaplins, which would be amenable for staining with a maleimide-based dye (Kim et al., 2008). Control constructs were first generated, by cloning PCR amplified sequences for *chpE*, *chpG*, and *chpH*, including their promoter and terminator regions, into the EcoRV site of the integrating plasmid pMS82 (Table 4.1 for plasmids and Table 4.2 for primers). To create cysteine-labelled chaplin variants, overlap extension PCR was used to mutagenize the last codon before the stop codon to TGC (Cys), and the resulting product was cloned into the EcoRV site of pMS82. Plasmids were then conjugated into wild type *S. venezuelae* containing the integrating plasmid pSET152 carrying ther *ermE** promoter driving the expression of *mcherry.*

Spores were spotted onto YP agar plates and grown for 7 days at 30˚C prior to staining. Colonies were floated off the agar surface using an excess of sterile Nanopure water and transferred to glass coverslips. Colonies were washed three times with PBS to neutralize pH, after which they were coated with 20 µg/mL maleimide-Alexa647 (Molecular Probes, United States of America) in PBS. The labelling reaction occurred for 2 h at room temperature in a humidity chamber in the dark. Colonies were then washed ten times with 1 mL of PBS and mounted in 100 µL PBS prior to imaging (see below).

4.3.9 Fluorescence microscopy

All samples for fluorescence microscopy were imaged on a Leica SP5 confocal microscope at 100× total magnification for samples stained with fluorescein conjugated lectins or TOTO-3, and 630× total magnification for samples stained with maleimide-Alexa 647 using LAS Advanced Fluorescence software. For fluorescein conjugated lectin probes, the argon laser line was set to 2.5% power and the photon multiplier tube captured 494-588 nm, gain set to 1000. For mCherry (cell imaging), the 561 nm laser was

set to 69% power and the photon multiplier tube captured 578-626 nm, with the gain set to 1100. Finally, for Alexa647 (chaplin protein imaging) and TOTO-3 (eDNA imaging), the 633 nm laser was set to 27%, gain to 1000 and the photon multiplier tube collected 640-700 nm. The pinhole was set to 1 Airy unit (96.44 um at 100×, and 102.91 at 630×). For Z stacks, the minimum section thickness was used for sectioning at 100× (20.01 µm) and 630× (0.89 µm). Samples were imaged sequentially for dual coloured images. Z stacks were processed using the Sum Stacks function in ImageJ (Schneider et al., 2012).

4.3.10 Antibiotic sensitivity assays

Sterile 6 mm filter disks were saturated with the indicated amount of antibiotics or sodium dodecyl sulphate (SDS) in water and left to dry. To measure resistance during classical development, 5 µL of wild type *S. venezuelae* spores were dispersed evenly over the surface of MYM agar plates. Once dry, disks were either immediately placed on top of inoculated spores, to measure resistance during germination, or after 24 h growth at 30˚C, to measure resistance during sporulation. Plates were incubated for a total of 48 h at 30˚C. To measure resistance during exploratory growth, 2 µL of a spore stock at $2x10^7$ cfu/mL was spotted into the middle of a YP agar plate. Disks were either immediately added 1.5 cm from the spot or added onto the surface of the colony after seven days incubation at 30˚C. Colonies were incubated at 30˚C for a total of 14 days.

Table 4.1: Strains and plasmids used in this study

Strain or plasmid	Genotype, characteristic(s), and/or use	Reference or source
***Streptomyces venezuelae* ATCC 10712 strains**		
5×Δ*chp*	*chpB::scar; chpC::scar; chpD::scar*; *chpF::scar; chpG::scar*	D.A. Crisante and M.A. Elliot, unpublished
Δ*cslA*	*cslA::acc(3)IV*	S.E. Jones and M.A. Elliot, unpublished
Δ*ebosin*	*ebosin::vph*	This study
Δ*eps*	*eps::acc(3)IV*	M. Zambri and M.A. Elliot, unpublished
Δ*rdlABC*	*rdlABC::vph*	This study
***Escherichia coli* stains**		
DH5α	Used for routine cloning	
ET12567/pUZ8002	*dam dcm*; with transmobilizing plasmid pUZ8002	(MacNeil et al., 1992; Paget et al., 1999)
BW25113	Construction of cosmid-based knockouts	(Datsenko and

		Wanner, 2000)
Plasmids		
Sv-4-G09	Cosmid used for deletion of ebosin gene cluster	
Sv-5-A10	Cosmid used for rodlin deletion	
pSET152	Apramycin resistant integrative plasmid *int* ϕC31	(Bierman et al., 1992)
pSET152+P*ermE**-*mcherry*	Constitutive expression of *mcherry* from *ermE** promoter, apramycin resistant integrative plasmid *int* ϕC31	S.E. Jones and M.A. Elliot, unpublished
pIJ82	Hygromycin resistant integrative plasmid *int* ϕC31	Gift from H. Kieser
pIJ82+P*ermE**-*mcherry*	Constitutive expression of *mcherry* from *ermE** promoter, hygromycin resistant integrative plasmid *int* ϕC31	S.E. Jones and M.A. Elliot, unpublished
pMS82	Hygromycin resistant integrative plasmid *int* ϕBT1	(Gregory et al., 2003)
pMS82+*chpE*	Control for reactive cysteine labelling	This work
pMS82+*chpE G81C*	Cysteine reactive labelling of ChpE	This work
pMS82+*chpG*	Control for reactive cysteine labelling	This work
pMS82+*chpG G91C*	Cysteine reactive labelling of ChpG	This work
pMS82+*chpH*	Control for reactive cysteine labelling	This work
pMS82+*chpH A77C*	Cysteine reactive labelling of ChpH	This work

Table 4.2: Oligonucleotides used in this study

Primer Name	Primer Sequence (5'→3')	Use
Ebosin KO fwd	CGGCCGACGCGGCCGGGCGGGCCCGCGGCTGACGCCGGG ATTCCGGGGATCGTCGACC	ebosin cluster deletion (*SVEN_7180-7200*)
Ebosin KO rev	AGGTATGGAGCGCCGCAACAACCGGTACGTCATCGCGGGT GTAGGCTGGAGCTGCTTC	ebosin cluster deletion (*SVEN_7180-7200*)
Ebosin KO check up fwd	ACCTGGTGGGACGCAC	Check for ebosin deletion - upstream of *SVEN_7180*
Ebosin KO check int fwd	CGATGGAAACGGGCTGACTA	Check for ebosin deletion – in *SVEN_ 7200*
Ebosin KO check rev	GGGGGAGGTACGGTTAGC	Check for ebosin deletion – downstream of *SVEN 7200*

rdlABC KO fwd	GCCCCTGACGTGTGAACGTCGTCGCGCGGAGGCGGAACG ATTCCGGGGATCGTCGACC	deletion of *rdlABC;* – upstream of *rdlC*
rdlABC KO rev	CGTGGATGTTCCCTCCGGCCCTGGCGTGCGCGACGCGGA TGTAGGCTGGAGCTGCTTC	deletion of *rdlABC*; downstream of *rdlA*
rdlABC check fwd	GCGACCTTCTTGCAGTTCAT	downstream of *rdlA*
rdlABC check rev	TGAAGTGACGGCACACGTA	upstream of *rdlC*
rdlABC check int fwd	CAGGGTTCCCTGAACAAGCC	internal to *rdlC*
chpE fwd	CGAGAACCTAGGATCCAAGCACCGGGAGATCGCCC	ChpE cysteine labelling
chpE G81C rev	AGCAGTTGAGGGCGTGGTT	ChpE cysteine labelling
chpE G81C fwd	ACCACGCCCTCAACTGCTGA	ChpE cysteine labelling
chpE rev	GCTCACTGGTACCATGCATAAGGTGGCCGCGTACAACG	ChpE cysteine labelling
chpG fwd	CGAGAACCTAGGATCCAAGCACACCCCCCGCCTTCCGCT CG	ChpG cysteine labelling
chpG G91C rev	TCAGCAGCCGTAGCCG	ChpG cysteine labelling
chpG G91C fwd	CGGCTACGGCTGCTGATCCCCCGCACC	ChpG cysteine labelling
chpG rev	GCTCACTGGTACCATGCATAGACGCCCAGTACCGCAAG	ChpG cysteine labelling
chpH fwd	CGAGAACCTAGGATCCAAGCCCGACGCCAAGTCCTTC	ChpH cysteine labelling
chpH A77C rev	AGCAGTTGACGCAGGTGTT	ChpH cysteine labelling
chpH A77C fwd	GGCAACACCTGCGTCAACTGCTGACGTTGAACCTCGCC	ChpH cysteine labelling
chpH rev	GCTCACTGGTACCATGCATAGGCGAGAACGCCTCCG	ChpH cysteine labelling
pMS82 EcoRV fwd	TTTTTGGCCTTGAAATCGTT	PCR screening for cloning
pMS82 EcoRV rev	GCTTGGATCCTAGGTTCTCG	PCR screening for cloning

4.4 RESULTS

4.4.1 Explorer cells are surrounded by an extracellular matrix

The wrinkled architecture of exploring cells was reminiscent of biofilms formed by other bacteria and fungi. As a first step to probing the biofilm potential of exploring cultures, we used cryogenic scanning electron microscopy (cryo SEM) to assess whether explorer cells were encased in an extracellular matrix. We found that explorer cells at the colony centre, where the colony was extremely wrinkly, and at the periphery, where the colony was flatter, were surrounded by what appeared to be an abundant extracellular matrix, when compared with sporulating growing *Streptomyces* cells (Fig 4.1A and B). Air space

was visible around the aerial hyphae and spore chains, and this was not observed for exploring hyphae, suggesting the presence of additional extracellular substances. A better control for this experiment would be to compare explorers to vegetatively growing cells from classical development, however this was not possible due to instrument limitations.

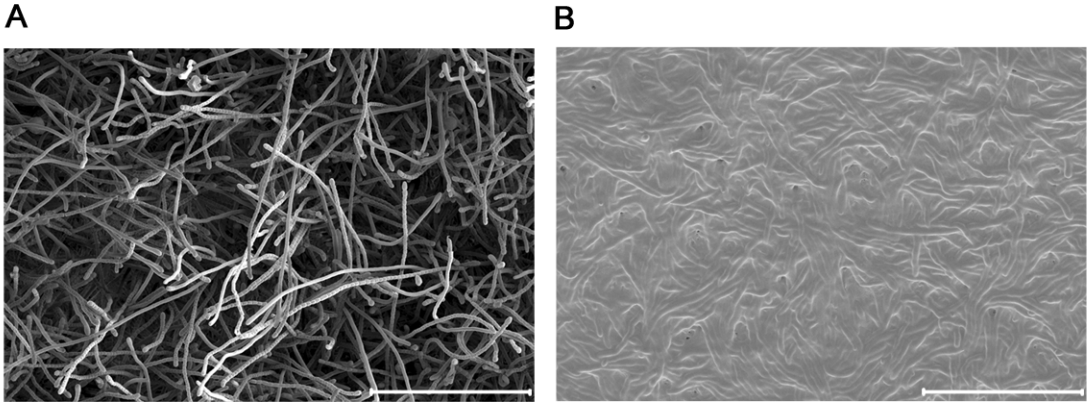

Figure 4.1: Explorer cells are encased in a thick extracellular matrix. (A) Cryo scanning electron micrograph of classically growing *S venezuelae* during sporulation. (B) Cryo-scanning electron micrograph of 7 day old *S. venezuelae* explorer cells from the middle of the colony. Scale bar = 25 μm.

4.1.2 Bioinformatic screen for potential matrix components

We next sought to identify components that may contribute to the apparent extracellular matrix. Using previously acquired RNA-seq data (Jones et al., 2017), we focused our attention on genes whose products could contribute to matrix formation, and examined their relative transcript levels during exploration versus static culture growth. Notably, the expression of the chaplin (*chp*) and rodlin (*rdl*) families of functional amyloid-encoding genes were up-regulated during exploratory growth (Fig. 4.2). This is suggestive of a potential role for these proteins in matrix formation. In classical development, the chaplin proteins form a hydrophobic sheath that coats the surface of aerial hyphae and spores (Claessen et al., 2003; Elliot et al., 2003). Interestingly, explorer colonies are not hydrophobic, apart from when they are associated with yeast, under specific growth conditions (and the RNA used for the analyses here was not harvested from these sporulating cells).

The polysaccharide component of the matrix was not immediately obvious from the RNA-seq data, with no polysaccharide biosynthetic clusters being upregulated in exploring cultures. So instead we turned to genomic searches, alongside information available for other biofilm-associated polysaccharides. We hypothesized that cellulose may be a component of the *S. venezuelae* biofilm matrix, due to the importance of

cellulose in static liquid culture and in biofilms produced by other bacteria. The cellulose synthase-encoding gene *cslA* is expressed at low levels in static and exploring colonies, although it is worth noting that its expression increases during exploratory growth.

To identify additional polysaccharide components, the *S. venezuelae* genome was searched on the *Streptomyces* annotation server StrepDB (http://strepdb.streptomyces.org.uk/) for genes annotated as glycosyltransferases. The resulting 16 hits were screened for the presence of adjacent genes annotated as being involved in production, modification, secretion or degradation of polysaccharides, alongside increased transcript levels in exploring *S. venezuelae* compared to static *S. venezuelae* (Jones et al., 2017). Two additional polysaccharide clusters of interest were identified using this method. The first, an *eps* cluster (*SVEN4634-4644)* was annotated as a capsular polysaccharide biosynthesis gene cluster (Fig. 4.3A, Table 4.3). This cluster was located immediately upstream of several *chp* and *rdl* genes, which made it of particular interest. The *eps* cluster included a putative β-mannosidase-encoding gene (Table 4.3), suggesting that the resulting polysaccharide may be mannose-rich, as gene clusters encoding polysaccharides often contain enzymes for degrading their product. This second cluster, the ebosin biosynthesis gene cluster (*SVEN_7180-7200*) (Fig. 4.3B, Table 4.4), was first characterized in *Streptomyces* sp. 139, where it directed the production of a complex extracellular polysaccharide composed of rhamnose, xylose, glucose, mannose, arabinose, fucose, and galactose (Jing et al., 2003). Both the *eps* and *ebosin* gene clusters were not expressed under static growth conditions, and were expressed at low levels in mature, 14 day old explorer colonies. Both clusters contain several putative glycosyltransferases, in addition to genes predicted to be involved in polysaccharide biosynthesis and modification, degradation, and secretion (Fig. 4.3).

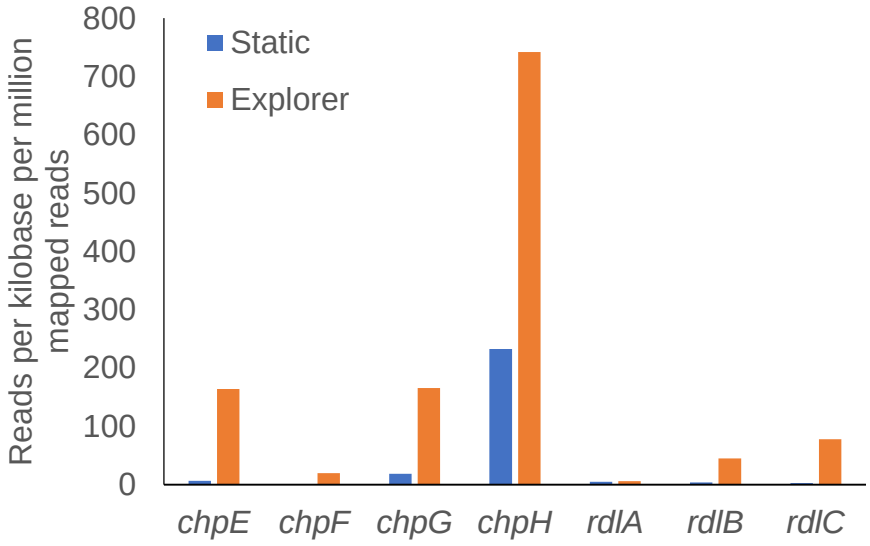

Figure 4.2: Expression of chaplin and rodlin genes during exploration and static culture. RNA abundance for the four annotated chaplin (*chp*) and three rodlin (*rdl*) genes in *S. venezuelae* ATCC 10712 were compared for cells grown under static (blue) and exploratory (orange) conditions. RNA abundance was measured using reads per kilobase per million mapped reads (RPKM). *chpD* is not annotated in the *S. venezuelae* ATCC 10712 genome, and thus no reads were assigned to it. Raw data were analyzed using the RNA-seq data generated by Jones *et al.*, 2017.

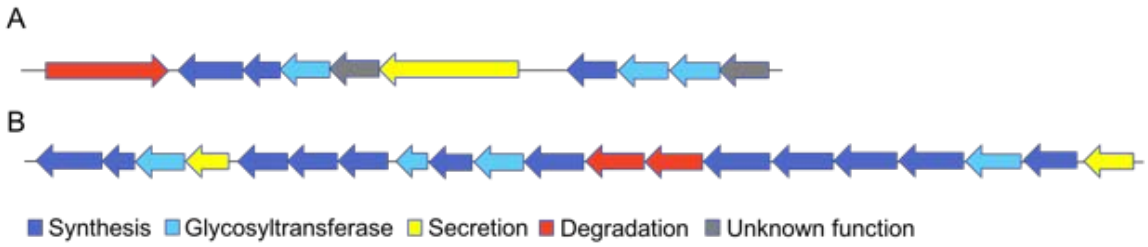

Figure 4.3: *eps* and *ebosin* gene clusters feature enzymes involved in all steps of exopolysaccharide biosynthesis. The (A) *eps* gene cluster and (B) *ebosin* gene cluster contain several predicted glycosyltransferases (light blue) in addition to other genes involved in tailoring or modifying polysaccharides (dark blue). These clusters also contain genes for putative secretory enzymes (yellow) and degradation enzymes (red). Genes of unknown function are marked in grey.

Table 4.3: *eps* gene cluster functional annotation

Gene	Predicted function	Classification
SVEN_4634	Putative β-mannosidase	Degradation
SVEN_4636	Acetyltransferase	Synthesis
SVEN_4637	Capsular polysaccharide biosynthesis protein	Synthesis
SVEN_4638	Glycosyltransferase	Glycosyltransferase
SVEN_4639	Carbohydrate esterase	Degradation
SVEN_4640	MurJ like protein	Secretion
SVEN_4641	Homologous to O-antigen ligase	Synthesis
SVEN_4642	Capsular polysaccharide biosynthesis protein – sugar transferase	Glycosyltransferase
SVEN_4643	Glycosyltransferase	Glycosyltransferase
SVEN_4644	Unknown function	Unknown function

Table 4.4: *ebosin* gene cluster functional annotation

Gene	Predicted function	Classification
SVEN_7180	Glutamate-1-semialdehyde 2,1-aminomutase	Synthesis

SVEN_7181	Isomerization of dTDP-4-dehydro-6-deoxy -D-glucose with dTDP-4-dehydro-6-deoxy-L-mannose	Synthesis
SVEN_7182	Glycosyltransferase	Glycosyltransferase
SVEN_7183	Glycosyltransferase	Glycosyltransferase
SVEN_7184	Similarities to translocase for O-antigen	Secretion
SVEN_7185	Zinc peptidase	Amino peptidase
SVEN_7186	Extended short chain dehydrogenase/reductase	Synthesis
SVEN_7187	GlcNAc-PI de-N-acetylase (GPI biosynthesis)	Synthesis
SVEN_7188	Glycosyltransferase	Glycosyltransferase
SVEN_7189	Methyltransferase	Synthesis
SVEN_7190	Glycosyltransferase	Glycosyltransferase
SVEN_7191	Weak similarity to O-antigen ligase	Synthesis
SVEN_7192	Pectate lyase	Degradation
SVEN_7193	Heparinase II/III –like/alginate lyase	Degradation
SVEN_7194	Sugar dehydrogenase	Synthesis
SVEN_7195	Glucosamine 6-phosphate synthetase	Synthesis
SVEN_7196	Hypothetical protein; Wzz superfmily domain – chain length determinate in O-antigen biosynthesis	Synthesis
SVEN_7197	Hypothetical protein; Wzz superfmily domain – chain length determinate in O-antigen biosynthesis	Synthesis
SVEN_7198	Glycosyltransferase	Glycosyltransferase
SVEN_7199	UDP-glucose or GDP-mannose dehydrogenase	Synthesis
SVEN_7200	Undecaprenyl-phosphategalactosephosphotransferase; EPS sugar transferase domain	Secretion

4.4.3 Deletion of putative matrix components affects explorer colony morphology

Different members of the lab focused on deleting the cellulose synthase-encoding gene (*cslA*; *SVEN_5061*), and the *eps* cluster (*SVEN_4634-4644*), while I deleted the ebosin biosynthesis cluster (*SVEN_7180-7200*). All twenty genes in the ebosin cluster were replaced with a viomycin resistance cassette. Another colleague has focused on deleting the chaplin genes from *S. venezuelae*. To determine if the products of these genes/clusters impacted exploratory growth, we examined these mutants under

exploration-promoting growth conditions, and tested to see whether they exhibited defects in exploration, colony formation or wrinkling patterns.

Compared to the wild type strain (Fig. 4.4A), the 5xΔ*chp* mutant explorer colonies were smaller and featured extremely pronounced wrinkles at the centre, with few wrinkles at the colony periphery (Fig. 4.4B and 4.5). The Δ*rdlABC* mutant was slightly smaller than wild type, but has a similar wrinkling pattern (Fig. 4.4C and 4.5) The Δ*cslA* mutant was also smaller than wild type, and the centre of the colony was white and very hydrophobic, reminiscent of aerial hyphae production during classical development (Fig. 4.4D and 4.5). In addition, the wrinkles at the colony periphery were taller and more pronounced than the wild type. By contrast, the Δ*ebosin* explorer colonies looked similar to wild type, although they may have had slightly reduced wrinkling in the centre (Fig. 4.4E and 4.5). Finally, the Δ*eps* explorers were much larger than wild type and featured a dramatically different wrinkling pattern (Fig. 4.4F and 4.5). The wrinkled core at the centre was almost non-existent, with large, tall wrinkles extending outward from the centre. Δ*eps* explorer colonies could be readily lifted off the agar surface for imaging; however, this led to release of the larger wrinkles, suggesting that these wrinkles were due to tissue buckling, as opposed to matrix-directed biofilm architecture. Complementation and cryo SEM imaging of these mutant strains are currently underway.

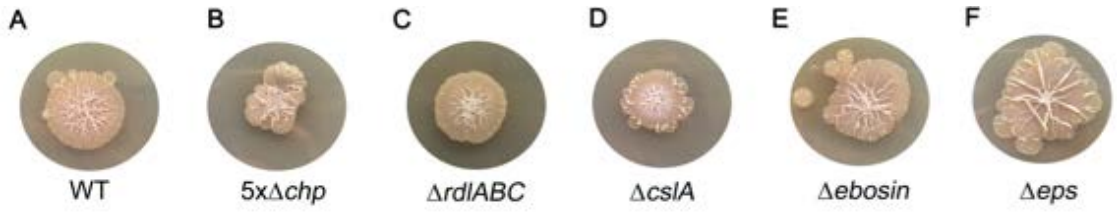

Figure 4.4: Deleting components of the extracellular matrix changes the biofilm phenotype. Images of 7 day old (A) wild type, (B) 5×Δ*chp*, (C) Δ*rdlABC*, (D) Δ*cslA*, (E) Δ*ebosin*, and (F) Δ*eps* explorer colonies grown on YP agar. Images are representative of three independent replicates. WT, wild type.

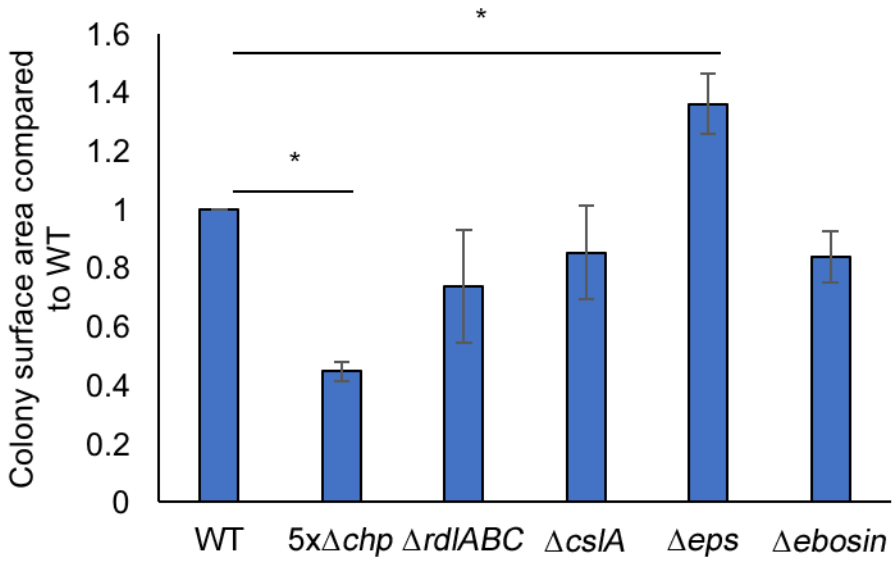

Figure 4.5: Colony surface area of mutant explorers compared to wild type. Colony surface area of mutant and wild type explorers was measured after 7 days growth. Data are average surface area of mutants divided by the wild type from three independent replicates ± one standard deviation. * denotes $p < 0.05$ using Student's t test. WT, wild type.

4.4.4 Chaplins coat hyphae on the exposed surface of explorer colonies

When working to image explorer colonies, we discovered that wild type biofilms lift off the plate readily when water is applied to the agar surface. Notably, however, 5xΔ*chp* explorer colonies failed to lift off the colony surface. This implied that the chaplins could coat the colony-substratum interface, and raised the tantalizing possibility that they functioned as motility-promoting surfactants.

To begin to localize the chaplin proteins within the explorer colonies, we used a reactive cysteine labelling approach coupled with confocal laser scanning microscopy. The carboxy termini of the chaplin proteins were predicted to be surface-exposed based on their predicted protein structure in amyloid fibrils (Capstick et al., 2011). Therefore, we substituted the terminal amino acid of ChpE, ChpH and ChpG (either a glycine or alanine), with a cysteine. These reactive cysteine-labeled chaplins were then expressed under their native regulatory elements *in trans* on an integrating plasmid in wild type *S. venezuelae*. To control for the addition of the second copy of these modified chaplin genes, a wild type (non-modified) version of each gene was also expressed using the same strategy. Explorer colonies constitutively producing mCherry, were then engineered to express ChpE G81C, ChpG G91C or ChpH A77C (or their wild type counterpart). After 7 days growth, the exploring cultures were stained with maleimide-Alexa647, a dye that reacts with free thiol groups (Fig. 4.6). Staining was not observed at lower magnification, so images were taken at 630× magnification to permit visualization

of individual hyphae, and at the periphery of the colony, where the colony was thinner. The hyphae were still densely packed, however, which made it difficult to distinguish individual hyphae in the brightfield images. For all three labeled chaplins examined in this study, fluorescence was associated strongly with hyphae on the surface of the colony. It was surprising to find that the ChpE G81C and ChpG G91C fluorescence signals were more intense than ChpH A77C, as our RNA-sequencing data had suggested that *chpH* was more highly expressed during exploratory growth (Fig 4.2).

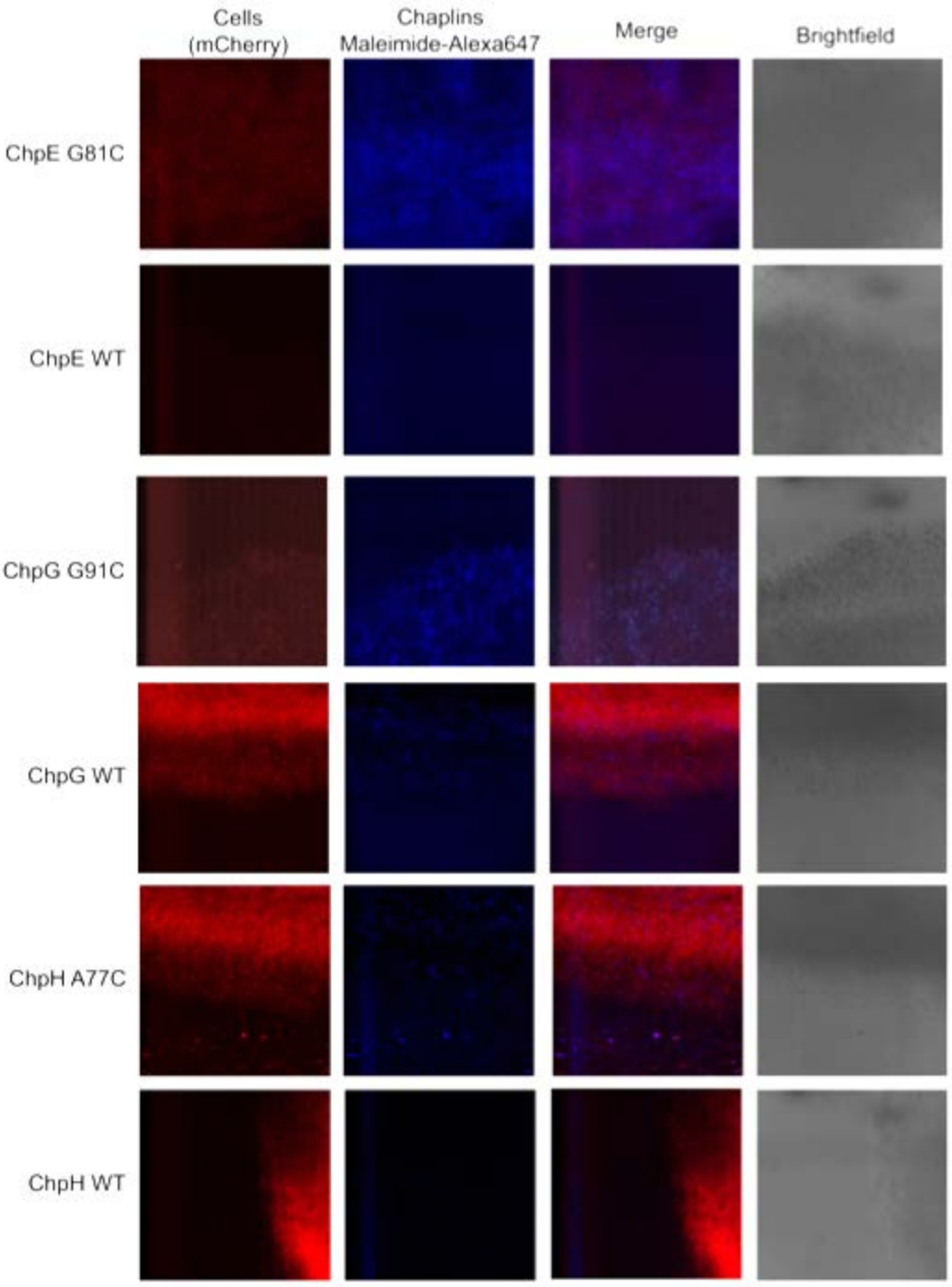

Figure 4.6: Chaplins are associated with hyphae during exploratory growth. Seven day old explorer colonies constitutively producing mCherry were stained with maleimide-Alexa647 and imaged at 630× magnification. Images are representative of three independent replicates.

4.4.5 The polysaccharide composition of explorer colony surfaces is different than that of classic vegetatively growing cells

In an effort to determine the composition of the matrix carbohydrates, and assess their localization, we used a series of fluorescein conjugated lectin probes that were specific for different carbohydrate modules. These probes were applied to both vegetative (classically growing) cells and explorer colonies, and these were imaged using confocal laser scanning microscopy. Each of the strains used for these analyses were constitutively producing mCherry, to facilitate co-localization of lectin staining with cells within the putative biofilm. Calcofluor white, used to visualize cellulose, was not used as this stain was not compatible with the laser lines on the microscope we had been using for these experiments.

We started by probing for conventional polymers associated with Gram- positive bacterial cell walls – specifically, the polysaccharides associated with the glycan strands of peptidoglycan, and those associated with teichoic acids. Concanavalin A (ConA) recognizes internal and nonreducing terminal α-D-glucosyl and α-D-mannosyl groups; these polysaccharides were expected to be found in teichoic acids, and possibly in the polysaccharides produced by the *eps* and ebosin clusters. Interestingly, we found that ConA did not bind to explorer colonies; however, it reacted strongly with the periphery of classic vegetatively growing colonies (Figs. 4.7 and 4.8, Table 4.5). Similarly, wheat germ agglutinin (WGA), which binds *N*-acetylglucosamine associated with bacterial peptidoglycan, strongly bound to the periphery of vegetatively growing *S. venezuelae* colonies, but bound with less affinity to explorer colonies (Figs. 4.7 and 4.8, Table 4.5). These results suggested that either explorer cultures had a different cell wall architecture than classically growing vegetative cells, or that their cell wall was simply not accessible to ConA and WGA stains in the same way as classically growing cells. It also raised the question of whether the products of the ebosin and *eps* clusters contributed to explorer colony architecture, or whether the associated polymers simply did not contain D-glucosyl or D-mannosyl groups.

We also tested a range of fluorescent lectins that recognized different sugars, including lectins with the potential to bind components of the predicted ebosin product (*e.g.* galactose). Soybean agglutinin (SBA) recognizes *N*-acetylgalactosamine and galactose, and could be seen binding strongly throughout vegetatively growing colonies, while weak binding was seen for explorer colonies (Fig. 4.7 and 4.8, Table 4.5). Other lectins, including *Dolichos biflorus* agglutinin (DBA), which also recognizes *N*-acetylgalactosamine; peanut agglutinin (PNA), which recognizes β-galactose-1,3-*N*-acetylgalactosamine; *Ricinus communis* agglutinin 120 (RCA120), which recognizes a non-reducing terminal β-D-galactose or *N*-acetylgalactosamine sugar, all failed to bind to either exploring or vegetatively growing colonies.

Collectively, our results suggested that there were significant differences between classic vegetatively growing cells and explorer cultures, with respect to their

polysaccharide profiles, although the reasons underlying these differences remain to be elucidated.

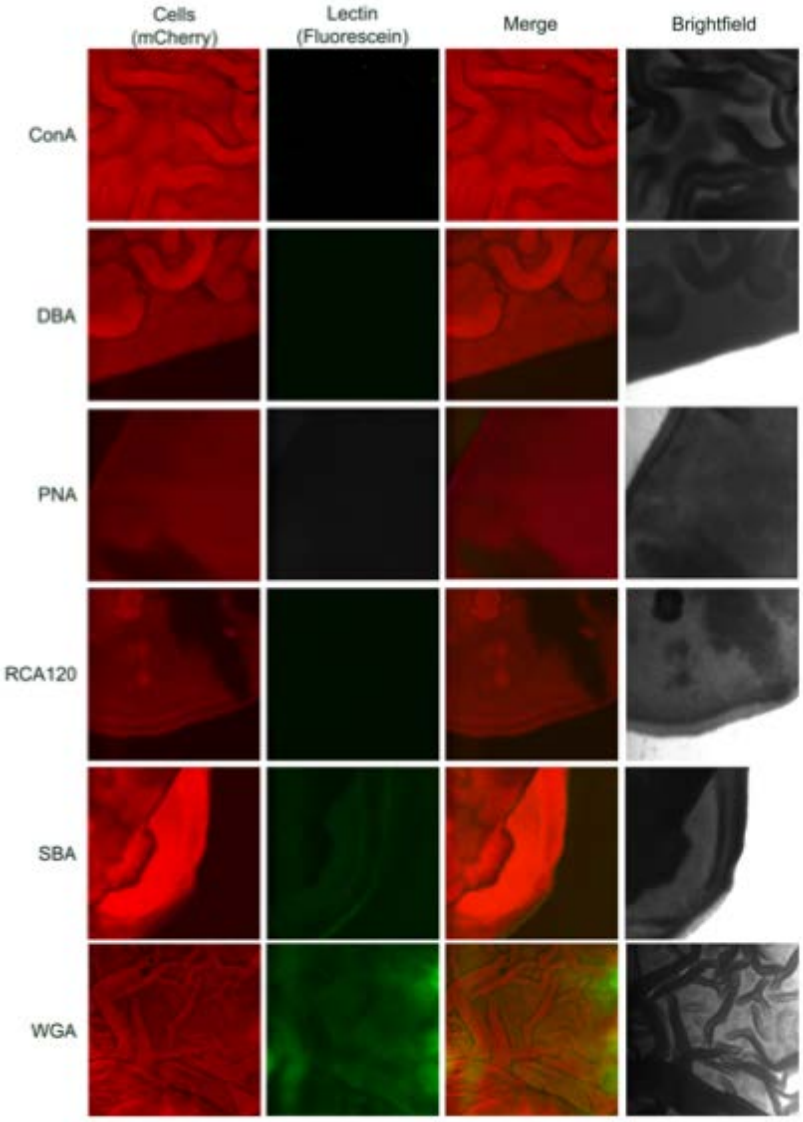

Figure 4.7: *S. venezuelae* explorers feature very little lectin binding. Seven day old wild type *S. venezuelae* explorer colonies constitutively producing mCherry were stained with the indicated lectins for polysaccharides. Images were taken at 10× total magnification, and are 1.5 mm × 1.5 mm in size. Experiments were conducted in biological triplicate, and representative images are shown. ConA, Concanavalin A; DBA, *Dolichos biflorus* agglutinin; PNA, Peanut agglutinin; RCA120, *Ricinus communis* agglutinin 120; SBA, Soybean agglutinin; WGA, Wheat germ agglutinin.

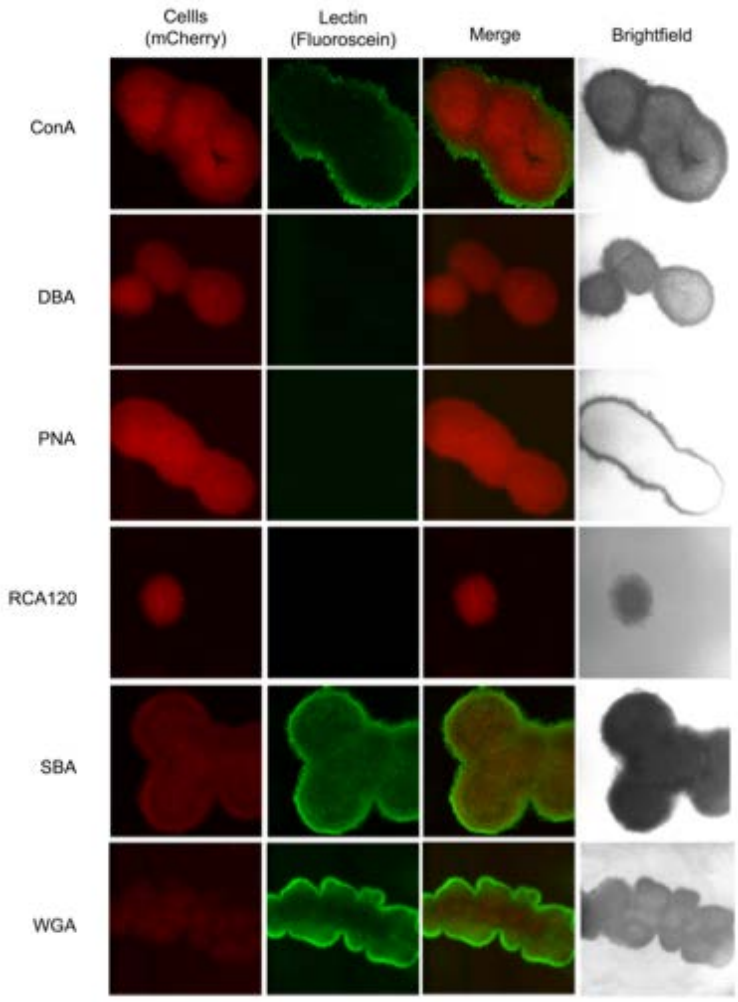

Figure 4.8: *S. venezuelae* vegetatively growing cells are bound by lectins specific for the bacterial cell wall. Twenty four hour old wild type *S. venezuelae* colonies (at the vegetative growth stage of their classical developmental cycle) were stained with the indicated lectins to assess surface polysaccharide composition. Cells were constitutively producing the mCherry fluorescent protein. Images were taken at 10× total magnification, and are 1.5 mm × 1.5 mm in size. Experiments were conducted in biological triplicate, and representative images are shown ConA, Concanavalin A; DBA, *Dolichos biflorus* agglutinin; PNA, Peanut agglutinin; RCA120, *Ricinus communis* agglutinin 120; SBA, Soybean agglutinin; WGA, Wheat germ agglutinin.

Table 4.5 Affinity of lectin probes for *S. venezuelae* cells

Lectin Probe	Recognition motif	Affinity for vegetative cells[1]	Affinity for explorer cells[1]
Concanavalin A	Internal and nonreducing terminal α-D-glucosyl and α-D-mannosyl groups	++	-
Dolichos biflorus agglutinin	*N*-acetylgalactosamine	-	-
Peanut agglutinin	β-galactose-1,3-*N*-acetylgalactosamine	-	-
Ricinus communis agglutinin	Non-reducing terminal β-D-galactose or *N*-acetylgalactosamine	-	-
Soybean agglutinin	*N*-acetylgalactosamine and galactose	+++	+
Wheat germ agglutinin	*N*-acetylglucosamine	+++	++

[1] High affinity: +++; Medium affinity: ++; Low affinity: +; No affinity: -. Affinity is determined based on fluorescence intensity.

4.4.6 Extracellular DNA is a component of the matrix surrounding explorer cells

Having examined the effect of chaplin amyloids and three possible polysaccharides on exploration, and assessed (where possible) their relative position within exploring cultures, we next turned our attention to eDNA. eDNA is a critical component of many bacterial and fungal biofilms (Hobley et al., 2015; Mitchell et al., 2016), and we sought to probe its presence and localization in exploring colonies. To do this, we used TOTO-3, a cell membrane impermeable dye that intercalates into the minor groove of DNA, and fluoresces at 647 nm (Milanovich et al., 1996). We found that mature,7 day old cultures have eDNA distributed throughout the explorer matrix (Fig. 4.9). To ensure this staining was specific for DNA, we treated cultures with DNase prior to staining, and observed significantly reduced fluorescence. This suggested that eDNA was an abundant polymer in exploring cultures. DNase treatment also reduced the cohesion of explorer cells as they were transferred off the agar plate and onto the slide for imaging, suggesting that eDNA promoted cohesion within explorer colonies. Very little eDNA was detectable in association with classically growing vegetative cells, suggesting that copious eDNA release is a feature specific to exploratory growth.

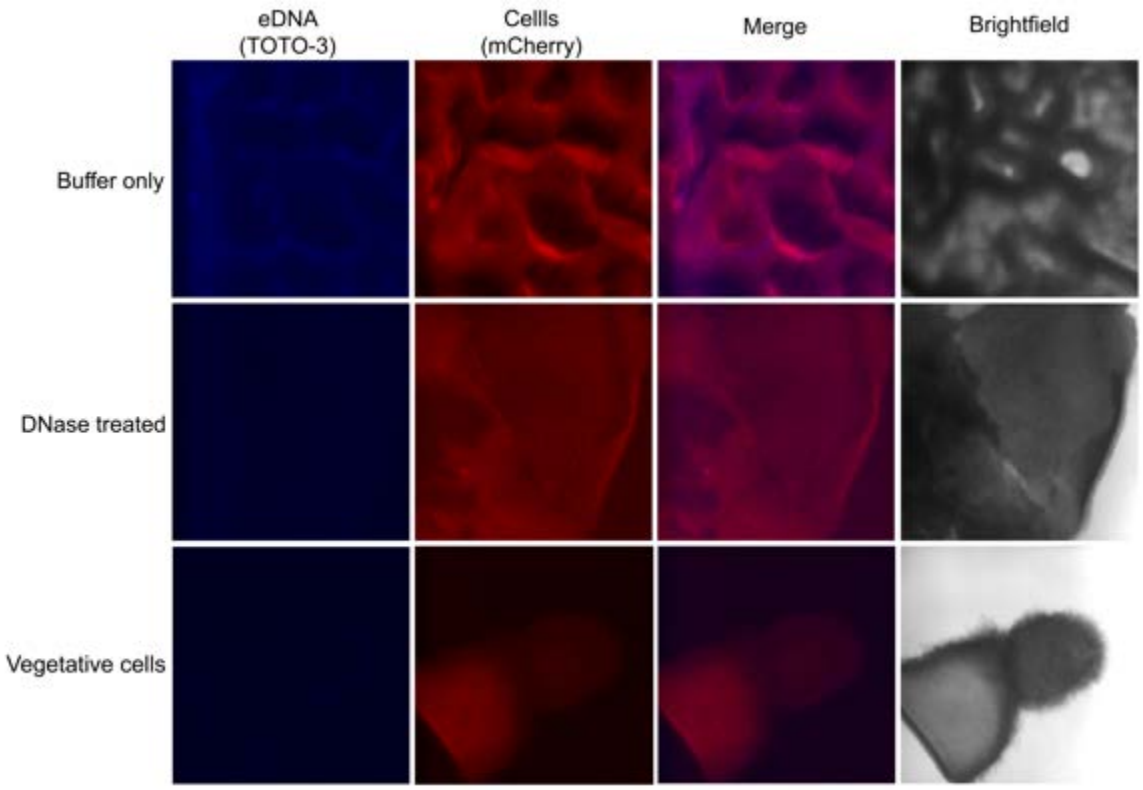

Figure 4.9: Extracellular DNA is a component of the explorer colony matrix. Seven day old explorer colonies constitutively producing mCherry were treated with DNase or buffer for 3 h prior to washing and staining with TOTO-3 for extracellular DNA. Vegetative cells from classical development were grown on MYM for 24 h prior to staining with TOTO-3. Images were taken at 100× magnification and are 1.55 mm × 1.55 mm. Experiments were conducted in biological triplicate, with at least three images take per replicate. Representative images are shown.

4.4.7 Mature explorer cells feature increased resistance to antimicrobial compounds

Biofilms provide cells with enhanced resistance to antimicrobial compounds, compared with their planktonically growing counterparts. To determine if this was a feature of *S. venezuelae* explorer colonies, we measured the response of mature and immature explorer colonies to three antimicrobial compounds: kanamycin, hygromycin and SDS (Fig. 4.10). To determine if this was a feature of exploratory growth specifically, we also examined the resistance of classically growing *S. venezuelae* to the same compounds. *S. venezuelae* was found to be more susceptible to antibiotics during germination than later on in growth, as determined by the zones of clearing surrounding the disks, particularly for kanamycin (Fig. 4.10A). When disks were applied during the aerial stages

of growth, it appears as though kanamycin and hygromycin led to a developmental block, as indicated by the white rings surrounding the disks (Fig. 4.10A). The inability to sporulate was also seen at the growing edge of SDS-exposed cells, although there was also significant cell death observed, as evidenced by the zone of clearing surrounding the SDS-saturated disk (Fig. 4.10B).

We expected that the leading edge of an explorer colony would be more susceptible to environmental insults than the interior of the colony, as we frequently observed individual hyphae to be extending out from the main body of the colony protected by the extracellular matrix (Fig. 4.11). In contrast, the centre of the explorer colony appears to be encased in a thick matrix. To determine if there was a difference in antimicrobial resistance between these two regions of the biofilm, a number of different approaches were taken. We initially attempted to overlay early-stage explorer colonies with antibiotics, but control experiments using static MYM-grown cultures routinely failed (colonies would simply break up and/or float away), making it challenging to draw meaningful conclusions. We next employed a disk diffusion assay. Disks were either placed on the agar surface at the same time spores were spotted, 1.5 cm away from the spot, or on the exploring colony surface after 7 days of growth. After 14 days of growth, colony morphology was then examined. The immature colonies that encountered the antimicrobial compounds with their leading edges appeared to exhibit an avoidance response when antibiotics were present at high concentrations (Fig. 4.10C). For hygromycin and kanamycin, growth in the directions of the disks was reduced. Colonies were longer than they were wide, but, the leading edge of the colony did extend right up to the disk in most cases. In the region closest to the disks, the colonies appeared thinner, and the wrinkling pattern was strikingly different from the control. Colonies were also observed to be producing melanin, a compound that is thought to assist with adaptation to stressful conditions (Kuznetsov et al., 1984). Together, these phenotypic changes suggested that the leading edges of the colony were affected by antimicrobial compounds, but to a lesser extent than classically growing cells. The mature colonies (exposed to the antimicrobial disks for 7 days) showed no differences in phenotype compared with the control, indicating that the centre of the colony was more resistant to antibiotics than aerial cultures grown on MYM (classic growth medium).

In contrast, SDS had a subtler effect than the two antibiotics on the leading edge of the biofilm (Fig. 4.10C). Growth towards the disks was inhibited to a lesser extent, and the thinner zone of cells closest to the disk was not observed, unlike when exposed to antibiotics. For the 4 mg SDS disk, the wrinkles piled up against each other at the edge of the zone of inhibition, almost as if there was an invisible barrier present. Notably, the zone of inhibition surrounding the disk was smaller than for classically growing cells (Fig. 4.10B). When the disks were applied to mature explorers, the area surround the disk appears to have thinned compared to the water only control. In addition, colony expansion seems to be reduced. Together, these results suggest that explorers are susceptible to detergents.

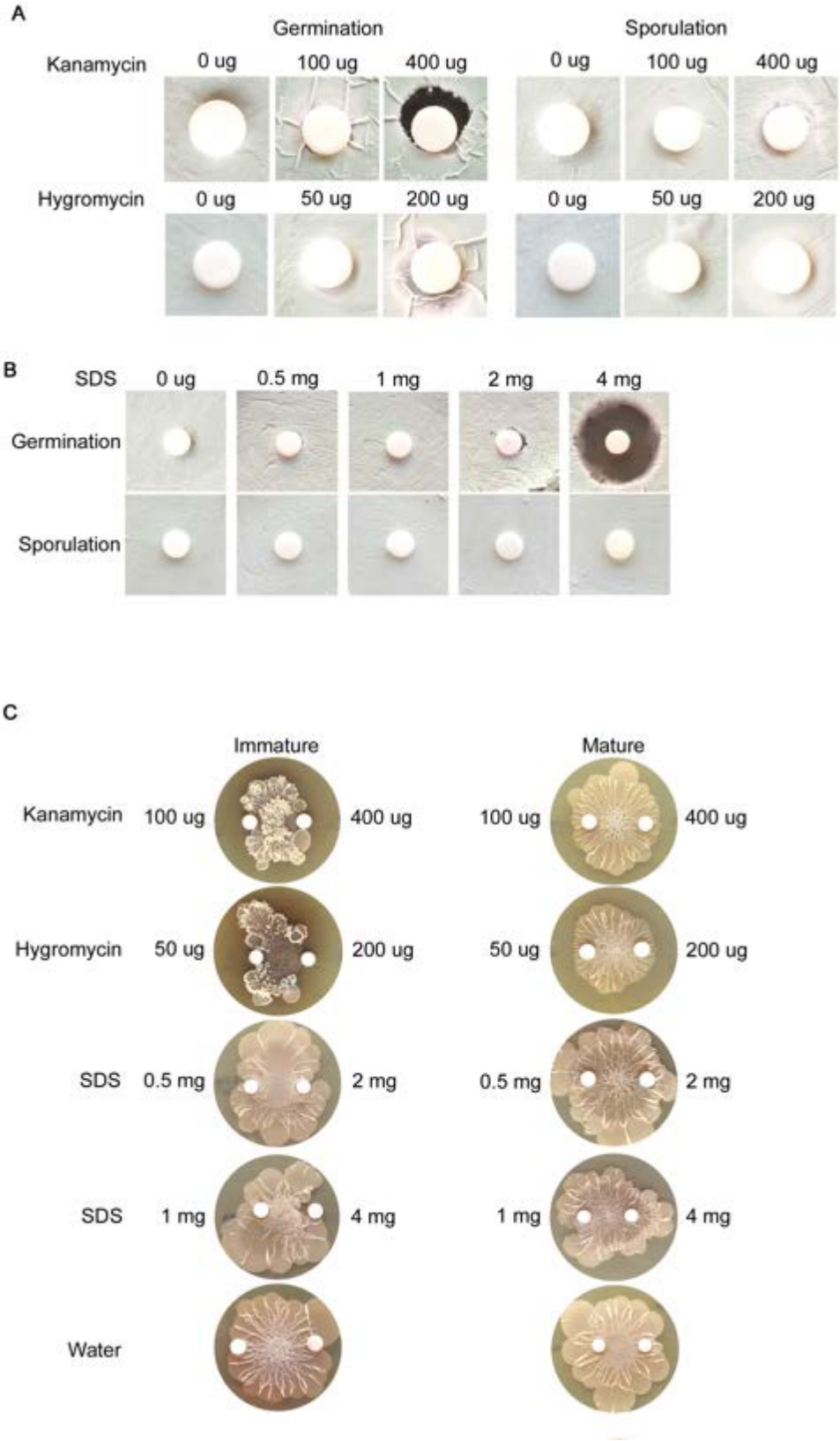
A
Germination
Sporulation
Kanamycin
0 ug
100 ug
400 ug
0 ug
100 ug
400 ug
Hygromycin
0 ug
50 ug
200 ug
0 ug
50 ug
200 ug
B
SDS
0 ug
0.5 mg
1 mg
2 mg
4 mg
Germination
Sporulation
C
Immature
Mature
Kanamycin
100 ug
400 ug
100 ug
400 ug
Hygromycin
50 ug
200 ug
50 ug
200 ug
SDS
0.5 mg
2 mg
0.5 mg
2 mg
SDS
1 mg
4 mg
1 mg
4 mg
Water

Figure 4.10: Mature biofilms have increases resistance to antimicrobial compounds. (A) Wild type *S. venezuelae* was plated on MYM agar to measure resistance to antimicrobial compounds during the germination and sporulation stages of classical development. To measure resistance during germination, spores were dispersed evenly across the surface of the agar and 6 mm disks containing the indicated amount of each antibiotic/detergent were placed on the surface immediately after drying. Resistance during sporulation was measured by placing disks containing the indicated amount of antibiotics/detergent on the surface of the colony once aerial growth commenced (24 h). Images were taken after 48 h growth at 30˚C. (B) Wild type *S. venezuelae* spores were dispersed as a lawn over the surface of MYM agar plates and disks containing the indicated amount of SDS were applied immediately for germination and after one day of growth at 30˚C for sporulation. Images were taken after 48 h growth at 30˚C and are representative of three independent replicates. (C) Spores were spotted onto the surface of YP agar plates and paper disks containing the indicated amount of antibiotics or SDS were either added immediately, for immature, or after 7 days growth at 30˚C, for mature cultures. Colonies were left to grow for 14 days total at 30˚C. Disks with water were used as a control for all experiments. Images are representative of three independent replicates.

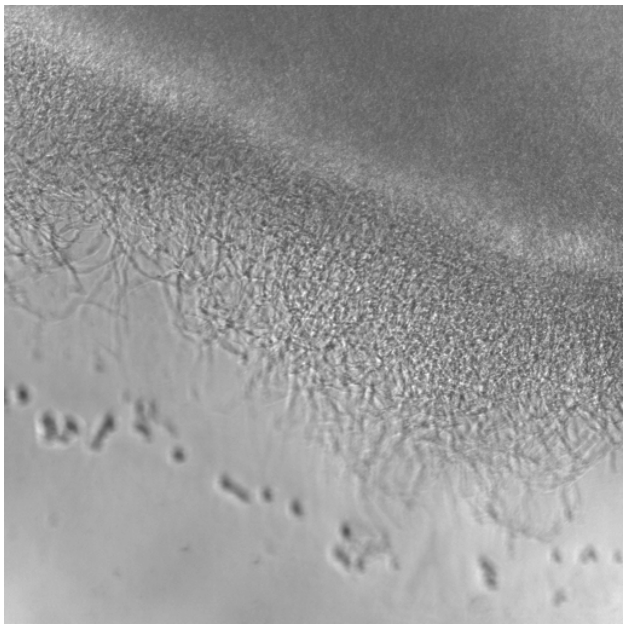

Figure 4.11: Hyphae are exposed on the leading edge of the explorer colony. Brightfield microscopy image of the leading edge of a wild type *S. venezuelae* explorer colony. The leading edge of the colony, upper right, has many layers of hyphae on top of each other. Individual hyphae extend outwards from the leading edge. Image taken at 630x magnification. Representative of >10 independent replicates.

4.5 DISCUSSION

Based on visual similarities to biofilms, we were curious if *S. venezuelae* explorer colonies had components and characteristics typically associated with biofilms. Biofilms feature aggregated cells or hyphae that are bundled together using an extracellular matrix. This matrix promotes cell adherence to the substratum, as well as to each other, so biofilm formation and motility are thought to be inversely related. Our results suggest that explorer cultures may constitute a biofilm, but one with properties that are in some instances distinct from the best-studied examples. We have identified several components of the matrix surrounding explorer cells, and examined the role of these in biofilm formation and colony expansion.

4.5.1 Chaplins form a coating on hyphae on the surface of the biofilm

Streptomyces produces two classes of amyloid proteins, rodlins and chaplins. In *S. coelicolor,* the chaplins are secreted and polymerize on the surface of the emerging aerial hyphae. This provides these hyphae with a hydrophobic coating and reduces surface tension, allowing the hyphae to pass through the air-medium interface efficiently (Claessen et al., 2003; Elliot et al., 2003). The chaplins also form fimbriae during standing liquid culturing, and these are predicted to facilitate surface attachment (de Jong et al., 2009). In contrast, the rodlins are thought to assist with organizing the chaplin proteins into a paired rodlet ultrastructure on the surface of aerial hyphae and spores (Claessen et al., 2004). It is not known whether the rodlins contribute to fimbriae formation, but they are not required for aerial hyphae formation (Claessen et al., 2002).

Here, we focused our attention on the chaplin and rodlin proteins and their contribution to exploration. In other bacterial biofilm systems, deleting the genes involved in amyloid formation results in flat colonies, suggesting a key role for amyloid proteins in colony architecture and wrinkling (Taglialegna et al., 2016). Intriguingly, we found that deleting five of the seven chaplin genes did not affect colony wrinkling. Instead, this strain featured smaller, wrinkled colonies that were more tightly associated with the substratum than wild type explorers. There are still two remaining chaplins in this strain, *chpE,* which is known to be conditionally essential in *S. coelicolor* (Di Berardo et al., 2008) and may be essential in *S. venezuelae,* and *chpH*, the most highly expressed chaplin gene during exploration (Fig. 4.2). It is possible that the two remaining chaplins functionally compensate for the deletion of the other five chaplins, with or without the assistance of the rodlins. Notably, deleting the rodlins did not have a significant effect on explorer colony phenotype (Fig. 4.4C and 4.5).

Our localization studies suggested that the three chaplins studied here, ChpE, ChpG, and ChpH, appeared to be associated with hyphae on the top of the exploring colony (Fig. 4.6). This was in contrast to other characterized systems, such as *B. subtilis* and *E. coli*, where amyloids are matrix associated and promote matrix stiffness (Taglialegna et al., 2016; Zeng et al., 2015), but similar to the localization of hydrophobins in *B. subtilis*

biofilms (Hobley et al., 2013). The surface of *B. subtilis* biofilms is hydrophobic due to the presence of hydrophobins, while the surface of *S. venezuelae* explorers is hydrophilic, suggesting that the chaplins do not function in a hydrophobin capacity. it is possible that the chaplins promote biofilm matrix integrity through a distinct mechanism than in these well-characterized systems. It also remains unclear if the chaplins affect colony expansion through altered matrix stiffness. To address the role of chaplins in biofilm formation, we will examine the matrix morphology of the 5×Δ*chp* mutant using cryo SEM, and use atomic force microscopy to measure biofilm elasticity.

As an alternative, it is possible that the chaplins function as a surfactant during sliding motility. This hypothesis is based on the increased adherence of the 5×Δ*chp* mutant to the substratum. The detected ChpE, ChpG, and ChpH were cell associated (Fig. 4.6); however, it possible that chaplins that are not tightly associated with the cell surface would be washed away during the staining process or are simply not accessible for labeling. It is also possible that ChpD and ChpF, not examined in this study, function in this capacity. Polymerization of ChpF into amyloid fibrils is inhibited at high pH due to changes protein structure, while amyloid formation by ChpE is enhanced at high pH (Dokouhaki et al., 2017b, 2017a). It is conceivable that the high pH associated with exploratory growth separates the chaplins into two classes: one that stays associated with hyphae and a second that coats the bottom of the colony to form a hydrophobic film upon which cells can slide across with ease. It is also possible that functional differentiation of chaplins may occur in response to different levels of oxygen. Assembly of hIAPP, the amyloid associated with type II diabetes, is regulated by redox state (Rodriguez Camargo et al., 2017). The oxidized form of the protein readily assembles into amyloid structures, while the reduced form does not (Rodriguez Camargo et al., 2017). A similar mechanism has been proposed for the assembly of the hydrophobin BslA on the surface of *B. subtilis* biofilms. BslA forms two distinct structures: one in reducing (colony-agar interface) and the other in oxidative (colony-air interface) conditions (Arnaouteli et al., 2017). Further work is required to determine the role of chaplins within exploratory growth.

It is important to note however that due to a lack of an *in vivo* functional test for individual chaplin activity at this time, we have not confirmed that the reactive cysteine-labeled chaplins are functional. The introduction of an additional cysteine residue may disrupt disulfide bond formation, which is critical for proper chaplin polymerization into amyloid fibres (Capstick et al., 2011). As a result, we cannot definitively conclude that these labeled chaplins function as wild type. To address this, we are working to develop a chaplin mutant system that will allow us to assess the phenotypes of individual wild type and mutant chaplins. If this approach is not successful, *in vitro* polymerization assays with synthesized chaplins could be used to confirm that the reactive cysteines do not disrupt amyloid formation.

When investigating the localization of the different chaplin proteins using maleimide staining, we noted that the levels of mCherry varied between samples (Fig. 4.6). This did not seem to be due to biofilm thickness at the edge, based on the brightfield images. Rather, the pSET152 based reporter used in these experiments was, for reasons unknown, routinely less intense when compared with the pIJ82-based version (which integrates into the same site, and differs only in its antibiotic resistance gene).

4.5.2 Polysaccharide composition of explorer cells differs from classically growing cells

We found that three lectins, ConA, SBA, and WGA, bound with high affinity to the edges of vegetatively growing *S. venezuelae* (Fig. 7, Table 4.5). In contrast, only WGA and SBA bound weakly to exploring colonies (Fig. 6, Table 4.5). This could be due to increased production of extracellular matrix surrounding the cells, obscuring the cell wall binding sites for the lectins. Alternatively, hyphae throughout the explorer colony could be coated in chaplins, which would also be expected to inhibit lectin binding. Finally, the cell wall of explorer cells may be completely different than that of vegetatively growing cells. At this point, we cannot draw any conclusions about whether polysaccharides comprise a portion of the extracellular matrix, and if so, what the nature of these molecules are. It interesting to note that the lectins used for analysis in this study bind with high affinity to a wide variety of biofilms (reviewed in Mlouka *et al.*, 2016). The absence of strong binding by any lectin probe is suggestive of a very different sort of extracellular polysaccharide composition in *S. venezuelae* explorers relative to other biofilm systems. We note, however, that deleting genes involved in polysaccharide synthesis, particularly the *cslA* gene and the *eps* cluster, altered explorer colony phenotypes, which could support a role for polysaccharides in contributing to exploratory growth. To identify these compounds, we will first work to investigate the possible localization of cellulose within the biofilm. We have now identified a microscope that is compatible with the calcafluor white stain used to stain cellulose, and will compare the staining of wild type and *cslA* under exploring conditions. In the non-exploring *S. coelicolor* strain, cellulose is produced during liquid growth, where it attaches chaplin fimbriae to the cell surface (de Jong et al., 2009). To identify other polysaccharides, we will extract them from the biofilm of wild type, *cslA* and the *eps* mutants, and compare their profiles using gas chromatography-mass spectrometry, similar to what has been used to identify polysaccharides from other microbial communities (Bales et al., 2013; Jiao et al., 2010; Li et al., 2016; Petruzzi et al., 2017).

4.5.3 Mature explorer colonies are resistant to antibiotics but not to detergents

Application of antibiotics to the leading edge of the explorer colony caused an intriguing stress response. Colony thickness and expansion were reduced in the region adjacent to the antimicrobial disk (Fig. 4.10C); however, growth continued right up to the disk, suggesting an increased tolerance to the antibiotics. Explorer colonies produce trimethylamine as a volatile signal to stimulate exploratory growth in neighbouring cells (Jones et al., 2017). This increases the pH of the surrounding media (Jones et al., 2017),

and this increased pH enhances the potency of aminoglycoside antibiotics (Létoffé et al., 2014). The increased resistance of exploring cells to aminoglycosides is therefore even more remarkable. We also observed the activation of melanin production. Melanin is typically thought to help with neutralizing reactive oxygen species (Nosanchuk and Casadevall, 2003), and aminoglycoside antibiotics are proposed to induce oxidative stress in their target organisms (Kohanski et al., 2007; Wang and Zhao, 2009). In contrast, applying the antimicrobial disks to the surface of mature explorer colonies had no obvious effect on growth, and did not induce melanin production (Fig. 4.10C). The increased antimicrobial tolerance of the mature colony, and even the edges of the exploring colony, therefore supports a similar function for explorer colonies as is seen for biofilms in other systems. It is unclear at this point what mechanism underlies this increased resistance/tolerance, whether it be through an altered metabolic state that reduce susceptibility, or through reduced uptake due to matrix sequestration of these compounds.

4.5.4 Explorers are a biofilm-like structure

Here, we have shown that explorer hyphal filaments are encased in a complex extracellular matrix. This matrix appears to comprise eDNA, as well as chaplin proteins, although the form taken by these proteins remains to be determined. Genetic results suggest a role for several different polysaccharide components, although this remains to be validated biochemically. Based on the presence of a complex extracellular matrix and dramatically different phenotype from classical development, the *S. venezuelae* explorer phenotype conforms to many of the features that define a biofilm: hyphae that are bundled together, an altered phenotype compared to classical development, presence of an extracellular matrix, and an increased resistance to antibiotics. There do, however, seem to be some differences, in that loss of individual components does not alter colony behaviour in expected ways. It will be interesting to see what the matrix of these mutant strains looks like using cryo SEM. Intriguingly, the expansion of the biofilm seems to be driven by growth powered motility, where growth in the centre of the biofilm powers the movement of the leading edge of the colony. This raises the tantalizing possibility of having a motile biofilm.

Chapter 5

General conclusions and future directions

Collectively, the work presented in this thesis has emphasized the importance of the cell surface, and its associated polymers, to *Streptomyces* growth and development. Our work on the Rpfs has provided insight into how these proteins function to promote both the exit from, and entry back into dormancy at the end of the *Streptomyces* lifecycle. Previous studies have focused on the transcriptional responses to germination, and on the signals that stimulate germination, but little work had been done to examine the mechanism by which the Rpfs stimulate spore germination. We established that the Rpfs are lytic transglycosylases that promote germination through cell wall remodeling once a signal has been received to resuscitate.

We have also revealed that explorer colonies formed by *S. venezuelae* can be classed as motile biofilms. These studies are reshaping our way of thinking about *Streptomyces* growth, and are opening up many new and exciting areas for *Streptomyces* biology and microbial community interactions.

5.1 DIRECTIONS FOR FUTURE WORK

5.1.1 Future work on germination in *Streptomyces*

Cells without the resuscitation promoting factors germinate more slowly than their wild type counterparts, and would likely be outcompeted in natural environments. A major outstanding question surrounding resuscitation is what other proteins contribute to cell wall remodeling during germination. Thus far, we know that SwlA, a secreted endopeptidase whose gene has the same cyclic di-AMP-sensing riboswitch as that of *rpfA*, has a more profound effect on germination rate than RpfA (Haiser et al., 2009). There are five additional genes – all encoding cell wall cleavage enzymes - that possess the equivalent riboswitch, and it will also be interesting to see if these enzymes work together to coordinate cellular resuscitation. Whether any, or all, of these enzymes physically associate with the Rpfs also remains to be seen. In *Mycobacterium*, Rpf binding partners have critical roles in cellular resuscitation, and indeed even in cell viability (Hett et al., 2007, 2008, 2010). The *S. coelicolor* chromosome encodes 60 additional cell wall lytic enzymes, and what effect these have on the ability of spores to germinate remains to be determined. Several of these putative cell wall lytic enzymes are upregulated during the initial stages of germination (Strakova et al., 2013), suggesting that they may be involved in cell wall remodeling during germination.

The link between the recognition of a germination signal and the expression/activation of cell wall lytic enzymes is still not well-understood. Here, we established that the role of Rpfs during spore germination in the streptomycetes is distinct from cellular

resuscitation in *Mycobacterium* and *Bacillus* species, where peptidoglycan fragments are predicted to stimulate germination.

We were unable to determine whether the defects in germination seen for the *rpf* null strains were due to defects in spore wall formation, due to the lack of lytic transglycosylase activity during sporulation, or due to a lack of lytic transglycosylase during germination causing a delay in outgrowth. Creating an inducible *rpf* expression strain in an *rpf* null background would allow us to tease apart whether the defect in outgrowth is due to the mutant cell walls, whether Rpf activity is required only at the initial stages of germination, or if it is required throughout development.

5.1.2 Further characterization of biofilms formed by *S. venezuelae*

Preliminary work is strongly suggestive of biofilm formation during exploratory growth; however, it remains to be seen how common biofilm characteristics, such as programmed cell death, division of labour, metabolic states, and social cheaters are dealt with in *S. venezuelae* biofilms. In biofilms produced by *B. subtilis*, programmed cell death is required for wrinkle formation (Asally et al., 2012). Wrinkle formation in turn generates channels to transport liquids to the centre of the biofilm (Wilking et al., 2013), and also allows for proper oxygenation of cells within the biofilm (Dietrich et al., 2013; Reineke et al., 2013). It would be interesting to see how changes in wrinkling pattern due to changes in biofilm composition affect nutrient accessibility and cell survival within the biofilm. Extracellular DNA is a component of the explorer matrix, suggesting that programmed cell death may be a part of explorer colony formation. However, the role programmed cell death plays in explorer colony architecture is not known.

In model biofilm systems, cells feature different levels of metabolic activity depending on their location in the colony, which influences nutrient availability. It is common to see cells producing different components based on metabolic state of the cells (Serra *et al.*, 2013a; Serra *et al.*, 2013b; Dragoš *et al.*, 2018). There is strong pressure for social cheaters, cells who do not produce matrix components, to arise as well. These cells are able to profit from the protective nature of the biofilm without expending energy towards its production. Presently, it is not known if all hyphae are equally metabolically active, and if all are producing all matrix components simultaneously within an exploring colony. Conducting mixed culture experiments with differentially labeled strains (*e.g.* mixing GFP-expressing chaplin producers with mCherry-expressing chaplin mutants) and examining both matrix production, using cryo-SEM, and cell distribution, using fluorescent microscopy, would allow us to begin to understand the community dynamics within explorer biofilms.

Explorers represent a unique example of a biofilm that expands using sliding motility. Typically, biofilm formation and motility are inversely correlated with each other; cells either form biofilms, or they are motile. The switch between planktonic and biofilm growth is governed by complex regulatory processes, with cyclic di-GMP (c-di-GMP)

being a major mediator of this switch. Rising levels of c-di-GMP inhibit the transcription of new flagellar components, and inhibit flagellum assembly and activity in a wide variety of bacteria (Baraquet and Harwood, 2013; Boehm et al., 2010; Davis et al., 2013; Jenal et al., 2017; Navarro et al., 2010; Russell et al., 2013; Trampari et al., 2015). There is a concomitant increase in the production of biofilm matrix components in response to the rising c-di-GMP concentration (Jenal et al., 2017; Park et al., 2015; Pesavento et al., 2008; Serra et al., 2013a). c-di-GMP does not seem to play a role in coordinating exploratory behaviour in contrast to other characterized systems (N. Tschowri, personal communication), highlighting how unique this behaviour is. It would be interesting to examine the interplay between biofilm formation and sliding motility in *S. venezuelae* explorers, to determine if they can occur independently of each other, or if these behaviours are inextricably linked. Identification of the surfactant that permits gliding motility will be critical for uncoupling motility from biofilm formation. Generating a strain that is not capable of producing major biofilm components could facilitate the separation of biofilm matrix formation from the motility aspect of exploration. Similarly, examining how the matrix elasticity is altered in mutants with reduced colony expansion using atomic force microscopy, could provide some additional insight into how the properties of the biofilm affect motility.

A key question that has yet to be addressed with respect to explorer colonies, is whether this is an ecologically relevant phenomenon. The concentration of nitrogen required to initiate exploratory behaviour is several orders of magnitude higher than what it found in soil (Alden et al., 2001). However, the soil is a heterogeneous environment, and there is the possibility of encountering conditions conducive to exploratory growth in the soil. This could be tested by inoculating sterilized soil with *S. venezuelae* and a strain that does not explore, such as *S. coelicolor* and measuring colony expansion using qPCR. Another possibility would be to measure colony expansion in soil supplemented with MYM or YP medium. Hopefully these experiments will allow us to determine how *S. venezuelae* traverses soil under a variety of environmental conditions.

In their native soil environment, *Streptomyces* would also be susceptible to a wide range of biotic and abiotic stresses. Dormant spores formed through classical development provide a robust mechanism for avoiding abiotic and biotic stresses. However, it will be interesting to determine whether biofilm formation through exploratory growth allows for protection against common soil phages, insects, predatory microorganisms, or environmental stresses, such as high pH or high nitrogen, and how components of the biofilm matrix contribute to resistance. There are a variety of different tests that could be used to explore these concepts. Plating classically growing *S. venezuelae* and explorers on media buffered to have high pH or high nitrogen concentration and monitoring their growth in these conditions compared to under standard growth conditions could be used to measure the robustness of explorers in response to environmental stress. To test phage susceptibility, we could isolate soil phages and test the susceptibility of classically growing cells and explorers using a plaque assay. Finally,

competing explorers and classically growing cells against predatory bacteria, such as *Myxococcus xanthus*, could be a method to determine if explorers are more protected against predation than classically growing *Streptomyces*.

Streptomyces are incredible bacteria which seem to be primed for survival in a wide variety of environments. They have evolved two potentially independent mechanisms for multicellular development, classical growth and exploratory growth, and two mechanisms for survival under stress conditions, dormancy and biofilm formation. It will be fascinating to see under which conditions these different growth and survival strategies are utilized.

References

van der Aart, L.T., Spijksma, G.K., Harms, A., Vollmer, W., Hankenmeier, T., and van Wezel, G.P. (2018). High-resolution analysis of the peptidoglycan composition in *Streptomyces coelicolor*. BioRxiv 1–26.

Alden, L., Demoling, F., and Baath, E. (2001). Rapid Method of Determining Factors Limiting Bacterial Growth in Soil. Appl. Environ. Microbiol. *67*, 1830–1838.

Arnaouteli, S., Ferreira, A.S., Schor, M., Morris, R.J., Bromley, K.M., Jo, J., Cortez, K.L., Sukhodub, T., Prescott, A.R., Dietrich, L.E.P., et al. (2017). Bifunctionality of a biofilm matrix protein controlled by redox state. Proc. Natl. Acad. Sci. U. S. A. *34*, 201707618–201707687.

Asally, M., Kittisopikul, M., Rue, P., Du, Y., Hu, Z., Cagatay, T., Robinson, A.B., Lu, H., Garcia-Ojalvo, J., and Suel, G.M. (2012). Localized cell death focuses mechanical forces during 3D patterning in a biofilm. Proc. Natl. Acad. Sci. *109*, 18891–18896.

Azuma, I., Thomas, D., Adam, A., Ghuysen, J., Bonaly, R., Petit, J., and Lederer, E. (1970). Occurence of N-glucosylmuramic acid in bacterial cell walls. Biochim Biophys Acta *20*, 444–451.

Bales, P.M., Renke, E.M., May, S.L., Shen, Y., and Nelson, D.C. (2013). Purification and Characterization of Biofilm-Associated EPS Exopolysaccharides from ESKAPE Organisms and Other Pathogens. PLoS One *8*.

Baraquet, C., and Harwood, C.S. (2013). Cyclic diguanosine monophosphate represses bacterial flagella synthesis by interacting with the Walker A motif of the enhancer-binding protein FleQ. Proc. Natl. Acad. Sci. *110*, 18478–18483.

Bateman, A., Holden, M.T.G., and Yeats, C. (2005). The G5 domain: a potential N-acetylglucosamine recognition domain involved in biofilm formation. Bioinformatics *21*, 1301–1303.

Beaman, T.C., and Gerhardt, P. (1986). Heat resistance of bacterial spores correlated with protoplast dehydration, mineralization, and thermal adaptation. Appl. Environ. Microbiol. *52*, 1242–1246.

Beauvais, A., Schmidt, C., Guadagnini, S., Roux, P., Perret, E., Henry, C., Paris, S., Mallet, A., Prévost, M.C., and Latgé, J.P. (2007). An extracellular matrix glues together the aerial-grown hyphae of *Aspergillus fumigatus*. Cell. Microbiol. *9*, 1588–1600.

Beeby, M., Gumbart, J.C., Roux, B., and Jensen, G.J. (2013). Architecture and assembly of the Gram-positive cell wall. Mol. Microbiol. *88*, 664–672.

Bera, A., Biswas, R., Herbert, S., Kulauzovic, E., Weidenmaier, C., Peschel, A., and Götz, F. (2007). Influence of wall teichoic acid on lysozyme resistance in *Staphylococcus aureus*. J. Bacteriol. *189*, 280–283.

Di Berardo, C., Capstick, D.S., Bibb, M.J., Findlay, K.C., Buttner, M.J., and Elliot, M.A. (2008). Function and Redundancy of the Chaplin Cell Surface Proteins in Aerial Hypha Formation, Rodlet Assembly, and Viability in *Streptomyces coelicolor*. J. Bacteriol. *190*, 5879–5889.

Bernard, E., Rolain, T., Courtin, P., Guillot, A., Langella, P., Hols, P., and Chapot-Chartier, M.P. (2011). Characterization of *O*-acetylation of *N*-acetylglucosamine: A novel structural variation of bacterial peptidoglycan. J. Biol. Chem. *286*, 23950–23958.

Bertani, and G (1951). Studies on lysogenesis. I. The mode of phage liberation by lysogenic *Escherichia coli* . J. Bacteriol. *62*, 293–300.

Bierman, M., Logan, R., O'Brien, K., Seno, E.T., Nagaraja Rao, R., and Schoner, B.E. (1992). Plasmid cloning vectors for the conjugal transfer of DNA from *Escherichia coli* to *Streptomyces* spp. Gene *116*, 43–49.

Biketov, S., Potapov, V., Ganina, E., Downing, K., Kana, B.D., and Kaprelyants, A. (2007). The role of resuscitation promoting factors in pathogenesis and reactivation of *Mycobacterium tuberculosis* during intra-peritoneal infection in mice. BMC Infect. Dis. *7*, 146.

Block, K.F., Hammond, M.C., and Breaker, R.R. (2010). Evidence for widespread gene control function by the *ydaO* riboswitch candidate. J. Bacteriol. *192*, 3983–3989.

Boehm, A., Kaiser, M., Li, H., Spangler, C., Kasper, C.A., Ackermann, M., Kaever, V., Sourjik, V., Roth, V., and Jenal, U. (2010). Second Messenger-Mediated Adjustment of Bacterial Swimming Velocity. Cell *141*, 107–116.

Bradford, M.M. (1976). A rapid and sensitive method for the quantitation of microgram quantities of protein utilizing the principle of protein-dye binding. Anal. Biochem. *72*, 248–254.

Bradley, S.G., and Ritzi, D. (1968). Composition and ultrastructure of *Streptomyces venezuelae*. J. Bacteriol. *95*, 2358–2364.

Branda, S.S., González-pastor, J.E., Ehrlich, S.D., Losick, R., Gonza, E., and Dervyn, E. (2004). Genes Involved in Formation of Structured Multicellular Communities by *Bacillus subtilis*. J. Bacteriol. *186*, 3970–3979.

Branda, S.S., Chu, F., Kearns, D.B., Losick, R., and Kolter, R. (2006). A major protein component of the *Bacillus subtilis* biofilm matrix. Mol. Microbiol. *59*, 1229–1238.

Brown, S., Xia, G., Luhachack, L.G., Campbell, J., Meredith, T.C., Chen, C., Winstel, V., Gekeler, C., Irazoqui, J.E., Peschel, A., et al. (2012). Methicillin resistance in *Staphylococcus aureus* requires glycosylated wall teichoic acids. Proc. Natl. Acad. Sci. *109*, 18909–18914.

Brown, S., Santa Maria Jr., J.P., and Walker, S. (2013). Wall Teichoic Acids of Gram-

Positive Bacteria. Annu. Rev. Microbiol. *67*, 313–336.

Cano, R., and Borucki, M. (1995). Revival and identification of bacterial spores in 25- to 40-million-year-old Dominican amber. Science. *2681*, 1060–1064.

Capstick, D.S., Willey, J.M., Buttner, M.J., and Elliot, M.A. (2007). SapB and the chaplins: connections between morphogenetic proteins in *Streptomyces coelicolor*. Mol. Microbiol. *64*, 602–613.

Capstick, D.S., Jomaa, A., Hanke, C., Ortega, J., and Elliot, M.A. (2011). Dual amyloid domains promote differential functioning of the chaplin proteins during *Streptomyces* aerial morphogenesis. Proc. Natl. Acad. Sci. *108*, 9821–9826.

Cava, F., and De Pedro, M.A. (2014). Peptidoglycan plasticity in bacteria: emerging variability of the murein sacculus and their associated biological functions. Curr. Opin. Microbiol. *18*, 46–53.

Celler, K., Koning, R.I., Willemse, J., Koster, A.J., and van Wezel, G.P. (2016). Cross-membranes orchestrate compartmentalization and morphogenesis in *Streptomyces*. Nat. Commun. *7*, ncomms11836.

Chapman, M.R., Robinson, L.S., Pinkner, J.S., Roth, R., Heuser, J., Hammar, M., Normark, S., and Hultgren, S.J. (2002). Role of *Escherichia coli* Curli Operons in Directing Amyloid Fiber Formation. Science (80-.). *295*, 851–855.

Claessen, D., Wösten, H.A.B., van Keulen, G., Faber, O.G., Alves, A.M.C.R., Meijer, W.G., and Dijkhuizen, L. (2002). Two novel homologous proteins of *Streptomyces coelicolor* and *Streptomyces lividans* are involved in the formation of the rodlet layer and mediate attachment to a hydrophobic surface. Mol. Microbiol. *44*, 1483–1492.

Claessen, D., Rink, R., de Jong, W., Siebring, J., de Vreugd, P., Boersma, F.G.H., Dijkhuizen, L., and Wosten, H.A.B. (2003). A novel class of secreted hydrophobic proteins is involved in aerial hyphae formation in *Streptomyces coelicolor* by forming amyloid-like fibrils. Genes Dev. *17*, 1714–1726.

Claessen, D., Stokroos, I., Deelstra, H.J., Penninga, N.A., Bormann, C., Salas, J.A., Dijkhuizen, L., and Wösten, H.A.B. (2004). The formation of the rodlet layer of streptomycetes is the result of the interplay between rodlins and chaplins. Mol. Microbiol. *53*, 433–443.

Claessen, D., Rozen, D.E., Kuipers, O.P., Søgaard-Andersen, L., and van Wezel, G.P. (2014). Bacterial solutions to multicellularity: a tale of biofilms, filaments and fruiting bodies. Nat. Rev. Microbiol. *12*, 115–124.

Clarke, A.J. (1993). Compositional analysis of peptidoglycan by high-performance anion-exchange chromatography. Anal. Biochem. *212*, 344–350.

Cohen-Gonsaud, M., Keep, N.H., Davies, A.P., Ward, J., Henderson, B., and Labesse, G.

(2004). Resuscitation-promoting factors possess a lysozyme-like domain. Trends Biochem. Sci. *29*, 7–10.

Cohen-Gonsaud, M., Barthe, P., Bagnéris, C., Henderson, B., Ward, J., Roumestand, C., and Keep, N.H. (2005). The structure of a resuscitation-promoting factor domain from *Mycobacterium tuberculosis* shows homology to lysozymes. Nat. Struct. & Mol. Biol. *12*, 270–273.

Collins, L.V., Kristian, S.A., Weidenmaier, C., Faigle, M., van Kessel, K.P.M., van Strijp, J.A.G., Götz, F., Neumeister, B., and Peschel, A. (2002). *Staphylococcus aureus* Strains Lacking D -Alanine Modifications of Teichoic Acids Are Highly Susceptible to Human Neutrophil Killing and Are Virulence Attenuated in Mice. J. Infect. Dis. *186*, 214–219.

Costa-Orlandi, C., Sardi, J., Pitangui, N., de Oliveira, H., Scorzoni, L., Galeane, M., Medina-Alarcón, K., Melo, W., Marcelino, M., Braz, J., et al. (2017). Fungal Biofilms and Polymicrobial Diseases. J. Fungi *3*, 22.

Cot, M., Ray, A., Gilleron, M., Vercellone, A., Larrouy-Maumus, G., Armau, E., Gauthier, S., Tiraby, G., Puzo, G., and Nigou, J. (2011). Lipoteichoic acid in *Streptomyces hygroscopicus*: Structural model and immunomodulatory activities. PLoS One *6*.

Craney, A., Hohenauer, T., Xu, Y., Navani, N.K., Li, Y., and Nodwell, J. (2007). A synthetic *luxCDABE* gene cluster optimized for expression in high-GC bacteria. Nucleic Acids Res. *35*, e46–e46.

Crowe, J.H., Crowe, L.M., and Chapman, D. (1984). Preservation of membranes in anhydrobiotic organisms: the role of trehalose. Science. *223*, 701–703.

Datsenko, K.A., and Wanner, B.L. (2000). One-step inactivation of chromosomal genes in *Escherichia coli* K-12 using PCR products. Proc. Natl. Acad. Sci. U. S. A. *97*, 6640–6645.

Davis, N.J., Cohen, Y., Sanselicio, S., Fumeaux, C., Ozaki, S., Luciano, J., Guerrero-Ferreira, R.C., Wright, E.R., Jenal, U., and Viollier, P.H. (2013). De- and repolarization mechanism of flagellar morphogenesis during a bacterial cell cycle. Genes Dev. *27*, 2049–2062.

Demina, G.R., Makarov, V.A., Nikitushkin, V.D., Ryabova, O.B., Vostroknutova, G.N., Salina, E.G., Shleeva, M.O., Goncharenko, A. V, and Kaprelyants, A.S. (2009). Finding of the Low Molecular Weight Inhibitors of Resuscitation Promoting Factor Enzymatic and Resuscitation Activity. PLoS One *4*, e8174.

Derouaux, A., Halici, S., Nothaft, H., Neutelings, T., Moutzourelis, G., Dusart, J., Titgemeyer, F., and Rigali, S. (2004). Deletion of a Cyclic AMP Receptor Protein Homologue Diminishes Germination and Affects Morphological Development of *Streptomyces coelicolor*. J. Bacteriol. *186*, 1893–1897.

Desmarais, S.M., De Pedro, M.A., Cava, F., and Huang, K.C. (2013). Peptidoglycan at its peaks: how chromatographic analyses can reveal bacterial cell wall structure and assembly. Mol. Microbiol. *89*, 1–13.

Dietrich, L.E.P., Okegbe, C., Price-Whelan, A., Sakhtah, H., Hunter, R.C., and Newmana, D.K. (2013). Bacterial community morphogenesis is intimately linked to the intracellular redox state. J. Bacteriol. *195*, 1371–1380.

Dokouhaki, M., Hung, A., Day, L., and Gras, S.L. (2017a). The pH-dependent assembly of Chaplin E from *Streptomyces coelicolor*. J. Struct. Biol. 1–10.

Dokouhaki, M., Prime, E., Hung, A., Qiao, G., Day, L., and Gras, S. (2017b). Structure-Dependent Interfacial Properties of Chaplin F from *Streptomyces coelicolor.* Biomolecules *7*, 15–68.

Downing, K.J., Mischenko, V. V, Shleeva, M.O., Young, D.I., Young, M., Kaprelyants, A.S., Apt, A.S., and Mizrahi, V. (2005). Mutants of *Mycobacterium tuberculosis* lacking three of the five *rpf*-like genes are defective for growth in vivo and for resuscitation in vitro. Infect. Immun. *73*, 3038–3043.

Dragoš, A., Kiesewalter, H., Martin, M., Hsu, C.Y., Hartmann, R., Wechsler, T., Eriksen, C., Brix, S., Drescher, K., Stanley-Wall, N., et al. (2018). Division of Labor during Biofilm Matrix Production. Curr. Biol. *28*, 1903–1913.

Dworkin, J., and Shah, I.M. (2010). Exit from dormancy in microbial organisms. Nat. Rev. Microbiol. *8*, 890–896.

Eaton, D., and Ensign, J.C. (1980). *Streptomyces viridochromogenes* spore germination initiated by calcium ions. J. Bacteriol. *143*, 377–382.

Eckert, C., Lecerf, M., Dubost, L., Arthur, M., and Mesnage, S. (2006). Functional analysis of AtlA, the major N-acetylglucosaminidase of *Enterococcus faecalis.* J. Bacteriol. *188*, 8513–8519.

Elliot, M.A., and Flardh, K. (2012). Streptomycete Spores. In Encyclopedia of Life Sciences eLS, (Chichester).

Elliot, M.A., Karoonuthaisiri, N., Huang, J., Bibb, M.J., Cohen, S.N., Kao, C.M., and Buttner, M.J. (2003). The chaplins: a family of hydrophobic cell-surface proteins involved in aerial mycelium formation in *Streptomyces coelicolor*. Genes Dev. *17*, 1727–1740.

Fan, D.P., and Beckman, M.M. (1971). Mutant of Bacillus subtilis demonstrating the requirement of lysis for growth. J. Bacteriol. *105*, 629–636.

Fan, D.P., Pelvit, M.C., and Cunningham, W.P. (1972). Structural difference between walls from ends and sides of the rod-shaped bacterium *Bacillus subtilis*. J. Bacteriol. *109*, 1266–1272.

Finn, R.D., Clements, J., Arndt, W., Miller, B.L., Wheeler, T.J., Schreiber, F., Bateman, A., and Eddy, S.R. (2015). HMMER web server: 2015 update. Nucleic Acids Res. *43*, W30-8.

Firczuk, M., and Bochtler, M. (2007). Folds and activities of peptidoglycan amidases. FEMS Microbiol. Rev. *31*, 676–691.

Firczuk, M., Mucha, A., and Bochtler, M. (2005). Crystal structures of active LytM. J. Mol. Biol. *354*, 578–590.

Flärdh, K., and Buttner, M.J. (2009). *Streptomyces* morphogenetics: dissecting differentiation in a filamentous bacterium. Nat. Rev. Microbiol. *7*, 36–49.

Flärdh, K., Richards, D.M., Hempel, A.M., Howard, M., and Buttner, M.J. (2012). Regulation of apical growth and hyphal branching in *Streptomyces*. Curr. Opin. Microbiol. *15*, 737–743.

Flemming, H.C., and Wingender, J. (2010). The biofilm matrix. Nat. Rev. Microbiol. *8*, 623–633.

Fontán, P.A., Voskuil, M.I., Gomez, M., Tan, D., Pardini, M., Manganelli, R., Fattorini, L., Schoolnik, G.K., and Smith, I. (2009). The *Mycobacterium tuberculosis* sigma factor σB is required for full response to cell envelope stress and hypoxia in vitro, but it is dispensable for in vivo growth. J. Bacteriol. *191*, 5628–5633.

Frankel, M.B., and Schneewind, O. (2012). Determinants of Murein Hydrolase Targeting to Cross-wall of *Staphylococcus aureus* Peptidoglycan. J. Biol. Chem. *287*, 10460–10471.

Gallo, P.M., Rapsinski, G.J., Wilson, R.P., Oppong, G.O., Sriram, U., Goulian, M., Buttaro, B., Caricchio, R., Gallucci, S., and Tükel, Ç. (2015). Amyloid-DNA Composites of Bacterial Biofilms Stimulate Autoimmunity. Immunity *42*, 1171–1184.

Gao, C., Hindra, Mulder, D., Yin, C., and Elliot, M.A. (2012). Crp Is a Global Regulator of Antibiotic Production in *Streptomyces*. mBio *3*, e00407-12-e00407-12.

Geer, L.Y., Domrachev, M., Lipman, D.J., and Bryant, S.H. (2002). CDART: protein homology by domain architecture. Genome Res. *12*, 1619–1623.

Gerhardt, P., and Black, S.H. (1961). Permeability of bacterial spores. II. Molecular variables affecting solute permeation. J. Bacteriol. *82*, 750–760.

Gietz, R.D., and Schiestl, R.H. (2008). High-efficiency yeast transformation using the LiAc / SS carrier DNA / PEG method. Nat. Protoc. *2*, 31–35.

Glauert, A.M., and Hopwood, D.A. (1961). The fine structure of *Streptomyces violaceoruber (S. coelicolor)*. III. The walls of the mycelium and spores. J. Biophys. Biochem. Cytol. *10*, 505–516.

Gottesman, S., and Storz, G. (2010). Bacterial Small RNA Regulators : Versatile Roles and Rapidly Evolving Variations. Cold Spring Harb. Perspect. Biol.

Grabowska, M., Jagielska, E., Czapinska, H., Bochtler, M., and Sabala, I. (2015). High resolution structure of an M23 peptidase with a substrate analogue. Sci. Rep. *5*, 14833.

Gregory, M.A., Till, R., and Smith, M.C.M. (2003). Integration site for *Streptomyces* phage ϕBT1 and development of site-specific integrating vectors. J. Bacteriol. *185*, 5320–5323.

Grund, A.D., and Ensign, J.C. (1982). Activation of *Streptomyces viridochromogenes* spores by detergents. Curr. Microbiol. *7*, 223–227.

Grund, A.D., and Ensign, J.C. (1985). Properties of the germination inhibitor of *Streptomyces viridochromogenes* spores. J. Gen. Microbiol. *131*, 833–847.

Gumbart, J.C., Beeby, M., Jensen, G.J., and Roux, B. (2014). *Escherichia coli* Peptidoglycan Structure and Mechanics as Predicted by Atomic-Scale Simulations. PLoS Comput. Biol. *10*.

Gupta, S., Ustok, F.I., Johnson, C.L., Bailey, D.M.D., Lowe, C.R., and Christie, G. (2013). Investigating the functional hierarchy of *Bacillus megaterium* PV361 spore germinant receptors. J. Bacteriol. *195*, 3045–3053.

Gust, B., Challis, G.L., Fowler, K., Kieser, T., and Chater, K.F. (2003). PCR-targeted *Streptomyces* gene replacement identifies a protein domain needed for biosynthesis of the sesquiterpene soil odor geosmin. Proc. Natl. Acad. Sci. U. S. A. *100*, 1541–1546.

Gust, B., Rourke, S.O., Bird, N., Kieser, T., and Chater, K. (2004). Recombineering in *Streptomyces coelicolor*. 1–22.

Haiser, H.J., Yousef, M.R., and Elliot, M.A. (2009). Cell wall hydrolases affect germination, vegetative growth, and sporulation in *Streptomyces coelicolor*. J. Bacteriol. *191*, 6501–6512.

Hall, C.W., and Mah, T.-F. (2017). Molecular mechanisms of biofilm-based antibiotic resistance and tolerance in pathogenic bacteria. FEMS Microbiol. Rev. *41*, 276–301.

Hanahan, D. (1983). Studies on transformation of *Escherichia coli* with plasmids. J. Mol. Biol. *166*, 557–580.

Harding, M.W., Marques, L.L.R., Howard, R.J., and Olson, M.E. (2009). Can filamentous fungi form biofilms? Trends Microbiol. *17*, 475–480.

Hardisson, C., Manzanal, M.B., Salas, J.A., and Suárez, J.E. (1978). Fine structure, physiology and biochemistry of arthrospore germination in *Streptomyces antibioticus*. J. Gen. Microbiol. *105*, 203–214.

Hartmann, M., Barsch, A., Niehaus, K., Pühler, A., Tauch, A., and Kalinowski, J. (2004). The glycosylated cell surface protein Rpf2, containing a resuscitation-promoting factor motif, is involved in intercellular communication of *Corynebacterium glutamicum*. Arch. Microbiol. *182*, 299–312.

Heckman, K.L., and Pease, L.R. (2007). Gene splicing and mutagenesis by PCR-driven overlap extension. Nat. Protoc. *2*, 924–932.

Heffron, J.D., Orsburn, B., and Popham, D.L. (2009). Roles of Germination-Specific Lytic Enzymes CwlJ and SleB in *Bacillus anthracis*. J. Bacteriol. *191*, 2237–2247.

Hempel, A.M., Cantlay, S., Molle, V., Wang, S.-B., Naldrett, M.J., Parker, J.L., Richards,

D.M., Jung, Y.-G., Buttner, M.J., and Flardh, K. (2012). The Ser/Thr protein kinase AfsK regulates polar growth and hyphal branching in the filamentous bacteria *Streptomyces*. Proc. Natl. Acad. Sci. *109*, E2371–E2379.

Henriques, A.O., and Moran, Jr., C.P. (2007). Structure, Assembly, and Function of the Spore Surface Layers. Annu. Rev. Microbiol. *61*, 555–588.

Herlihey, F.A., Moynihan, P.J., and Clarke, A.J. (2014). The essential protein for bacterial flagella formation FlgJ functions as a β-N-acetylglucosaminidase. J. Biol. Chem. *289*, 31029–31042.

Hesketh, A., Chen, W.J., Ryding, J., Chang, S., and Bibb, M. (2007). The global role of ppGpp synthesis in morphological differentiation and antibiotic production in *Streptomyces coelicolor* A3(2). Genome Biol. *8*.

Hesketh, A., Hill, C., Mokhtar, J., Novotna, G., Tran, N., Bibb, M., and Hong, H.-J. (2011). Genome-wide dynamics of a bacterial response to antibiotics that target the cell envelope. BMC Genomics *12*, 226.

Hett, E.C., Chao, M.C., Steyn, A.J., Fortune, S.M., Deng, L.L., and Rubin, E.J. (2007). A partner for the resuscitation-promoting factors of *Mycobacterium tuberculosis*. Mol. Microbiol. *66*, 658–668.

Hett, E.C., Chao, M.C., Deng, L.L., and Rubin, E.J. (2008). A mycobacterial enzyme essential for cell division synergizes with resuscitation-promoting factor. PLoS Pathog. *4*, e1000001.

Hett, E.C., Chao, M.C., and Rubin, E.J. (2010). Interaction and Modulation of Two Antagonistic Cell Wall Enzymes of Mycobacteria. PLoS Pathog. *6*, e1001020.

Higgins, D., and Dworkin, J. (2012). Recent progress in *Bacillus subtilis* sporulation. FEMS Microbiol. Rev. *36*, 131–148.

Hirsch, C.F., and Ensign, J.C. (1976a). Nutritionally defined conditions for germination of *Streptomyces viridochromogenes* spores. J. Bacteriol. *126*, 13–23.

Hirsch, C.F., and Ensign, J.C. (1976b). Heat activation of *Streptomyces viridochromogenes* spores. J. Bacteriol. *126*, 24–30.

Hobley, L., Ostrowski, A., Rao, F. V, Bromley, K.M., Porter, M., Prescott, A.R., MacPhee, C.E., van Aalten, D.M.F., and Stanley-Wall, N.R. (2013). BslA is a self-assembling bacterial hydrophobin that coats the *Bacillus subtilis* biofilm. Proc. Natl. Acad. Sci. *110*, 13600–13605.

Hobley, L., Harkins, C., MacPhee, C.E., and Stanley-Wall, N.R. (2015). Giving structure to the biofilm matrix: an overview of individual strategies and emerging common themes. FEMS Microbiol. Rev. *39*, 649–669.

Hopwood, D.A. (2007). *Streptomyces* in Nature and Medicine: The Antibiotic Makers

(Oxford: Oxford University Press).

Hugonnet, J.E., Haddache, N., Veckerle, C., Dubost, L., Marie, A., Shikura, N., Mainardi, J.L., Rice, L.B., and Arthur, M. (2014). Peptidoglycan cross-linking in glycopeptide resistant Actinomycetales. Antimicrob. Agents Chemother.

Jakimowicz, D., and Van Wezel, G.P. (2012). Cell division and DNA segregation in *Streptomyces*: How to build a septum in the middle of nowhere? Mol. Microbiol. *85*, 393–404.

Jenal, U., Reinders, A., and Lori, C. (2017). Cyclic di - GMP : second messenger extraordinaire. Nat. Rev. Microbiol. *15*, 271–284.

Jenni, R., and Berger-Bächi, B. (1998). Teichoic acid content in different lineages of *Staphylococcus aureus* NCTC8325. Arch. Microbiol. *170*, 171–178.

Jiao, Y., Cody, G.D., Harding, A.K., Wilmes, P., Schrenk, M., Wheeler, K.E., Banfield, J.F., and Thelen, M.P. (2010). Characterization of extracellular polymeric substances from acidophilic microbial biofilms. Appl. Environ. Microbiol. *76*, 2916–2922.

Jing, C., Jianbo, W., Yuan, L., Rong, J., and Baoyi, L. (2003). A new IL-1 receptor inhibitor 139A: Fermentation, isolation, physico-chemical properties and structure. J. Antibiot. (Tokyo). *56*, 87–90.

Jones, S.E., Ho, L., Rees, C.A., Hill, J.E., Nodwell, J.R., and Elliot, M.A. (2017). *Streptomyces* exploration is triggered by fungal interactions and volatile signals. eLife *6*, 33.

de Jong, W., Wösten, H.A.B., Dijkhuizen, L., and Claessen, D. (2009). Attachment of *Streptomyces coelicolor* is mediated by amyloidal fimbriae that are anchored to the cell surface via cellulose. Mol. Microbiol. *73*, 1128–1140.

Jungwirth, B., Emer, D., Brune, I., Hansmeier, N., Pühler, A., Eikmanns, B.J., and Tauch, A. (2008). Triple transcriptional control of the resuscitation promoting factor 2 (*rpf2*) gene of *Corynebacterium glutamicum* by the regulators of acetate metabolism RamA and RamB and the cAMP-dependent regulator GlxR. FEMS Microbiol. Lett. *281*, 190–197.

Jungwirth, B., Sala, C., Kohl, T.A., Uplekar, S., Baumbach, J., Cole, S.T., Puhler, A., and Tauch, A. (2013). High-resolution detection of DNA binding sites of the global transcriptional regulator GlxR in *Corynebacterium glutamicum*. Microbiology *159*, 12–22.

Kahramanoglou, C., Cortes, T., Matange, N., Hunt, D.M., Visweswariah, S.S., Young, D.B., and Buxton, R.S. (2014). Genomic mapping of cAMP receptor protein (CRPMt) in *Mycobacterium tuberculosis*: Relation to transcriptional start sites and the role of CRPMtas a transcription factor. Nucleic Acids Res. *42*, 8320–8329.

Kana, B.D., Gordhan, B.G., Downing, K.J., Sung, N., Vostroktunova, G., Machowski, E.E., Tsenova, L., Young, M., Kaprelyants, A., Kaplan, G., et al. (2008). The resuscitation-

promoting factors of *Mycobacterium tuberculosis* are required for virulence and resuscitation from dormancy but are collectively dispensable for growth in vitro. Mol. Microbiol. *67*, 672–684.

Kearns, D.B. (2010). A field guide to bacterial swarming motility. Nat. Rev. Microbiol. *8*, 634–644.

Keep, N.H., Ward, J.M., Robertson, G., Cohen-Gonsaud, M., and Henderson, B. (2006a). Bacterial resuscitation factors: Revival of viable but non-culturable bacteria. Cell. Mol. Life Sci. *63*, 2555–2559.

Keep, N.H., Ward, J.M., Cohen-Gonsaud, M., and Henderson, B. (2006b). Wake up! Peptidoglycan lysis and bacterial non-growth states. Trends Microbiol. *14*, 271–276.

Kieser, T., Bibb, M.J., Buttner, M.J., Chater, K.F., and Hopwood, D.A. (2000). Practical Streptomyces Genetics.

Kim, H.S., Lee, E.J., Cho, Y.H., and Roe, J.H. (2013a). Post-translational regulation of a developmental catalase, CatB, involves a metalloprotease, SmpA and contributes to proper differentiation and osmoprotection of *Streptomyces coelicolor*. Res. Microbiol. *164*, 327–334.

Kim, J.-H., O'Brien, K.M., Sharma, R., Boshoff, H.I.M., Rehren, G., Chakraborty, S., Wallach, J.B., Monteleone, M., Wilson, D.J., Aldrich, C.C., et al. (2013b). A genetic strategy to identify targets for the development of drugs that prevent bacterial persistence. Proc. Natl. Acad. Sci. *110*, 19095–19100.

Kim, Y., Ho, S.O., Gassman, N.R., Korlann, Y., Landorf, E. V., Collart, F.R., and Weiss, S. (2008). Efficient Site-Specific Labeling of Proteins via Cysteines. Bioconj. Chem. *19*, 786.

Kleinschnitz, E.-M., Heichlinger, A., Schirner, K., Winkler, J., Latus, A., Maldener, I., Wohlleben, W., and Muth, G. (2011a). Proteins encoded by the mre gene cluster in *Streptomyces coelicolor* A3(2) cooperate in spore wall synthesis. Mol. Microbiol. *79*, 1367–1379.

Kleinschnitz, E.M., Latus, A., Sigle, S., Maldener, I., Wohlleben, W., and Muth, G. (2011b). Genetic analysis of SCO2997, encoding a *tagF* homologue, indicates a role for wall teichoic acids in sporulation of *Streptomyces coelicolor* A3(2). J. Bacteriol. *193*, 6080–6085.

Kohanski, M.A., Dwyer, D.J., Hayete, B., Lawrence, C.A., and Collins, J.J. (2007). A Common Mechanism of Cellular Death Induced by Bactericidal Antibiotics. Cell *130*, 797–810.

Kruse, T., Bork-Jensen, J., and Gerdes, K. (2005). The morphogenetic MreBCD proteins of *Escherichia coli* form an essential membrane-bound complex. Mol. Microbiol. *55*, 78–89.

Kuznetsov, V.D., Filippova, S.N., and Rybakova, A.M. (1984). Nature of the brown

pigment and the composition of the phenol oxidases of *Streptomyces galbus* . Mikrobiologiia *53*, 251–256.

Lattif, A.A., Mukherjee, P.K., Chandra, J., Roth, M.R., Welti, R., Rouabhia, M., and Ghannoum, M.A. (2011). Lipidomics of *Candida albicans* biofilms reveals phase-dependent production of phospholipid molecular classes and role for lipid rafts in biofilm formation. Microbiology *157*, 3232–3242.

Lee, E., Cho, Y., Kim, H., Ahn, B., and Roe, J. (2004). Regulation of σ B by an Anti- and an Anti-Anti-Sigma Factor in *Streptomyces coelicolor* in Response to Osmotic Stress. J. Bacteriol. *186*, 8490–8498.

Lenarcic, R., Halbedel, S., Visser, L., Shaw, M., Wu, L.J., Errington, J., Marenduzzo, D., and Hamoen, L.W. (2009). Localisation of DivIVA by targeting to negatively curved membranes. EMBO J. *28*, 2272–2282.

Létoffé, S., Audrain, B., Bernier, S.P., Delepierre, M., and Ghigo, J.M. (2014). Aerial exposure to the bacterial volatile compound trimethylamine modifies antibiotic resistance of physically separated bacteria by raising culture medium pH. mBio *5*, 1–12.

Li, Z., Hwang, S., and Bar-Peled, M. (2016). Discovery of a unique extracellular polysaccharide in members of the pathogenic *Bacillus* that can co-form with spores. J. Biol. Chem. *291*, 19051–19067.

Lu, J.Z., Fujiwara, T., Komatsuzawa, H., Sugai, M., and Sakon, J. (2006). Cell wall-targeting domain of glycylglycine endopeptidase distinguishes among peptidoglycan cross-bridges. J. Biol. Chem. *281*, 549–558.

Lyons, N.A., and Kolter, R. (2015). On the evolution of bacterial multicellularity. Curr. Opin. Microbiol. *24*, 21–28.

Machowski, E.E., Senzani, S., Ealand, C., and Kana, B.D. (2014). Comparative genomics for mycobacterial peptidoglycan remodelling enzymes reveals extensive genetic multiplicity. BMC Microbiol. *14*, 75.

MacNeil, D.J., Gewain, K.M., Ruby, C.L., Dezeny, G., Gibbons, P.H., and MacNeil, T. (1992). Analysis of *Streptomyces avermitilis* genes required for avermectin biosynthesis utilizing a novel integration vector. Gene *111*, 61–68.

Mahne, M., Tauch, A., Pühler, A., and Kalinowski, J. (2006). The *Corynebacterium glutamicum* gene *pmt* encoding a glycosyltransferase related to eukaryotic protein-O-mannosyltransferases is essential for glycosylation of the resuscitation promoting factor (Rpf2) and other secreted proteins. FEMS Microbiol. Lett. *259*, 226–233.

Manganelli, R., Voskuil, M.I., Schoolnik, G.K., and Smith, I. (2001). The *Mycobacterium tuberculosis* ECF sigma factor SigmaE: role in global gene expression and survival in macrophages. Mol. Microbiol. *41*, 423–437.

Mazza, P., Noens, E.E., Schirner, K., Grantcharova, N., Mommaas, A.M., Koerten, H.K., Muth, G., Flärdh, K., van Wezel, G.P., and Wohlleben, W. (2006). MreB of *Streptomyces coelicolor* is not essential for vegetative growth but is required for the integrity of aerial hyphae and spores. Mol. Microbiol. *60*, 838–852.

Mckenney, P.T., Driks, A., and Eichenberger, P. (2013). The *Bacillus subtilis* endospore: Assembly and functions of the multilayered coat. Nat. Rev. Microbiol. *11*, 33–44.

Meador-parton, J., and Popham, D.L. (2000). Structural Analysis of *Bacillus subtilis* Spore Peptidoglycan during Sporulation. J. Bacteriol. *182*, 4491–4499.

Mesnage, S., Dellarole, M., Baxter, N.J., Rouget, J.-B., Dimitrov, J.D., Wang, N., Fujimoto, Y., Hounslow, A.M., Lacroix-Desmazes, S., Fukase, K., et al. (2014). Molecular basis for bacterial peptidoglycan recognition by LysM domains. Nat. Commun. *5*, 4269.

Milanovich, N., Suh, M., Jankowiak, R., Small, G.J., and Hayes, J.M. (1996). Binding of TO-PRO-3 and TOTO-3 to DNA: Fluorescence and hole-burning studies. J. Phys. Chem. *100*, 9181–9186.

Mir, M., Asong, J., Li, X., Cardot, J., Boons, G.-J., and Husson, R.N. (2011). The Extracytoplasmic Domain of the *Mycobacterium tuberculosis* Ser/Thr Kinase PknB Binds Specific Muropeptides and Is Required for PknB Localization. PLoS Pathog. *7*, e1002182.

Mitchell, K.F., Zarnowski, R., and Andes, D.R. (2016). Fungal Super Glue: The Biofilm Matrix and Its Composition, Assembly, and Functions. PLoS Pathog. *12*, 1–6.

Mlouka, M.A. Ben, Cousseau, T., and Di Martino, P. (2016). Application of fluorescently labelled lectins for the study of polysaccharides in biofilms with a focus on biofouling of nanofiltration membranes. AIMS Mol. Sci. *3*, 338–356.

Moody, M.J., Young, R.A., Jones, S.E., and Elliot, M.A. (2013). Comparative analysis of non-coding RNAs in the antibiotic-producing Streptomyces bacteria. BMC Genomics *14*, 558.

Mukamolova, G. V, Kaprelyants, A.S., Young, D.I., Young, M., and Kell, D.B. (1998). A bacterial cytokine. Proc. Natl. Acad. Sci. U. S. A. *95*, 8916–8921.

Mukamolova, G. V, Turapov, O.A., Kazarian, K., Telkov, M., Kaprelyants, A.S., Kell, D.B., and Young, M. (2002a). The *rpf* gene of *Micrococcus luteus* encodes an essential secreted growth factor. Mol. Microbiol. *46*, 611–621.

Mukamolova, G. V, Turapov, O.A., Young, D.I., Kaprelyants, A.S., Kell, D.B., and Young, M. (2002b). A family of autocrine growth factors in *Mycobacterium tuberculosis*. Mol. Microbiol. *46*, 623–635.

Mukamolova, G. V, Murzin, A.G., Salina, E.G., Demina, G.R., Kell, D.B., Kaprelyants, A.S., and Young, M. (2006). Muralytic activity of *Micrococcus luteus* Rpf and its relationship to physiological activity in promoting bacterial growth and resuscitation. Mol. Microbiol.

59, 84–98.

Nakashio, S., and Gerhardt, P. (1985). Protoplast dehydration correlated with heat resistance of bacterial spores. J. Bacteriol. *162*, 571–578.

Navarro, M.V.A.S., Yildiz, F.H., and Sondermann, H. (2010). *Vibrio cholerae* VpsT Regulates by Directly Sensing Cyclic di-GMP. Science. *327*, 866–869.

Nelson, J.W., Sudarsan, N., Furukawa, K., Weinberg, Z., Wang, J.X., and Breaker, R.R. (2013). Riboswitches in eubacteria sense the second messenger c-di-AMP. Nat. Chem. Biol. *9*, 834–839.

Neuhaus, F.C., and Baddiley, J. (2003). A Continuum of Anionic Charge: Structures and Functions of D- Alanyl- Teichoic Acids in Gram- Positive Bacteria. Microbiol. Mol. Biol. Rev. *67*, 686.

Nikitushkin, V.D., Demina, G.R., Shleeva, M.O., and Kaprelyants, A.S. (2013). Peptidoglycan fragments stimulate resuscitation of non-culturable mycobacteria. Antonie Van Leeuwenhoek *103*, 37–46.

Nikitushkin, V.D., Demina, G.R., Shleeva, M.O., Guryanova, S. V, Ruggiero, A., Berisio, R., and Kaprelyants, A.S. (2015). A product of RpfB and RipA joint enzymatic action promotes the resuscitation of dormant mycobacteria. FEBS J. *282*, 2500–2511.

Noens, E.E., Mersinias, V., Willemse, J., Traag, B.A., Laing, E., Chater, K.F., Smith, C.P., Koerten, H.K., and van Wezel, G.P. (2007). Loss of the controlled localization of growth stage-specific cell-wall synthesis pleiotropically affects developmental gene expression in an *ssgA* mutant of *Streptomyces coelicolor*. Mol. Microbiol. *64*, 1244–1259.

Noens, E.E.E., Mersinias, V., Traag, B.A., Smith, C.P., Koerten, H.K., and van Wezel, G.P. (2005). SsgA-like proteins determine the fate of peptidoglycan during sporulation of *Streptomyces coelicolor*. Mol. Microbiol. *58*, 929–944.

Nosanchuk, J.D., and Casadevall, A. (2003). The contribution of melanin to microbial pathogenesis. Cell. Microbiol. *5*, 203–223.

Odintsov, S.G., Sabala, I., Marcyjaniak, M., and Bochtler, M. (2004). Latent LytM at 1.3 Å resolution. J. Mol. Biol. *335*, 775–785.

Oliver, J.D. (2005). The Viable but Nonculturable State in Bacteria. J. Microbiol. *43*, 93–100.

Oliver, J.D. (2010). Recent findings on the viable but nonculturable state in pathogenic bacteria. FEMS Microbiol. Rev. *34*, 415–425.

Ostash, B., Shashkov, A., Streshinskaya, G., Tul'skaya, E., Baryshnikova, L., Dmitrenok, A., Dacyuk, Y., and Fedorenko, V. (2014). Identification of *Streptomyces coelicolor* M145 genomic region involved in biosynthesis of teichulosonic acid-cell wall glycopolymer. Folia Microbiol. (Praha). *59*, 355–360.

Ostrowski, A., Mehert, A., Prescott, A., Kiley, T.B., and Stanley-Wall, N.R. (2011). YuaB functions synergistically with the exopolysaccharide and TasA amyloid fibers to allow biofilm formation by *Bacillus subtilis*. J. Bacteriol. *193*, 4821–4831.

Paget, M.S., Chamberlin, L., Atrih, A., Foster, S.J., and Buttner, M.J. (1999). Evidence that the extracytoplasmic function sigma factor SigmaE is required for normal cell wall structure in *Streptomyces coelicolor* A3(2). J. Bacteriol. *181*, 204–211.

Paidhungat, M., and Setlow, P. (2000). Role of ger proteins in nutrient and nonnutrient triggering of spore germination in *Bacillus subtilis*. J. Bacteriol. *182*, 2513–2519.

Park, J.H., Jo, Y., Jang, S.Y., Kwon, H., and Irie, Y. (2015). The *cabABC* Operon Essential for Biofilm and Rugose Colony Development in *Vibrio vulnificus*. PLoS Pathog. *11*, e1005192.

Peirson, S.N. (2003). Experimental validation of novel and conventional approaches to quantitative real-time PCR data analysis. Nucleic Acids Res. *31*, 73e–73.

Pesavento, C., Becker, G., Sommerfeldt, N., Possling, A., Tschowri, N., Mehlis, A., and Hengge, R. (2008). Inverse regulatory coordination of motility and curli-mediated adhesion in *Escherichia coli*. Genes Dev. *22*, 2434–2446.

Petersen, F., Zähner, H., Metzger, J.W., Freund, S., and Hummel, R.P. (1993). Germicidin, an autoregulative germination inhibitor of *Streptomyces viridochromogenes* NRRL B-1551. J. Antibiot. (Tokyo). *46*, 1126–1138.

Petersen, T.N., Brunak, S., von Heijne, G., and Nielsen, H. (2011). SignalP 4.0: discriminating signal peptides from transmembrane regions. Nat. Methods *8*, 785–786.

Petruzzi, B., Briggs, R.E., Swords, W.E., de Castro, C., Molinaro, A., and Inzana, T.J. (2017). Capsular polysaccharide interferes with biofilm formation by *Pasteurella multocida* serogroup A. mBio *8*, 1–17.

Pisu, D., Provvedi, R., Espinosa, D.M., Payan, J.B., Boldrin, F., Palù, G., Hernandez-Pando, R., and Manganelli, R. (2017). The alternative sigma factors SigE and SigB are involved in tolerance and persistence to antitubercular drugs. Antimicrob. Agents Chemother. *61*, 1–11.

Potúcková, L., Kelemen, G.H., Findlay, K.C., Lonetto, M.A., Buttner, M.J., and Kormanec, J. (1995). A new RNA polymerase sigma factor, SigmaF is required for the late stages of morphological differentiation in *Streptomyces* spp. Mol. Microbiol. *17*, 37–48.

Rahman, O., Pfitzenmaier, M., Pester, O., Morath, S., Cummings, S.P., Hartung, T., and Sutcliffe, I.C. (2009). Macroamphiphilic components of thermophilic actinomycetes: Identification of lipoteichoic acid in *Thermobifida fusca*. J. Bacteriol. *91*, 152–160.

Ramamurthi, K.S., and Losick, R. (2009). Negative membrane curvature as a cue for subcellular localization of a bacterial protein. Proc. Natl. Acad. Sci. *106*, 13541–13545.

Raman, S., Hazra, R., Dascher, C.C., and Husson, R.N. (2004). Transcription Regulation by

the *Mycobacterium tuberculosis* Alternative Sigma Factor SigD and Its Role in Virulence. J. Bacteriol. *186*, 6605–6616.

Ravagnani, A., Finan, C.L., and Young, M. (2005). A novel firmicute protein family related to the actinobacterial resuscitation-promoting factors by non-orthologous domain displacement. BMC Genomics *6*, 1–14.

Raymond, J.B., Mahapatra, S., Crick, D.C., and Pavelka, M.S. (2005). Identification of the *namH* gene, encoding the hydroxylase responsible for the N-glycolylation of the mycobacterial peptidoglycan. J. Biol. Chem. *280*, 326–333.

Redenbach, M., Kieser, H.M., Denapaite, D., Eichner, A., Cullum, J., Kinashi, H., and Hopwood, D.A. (1996). A set of ordered cosmids and a detailed genetic and physical map for the 8 Mb *Streptomyces coelicolor* A3(2) chromosome. Mol. Microbiol. *21*, 77–96.

Reichmann, N.T., and Gründling, A. (2011). Location, synthesis and function of glycolipids and polyglycerolphosphate lipoteichoic acid in Gram-positive bacteria of the phylum Firmicutes. FEMS Microbiol. Lett. *319*, 97–105.

Reineke, K., Mathys, A., Heinz, V., and Knorr, D. (2013). Mechanisms of endospore inactivation under high pressure. Trends Microbiol. *21*, 296–304.

Renberg, I., and Nilsson, M. (1992). Dormant bacteria in lake sediments as palaeoecological indicators. J. Paleolimnol. *7*, 127–135.

Rioseras, B., Yagüe, P., López-García, M.T., Gonzalez-Quiñonez, N., Binda, E., Marinelli, F., and Manteca, A. (2016). Characterization of SCO4439, a D-alanyl-D-alanine carboxypeptidase involved in spore cell wall maturation, resistance, and germination in *Streptomyces coelicolor*. Sci. Rep. *6*, 21659.

Rittershaus, E.S.C., Baek, S.H., and Sassetti, C.M. (2013). The normalcy of dormancy: Common themes in microbial quiescence. Cell Host Microbe *13*, 643–651.

Rode, L., Willard Lewis, C., and Foster, J.W. (1962). Electron microscopy of spores of *Bacillus megaterium* with special reference to the effects of fixation and thin sectioning. J. Cell Biol. *13*, 423–435.

Rodriguez Camargo, D.C., Tripsianes, K., Buday, K., Franko, A., Göbl, C., Hartlmüller, C., Sarkar, R., Aichler, M., Mettenleiter, G., Schulz, M., et al. (2017). The redox environment triggers conformational changes and aggregation of hIAPP in Type II Diabetes. Sci. Rep. *7*, 1–11.

Romero, D., Aguilar, C., Losick, R., and Kolter, R. (2010). Amyloid fibers provide structural integrity to *Bacillus subtilis* biofilms. Proc. Natl. Acad. Sci. *107*, 2230–2234.

Rossetti, V., and Bagheri, H.C. (2012). Advantages of the division of labour for the long-term population dynamics of cyanobacteria at different latitudes. Proc. R. Soc. B Biol. Sci. *279*, 3457–3466.

Ruggiero, A., Tizzano, B., Pedone, E., Pedone, C., Wilmanns, M., and Berisio, R. (2009). Crystal Structure of the Resuscitation-Promoting FactorΔDUFRpfB from *M. tuberculosis*. J. Mol. Biol. *385*, 153–162.

Ruggiero, A., Squeglia, F., Romano, M., Vitagliano, L., De Simone, A., and Berisio, R. (2016). The structure of Resuscitation promoting factor B from *M. tuberculosis* reveals unexpected ubiquitin-like domains. Biochim. Biophys. Acta *1860*, 445–451.

Ruggiero, A., Squeglia, F., Romano, M., Vitagliano, L., De Simone, A., and Berisio, R. (2017). Structure and dynamics of the multi-domain resuscitation promoting factor RpfB from *Mycobacterium tuberculosis*. J. Biomol. Struct. Dyn. *35*, 1322–1330.

Russell-Goldman, E., Xu, J., Wang, X., Chan, J., and Tufariello, J.M. (2008). A *Mycobacterium tuberculosis* Rpf double-knockout strain exhibits profound defects in reactivation from chronic tuberculosis and innate immunity phenotypes. Infect. Immun. *76*, 4269–4281.

Russell, M.H., Bible, A.N., Fang, X., Gooding, J.R., Campagna, S.R., Gomelsky, M., and Alexandrea, G. (2013). Integration of the second messenger c-di-GMP into the chemotactic signaling pathway. mBio *4*, 1–11.

Schägger, H. (2006). Tricine–SDS-PAGE. Nat. Protoc. *1*, 16–22.

Scheurwater, E., Reid, C.W., and Clarke, A.J. (2008). Lytic transglycosylases: Bacterial space-making autolysins. Int. J. Biochem. & Cell Biol. *40*, 586–591.

Schirrmeister, B.E., Antonelli, A., and Bagheri, H.C. (2011). The origin of multicellularity in cyanobacteria. BMC Evol. Biol. *11*.

Schlag, M., Biswas, R., Krismer, B., Kohler, T., Zoll, S., Yu, W., Schwarz, H., Peschel, A., and Götz, F. (2010). Role of staphylococcal wall teichoic acid in targeting the major autolysin Atl. Mol. Microbiol. *75*, 864–873.

Schleifer, K.H., and Kandler, O. (1972). Peptidoglycan types of bacterial cell walls and their taxonomic implications. Bacteriol. Rev. *36*, 407–477.

Schlimpert, S., Wasserstrom, S., Chandra, G., Bibb, M.J., Findlay, K.C., Flärdh, K., and Buttner, M.J. (2017). Two dynamin-like proteins stabilize FtsZ rings during *Streptomyces* sporulation. Proc. Natl. Acad. Sci. *393*, 201704612.

Schneider, C.A., Rasband, W.S., and Eliceiri, K.W. (2012). NIH Image to ImageJ: 25 years of image analysis. Nat. Methods *9*, 671–675.

Schooling, S.R., and Beveridge, T.J. (2006). Membrane vesicles: An overlooked component of the matrices of biofilms. J. Bacteriol. *188*, 5945–5957.

Schooling, S.R., Hubley, A., and Beveridge, T.J. (2009). Interactions of DNA with biofilm-derived membrane vesicles. J. Bacteriol. *191*, 4097–4102.

Segev, E., Rosenberg, A., Mamou, G., Sinai, L., and Ben-Yehuda, S. (2013). Molecular

Kinetics of Reviving Bacterial Spores. J. Bacteriol. *195*, 1875–1882.

Seiler, P., Ulrichs, T., Bandermann, S., Pradl, L., Jörg, S., Krenn, V., Morawietz, L., Kaufmann, S.H.E., and Aichele, P. (2003). Cell-wall alterations as an attribute of *Mycobacterium tuberculosis* in latent infection. J. Infect. Dis. *188*, 1326–1331.

Serra, D.O., Richter, A.M., Klauck, G., Mika, F., and Hengge, R. (2013a). Microanatomy at Cellular Resolution and Spatial Order of Physiological Differentiation in a Bacterial Biofilm. mBio *4*, e00103-13-e00103-13.

Serra, D.O., Richter, A.M., and Hengge, R. (2013b). Cellulose as an architectural element in spatially structured *Escherichia coli* biofilms. J. Bacteriol. *195*, 5540–5554.

Setlow, P. (2006). Spores of *Bacillus subtilis*: Their resistance to and killing by radiation, heat and chemicals. In Journal of Applied Microbiology, pp. 514–525.

Setlow, P. (2013). Summer meeting 2013 - when the sleepers wake: The germination of spores of *Bacillus* species. J. Appl. Microbiol. *115*, 1251–1268.

Setlow, P. (2014). Germination of spores of *Bacillus* species: what we know and do not know. J. Bacteriol. *196*, 1297–1305.

Sexton, D.L., St-Onge, R.J., Haiser, H.J., Yousef, M.R., Brady, L., Gao, C., Leonard, J., and Elliot, M.A. (2015). Resuscitation-promoting factors are cell wall-lytic enzymes with important roles in the germination and growth of *Streptomyces coelicolor*. J. Bacteriol.

Shah, I.M., Laaberki, M.-H., Popham, D.L., and Dworkin, J. (2008). A Eukaryotic-like Ser/Thr Kinase Signals Bacteria to Exit Dormancy in Response to Peptidoglycan Fragments. Cell *135*, 486–496.

Sharma, A.K., Chatterjee, A., Gupta, S., Banerjee, R., Mandal, S., Mukhopadhyay, J., Basu, J., and Kundu, M. (2015). MtrA, an essential response regulator of the MtrAB two-component system, regulates the transcription of resuscitation-promoting factor B of *Mycobacterium tuberculosis*. Microbiol. (United Kingdom) *161*, 1271–1281.

Shashkov, A.S., Ostash, B.E., Fedorenko, V.A., Streshinskaya, G.M., Tul'skaya, E.M., Senchenkova, S.N., Baryshnikova, L.M., and Evtushenko, L.I. (2012). Novel teichulosonic acid from cell wall of *Streptomyces coelicolor* M145. Carbohydr. Res. *359*, 70–75.

Shleeva, M., Goncharenko, A., Kudykina, Y., Young, D., Young, M., and Kaprelyants, A. (2013). Cyclic Amp-Dependent Resuscitation of Dormant Mycobacteria by Exogenous Free Fatty Acids. PLoS One *8*, e82914.

Sigle, S., Steblau, N., Wohlleben, W., and Muth, G. (2016). Polydiglycosylphosphate Transferase PdtA (SCO2578) of *Streptomyces coelicolor* A3(2) Is Crucial for Proper Sporulation and Apical Tip Extension under Stress Conditions. Appl. Environ. Microbiol. *82*, 5661–5672.

Soufo, H.J.D., and Graumann, P.L. (2006). Dynamic localization and interaction with

other *Bacillus subtilis* actin-like proteins are important for the function of MreB. Mol. Microbiol. *62*, 1340–1356.

Squeglia, F., Marchetti, R., Ruggiero, A., Lanzetta, R., Marasco, D., Dworkin, J., Petoukhov, M., Molinaro, A., Berisio, R., and Silipo, A. (2011). Chemical basis of peptidoglycan discrimination by PrkC, a key kinase involved in bacterial resuscitation from dormancy. J. Am. Chem. Soc. *133*, 20676–20679.

St-Onge, R.J., and Elliot, M.A. (2017). Regulation of a muralytic enzyme-encoding gene by two non-coding RNAs. RNA Biol. *14*, 1592–1605.

St-Onge, R.J., Haiser, H.J., Yousef, M.R., Sherwood, E., Tschowri, N., Al-Bassam, M., and Elliot, M.A. (2015). Nucleotide second messenger-mediated regulation of a muralytic enzyme in *Streptomyces*. Mol. Microbiol. *96*, 779–795.

Steen, A., Buist, G., Horsburgh, G.J., Venema, G., Kuipers, O.P., Foster, S.J., and Kok, J. (2005). AcmA of *Lactococcus lactis* is an N-acetylglucosaminidase with an optimal number of LysM domains for proper functioning. FEBS J. *272*, 2854–2868.

Strakova, E., Bobek, J., Zikova, A., and Vohradsky, J. (2013). Global Features of Gene Expression on the Proteome and Transcriptome Levels in *S. coelicolor* during Germination. PLoS One *8*, e72842.

Süsstrunk, U., Pidoux, J., Taubert, S., Ullmann, A., and Thompson, C.J. (1998). Pleiotropic effects of cAMP on germination, antibiotic biosynthesis and morphological development in *Streptomyces coelicolor*. Mol. Microbiol. *30*, 33–46.

Swerdlow, B.M., Setlow, B., and Setlow, P. (1981). Levels of H+ and other monovalent cations in dormant and germinating spores of *Bacillus megaterium*. J. Bacteriol. *148*, 20–29.

Swiercz, J.P., and Elliot, M.A. (2011). Streptomyces Sporulation. In Bacterial Spores Current Research and Applications, (Horizon Scientific Press.), pp. 1–18.

Swiercz, J.P., Hindra, Bobek, J., Haiser, H.J., Di Berardo, C., Tjaden, B., and Elliot, M.A. (2008). Small non-coding RNAs in *Streptomyces coelicolor*. Nucleic Acids Res. *36*, 7240–7251.

Swiercz, J.P., Nanji, T., Gloyd, M., Guarné, A., and Elliot, M.A. (2013). A novel nucleoid-associated protein specific to the actinobacteria. Nucleic Acids Res. *41*, 4171–4184.

Taglialegna, A., Lasa, I., and Valle, J. (2016). Amyloid Structures as Biofilm Matrix Scaffolds. J. Bacteriol. *198*, 2579–2588.

Telkov, M. V, Demina, G.R., Voloshin, S.A., Salina, E.G., Dudik, T. V, Stekhanova, T.N., Mukamolova, G. V, Kazaryan, K.A., Goncharenko, A. V, Young, M., et al. (2006). Proteins of the Rpf (resuscitation promoting factor) family are peptidoglycan hydrolases. Biochemistry. (Mosc). *71*, 414–422.

Tomitani, A., Knoll, A.H., Cavanaugh, C.M., and Ohno, T. (2006). The evolutionary diversification of cyanobacteria: Molecular-phylogenetic and paleontological perspectives. Proc. Natl. Acad. Sci. *103*, 5442–5447.

Traag, B.A., and Wezel, G.P. (2008). The SsgA-like proteins in actinomycetes: small proteins up to a big task. Antonie Van Leeuwenhoek *94*, 85–97.

Trampari, E., Stevenson, C.E.M., Little, R.H., Wilhelm, T., Lawson, D.M., and Malone, J.G. (2015). Bacterial rotary export ATPases are allosterically regulated by the nucleotide second messenger cyclic-di-GMP. J. Biol. Chem. *290*, 24470–24483.

Tufariello, J.M., Jacobs, W.R., and Chan, J. (2004). Individual *Mycobacterium tuberculosis* resuscitation-promoting factor homologues are dispensable for growth in vitro and in vivo. Infect. Immun. *72*, 515–526.

Tufariello, J.M., Mi, K., Xu, J., Manabe, Y.C., Kesavan, A.K., Drumm, J., Tanaka, K., Jacobs, W.R., and Chan, J. (2006). Deletion of the *Mycobacterium tuberculosis* resuscitation-promoting factor Rv1009 gene results in delayed reactivation from chronic tuberculosis. Infect. Immun. *74*, 2985–2995.

Turapov, O., Loraine, J., Jenkins, C.H., Barthe, P., McFeely, D., Forti, F., Ghisotti, D., Hesek, D., Lee, M., Bottrill, A.R., et al. (2015). The external PASTA domain of the essential serine/threonine protein kinase PknB regulates mycobacterial growth. Open Biol. *5*, 150025.

Turner, R.D., Vollmer, W., and Foster, S.J. (2014). Different walls for rods and balls: The diversity of peptidoglycan. Mol. Microbiol. *91*, 862–874.

Turner, R.D., Mesnage, S., Hobbs, J.K., and Foster, S.J. (2018). Molecular imaging of glycan chains couples cell-wall polysaccharide architecture to bacterial cell morphology. Nat. Commun. *9*.

Typas, A., Banzhaf, M., Gross, C.A., and Vollmer, W. (2012). From the regulation of peptidoglycan synthesis to bacterial growth and morphology. Nat. Rev. Microbiol. *10*, 123–136.

Uchida, K., and Aida, K. (1979). Taxonomical significance of cell-wall acyl type in *Corynebacterium-Mycobacterium-Nocardia* group by glycolate test. J Gen Appl Microbiol *25*, 169–183.

Uehara, T., and Bernhardt, T.G. (2011). More than just lysins: peptidoglycan hydrolases tailor the cell wall. Curr. Opin. Microbiol. *14*, 698–703.

Uehara, T., Parzych, K.R., Dinh, T., and Bernhardt, T.G. (2010). Daughter cell separation is controlled by cytokinetic ring-activated cell wall hydrolysis. EMBO J. *29*, 1412–1422.

Vilain, S., Pretorius, J.M., Theron, J., and Brözel, V.S. (2009). DNA as an adhesin: *Bacillus cereus* requires extracellular DNA to form biofilms. Appl. Environ. Microbiol. *75*, 2861–

2868.

Vlamakis, H., Chai, Y., Beauregard, P., Losick, R., and Kolter, R. (2013). Sticking together: building a biofilm the *Bacillus subtilis* way. Nat. Rev. Microbiol. *11*, 157–168.

Vocadlo, D.J., Davies, G.J., Laine, R., and Withers, S.G. (2001). Catalysis by hen egg-white lysozyme proceeds via a covalent intermediate. Nature *412*, 835–838.

Vockenhuber, M.P., Heueis, N., and Suess, B. (2015). Identification of *metE* as a second target of the sRNA scr5239 in *Streptomyces coelicolor* . PLoS One *10*, 1–15.

Vollmer, W. (2008). Structural variation in the glycan strands of bacterial peptidoglycan. FEMS Microbiol. Rev. *32*, 287–306.

Vollmer, W., Blanot, D., and De Pedro, M.A. (2008a). Peptidoglycan structure and architecture. FEMS Microbiol. Rev. *32*, 149–167.

Vollmer, W., Joris, B., Charlier, P., and Foster, S. (2008b). Bacterial peptidoglycan (murein) hydrolases. FEMS Microbiol. Rev. *32*, 259–286.

Wang, X., and Zhao, X. (2009). Contribution of oxidative damage to antimicrobial lethality. Antimicrob. Agents Chemother. *53*, 1395–1402.

Wang, G., Olczak, A., Forsberg, L.S., and Maier, R.J. (2009). Oxidative stress-induced Peptidoglycan deacetylase in *Helicobacter pylori* . J. Biol. Chem. *284*, 6790–6800.

Weadge, J.T., Pfeffer, J.M., and Clarke, A.J. (2005). Identification of a new family of enzymes with potential *O*-acetylpeptidoglycan esterase activity in both Gram-positive and Gram-negative bacteria. BMC Microbiol. *5*.

Wilking, J.N., Zaburdaev, V., De Volder, M., Losick, R., Brenner, M.P., and Weitz, D.A. (2013). Liquid transport facilitated by channels in *Bacillus subtilis* biofilms. Proc. Natl. Acad. Sci. *110*, 848–852.

Willemse, J., Borst, J.W., De Waal, E., Bisseling, T., and Van Wezel, G.P. (2011). Positive control of cell division: FtsZ is recruited by SsgB during sporulation of *Streptomyces*. Genes Dev. *25*, 89–99.

Willey, J., Santamaria, R., Guijarro, J., Geistlich, M., and Losick, R. (1991). Extracellular complementation of a developmental mutation implicates a small sporulation protein in aerial mycelium formation by *S. coelicolor*. Cell *65*, 641–650.

Williams, E.P., Lee, J.H., Bishai, W.R., Colantuoni, C., and Karakousis, P.C. (2007). *Mycobacterium tuberculosis* SigF regulates genes encoding cell wall-associated proteins and directly regulates the transcriptional regulatory gene *phoY1*. J. Bacteriol. *189*, 4234–4242.

Wolanski, M., Donczew, R., Kois-Ostrowska, A., Masiewicz, P., Jakimowicz, D., and Zakrzewska-Czerwinska, J. (2011). The Level of AdpA Directly Affects Expression of Developmental Genes in *Streptomyces coelicolor*. J. Bacteriol. *193*, 6358–6365.

Wong, J.E.M.M., Alsarraf, H.M.A.B., Kaspersen, J.D., Pedersen, J.S., Stougaard, J., Thirup, S., and Blaise, M. (2014). Cooperative binding of LysM domains determines the carbohydrate affinity of a bacterial endopeptidase protein. FEBS J. *281*, 1196–1208.

Wood, T.K., Knabel, S.J., and Kwan, B.W. (2013). Bacterial persister cell formation and dormancy. Appl. Environ. Microbiol. *79*, 7116–7121.

Xia, G., Kohler, T., and Peschel, A. (2010). The wall teichoic acid and lipoteichoic acid polymers of *Staphylococcus aureus*. Int. J. Med. Microbiol. *300*, 148–154.

Xu, Y., and Vetsigian, K. (2017). Phenotypic variability and community interactions of germinating *Streptomyces* spores. Sci. Rep. *7*, 1–13.

Xu, Q., Mengin-Lecreulx, D., Liu, X.W., Patin, D., Farr, C.L., Grant, J.C., Chiu, H.J., Jaroszewski, L., Knuth, M.W., Godzik, A., et al. (2015). Insights into substrate specificity of NlpC/P60 cell wall hydrolases containing bacterial SH3 domains. mBio *6*, 1–12.

Yahashiri, A., Jorgenson, M.A., and Weiss, D.S. (2015). Bacterial SPOR domains are recruited to septal peptidoglycan by binding to glycan strands that lack stem peptides. Proc. Natl. Acad. Sci. *112*, 11347–11352.

Yeats, C., Finn, R.D., and Bateman, A. (2002). The PASTA domain: a beta-lactam-binding domain. Trends Biochem. Sci. *27*, 438.

Yi, X., and Setlow, P. (2010). Studies of the commitment step in the germination of spores of *Bacillus* species. J. Bacteriol. *192*, 3424–3433.

Zeng, G., Vad, B.S., Dueholm, M.S., Christiansen, G., Nilsson, M., Tolker-Nielsen, T., Nielsen, P.H., Meyer, R.L., and Otzen, D.E. (2015). Functional bacterial amyloid increases *Pseudomonas* biofilm hydrophobicity and stiffness. Front. Microbiol. *6*, 1–14.

Zhang, P., Wu, L., Zhu, Y., Liu, M., Wang, Y., Cao, G., Chen, X.L., Tao, M., and Pang, X. (2017). Deletion of *mtrA* inhibits cellular development of *Streptomyces coelicolor* and alters expression of developmental regulatory genes. Front. Microbiol. *8*, 1–18.